2020 Doctoral Dissertation

Photoinjection of Macromolecules into Single Plant Cells Applying Femtosecond Laser Amplifier

(フェムト秒レーザー増幅器を利用した単一植物細胞への巨大分子の導入)

Taufiq Indra Rukmana

Nara Institute of Science and Technology

Division of Materials Science

Bio-Process Engineering Laboratory

（Main Supervisor: Prof. Yoichiroh Hosokawa）

Submission Date: July 14, 2020

Table of Contents

Chapter 1

General Introduction

1.1 Molecular introduction into plant cells

Methods for molecular introduction into plant cells have become increasingly crucial in the study of plant physiology and genetic engineering.[1] Indeed, various functional molecules, such as fluorescent dyes, proteins, chemical agents, and genes, are introduced into plant cells. In basic studies of plant physiology, molecular introduction is an important way for ascertaining and designing plant functions.[2-5] The green fluorescent protein (GFP) was fused to prolamins, a group of rice (*Oryza sativa*) seed storage proteins, in order to examine the accumulation mechanism of prolamins in endoplasmic reticulum.[3] The presence of extracellular adenosine triphosphate (eATP), closely correlated with active growth and cell expansion, in plants (*Medicago truncatula*) was detected using a new reporter, by fusing a cellulose-binding domain peptide to the ATP-requiring enzyme luciferase, that permitted visualization of eATP with the occurrence of the substrate luciferin in the plant roots.[4] The GFP was also used to identify the genes whose expression is linked to auxin, a plant hormone, that regulates the initiation of flower primordium.[5] In agriculture, addition of intended properties to agricultural crops is commonly applied. Crops with high yield production and disease-and-stress resistances are usually desirable by farmers.[6] Other active fields in plant research also include production of useful materials, such as drugs and antibodies, and environmental purification through genetically modified plants.[2, 7-8] The genes from *Artemisia annua* that involved in the production of artemisinin, a medicine for malaria, were inserted into tobacco plants for mass production of the drug.[7] Recently, the large scale production of biopharmaceutical proteins, such as monoclonal antibodies (mAbs) utilizing transgenic plants is also promising.[8]

In another development, the introduction of functional molecules into plant cells could be combined with the utilization of nanoparticles as transporters for various functional materials ranging from small agrochemicals to large DNA and proteins.[9-11] The nanoparticle application in agriculture has many benefits in plant production, including the controlled release of agrochemicals, such as fertilizers, pesticides, and herbicides, and target-specific delivery of biomolecules, such as nucleotides and proteins.[9] Those benefits are mainly due to the unique physicochemical properties of nanoparticles, such as surface area, reactivity, particle size, and particle morphology, which could be designed as necessary for the nanoparticle application.[10-11] The nanoparticles internalization into intact plant cells is usually administered either by diffusion or by active uptake managed by cellular processes.[12-14] Nevertheless, such passive method applicability is highly material dependent. Thus, recent molecular delivery techniques usually also use a more active approach.

Meanwhile, many introduction techniques into plants, such as polyethylene glycol and electroporation, need protoplast preparation.[15-16] Polyethylene glycol (PEG), under presence of divalent cations, makes the plasma membrane of protoplasts unstable and permeable to DNA. After incubation, the DNA would enter and transform the protoplasts.[15] In electroporation, the protoplast plasma membrane becomes permeable to extracellular macromolecules, such as nucleotides, nucleic acids, indicator dyes, and proteins, after receiving high-voltage electric shocks.[16] The use of protoplasts, which are plant cells without cell wall, requires careful handling and is time consuming due to laborious protocols; therefore such methods are not frequently used today.[1-2, 6] Instead, methods using *Agrobacterium* and particle gun are usually applied. In nature, *Agrobacterium* infects the host plant cell with a tumor inducing (Ti) plasmid and then transfers a portion of its gene, called transferred DNA (T-DNA), which makes the host cell continue to grow and produce opines, amino acid derivatives that are exclusively used by the bacteria. To transform the plant cell, recombinant *Agrobacterium* strains, in which the native

T-DNA has been replaced by the genes of interest, are used. However, the *Agrobacterium* usage has a safety risk of unexpected gene modifications.[1, 17] The particle gun is relatively safe and applicable to various kinds of plants. For the transformation, it uses a device to fire micro-projectiles, made of metal coated by the genes of interest, into plant cells. It also permits the delivery of gold or tungsten nanoparticles coated with genetic substances (DNA, RNA, etc.) through cell walls. However, it has a low introduction efficiency and a risk of damaging target samples or transported substances.[1-2, 6, 14, 18-19]

In the methods above, plant cells are randomly transfected. So far, injection techniques for plant cells at single cell level have not been well established. There are several advantages of molecular introduction at single cell level, such as the ability to manipulate specific cells of intact plant organs, instead of callus or protoplast; to examine the role of individual cells, and to study intercellular communication.[24] An introduction method that can be used for this purpose is microinjection. It utilizes a glass microcapillary-injection pipette with micromanipulator to inject molecules, usually genes, into a single cell. However, this method is tedious, invasive, requires physical contact, and with low throughput.[1]

Laser photoinjection is promising as an alternative method for molecular introduction to intact plant cells at single cell level, which is non-invasive, non-contact, and with relatively high throughput if compared to microinjection. It uses a pulsed laser that is focused onto a cell to form a transient pore for the injection of extracellular substances into cells. This is conducted in a hypertonic solution in order to reduce the plant turgor pressure, which is caused by the inner pressure from plant cell vacuoles. A UV nanosecond laser was utilized by Weber *et al.* for the first time in 1988 to introduce DNA plasmid into plant cells of *Brassica napus* in a buffer containing 0.4 M of sorbitol. A hole was punctured on the cell wall and plasma membrane for this purpose. About 80% of the irradiated cells survived, indicated by their cytoplasmic streaming. However, the introduction efficiency was not stated.[20-21] Subsequent work in 1995

by Guo *et al.* confirmed gene transformation in rice cells with a UV nanosecond Nd:YAG laser, even though only 0.48% of cells was transformed. Before injection, the cells were pre-treated in a hypertonic buffer containing 0.75 M $CaCl_2$ because without the pre-treatment, an outflow of cell contents was observed.[22] Moreover, the intense UV laser light has photochemical damage risk in its optical path that compromises cell viability and ability for gene expression.

Recently, a near infrared (NIR) femtosecond (fs) laser has been used for the nanoprocessing and photoinjection to plants.[23-25] One of the fs laser photoinjection main advantages is its ability for precise perforation at a subcellular level due to effective non-linear processes such as a multi-photon absorption at a laser focal point, which minimizes collateral damage in the optical path (Fig. 1).[26-27] Water and nearly all biological materials have little absorption between 600–900 nm. Thus, a multiphoton absorption would be dominant in the excitation using intense 800 nm fs pulse. It needs four-photon absorption to excite water molecules with maximum absorption at about 200 nm and energy of 6.24 eV using 800 nm fs laser pulse (1.56 eV). An objective lens would focus the pulse and induce the absorption at the laser focal point. Following that, propagation of mechanical effects, such as stress and shock waves, would occur as a cavitation bubble with less thermal accumulation formed near the focal point. [26-29]

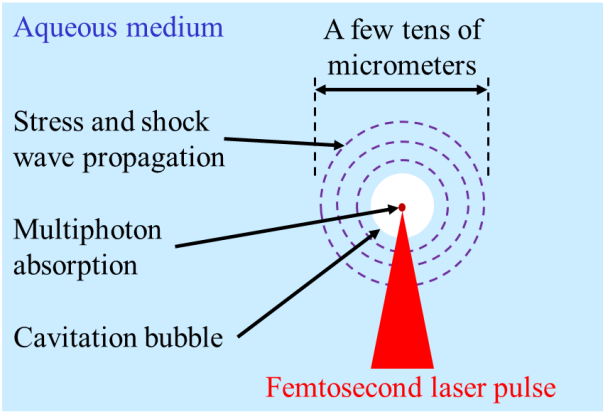

Figure 1. Illustration of fs laser pulse inducing multiphoton absorption at the laser focal point. When the fs laser pulse is focused in aqueous medium, cavitation bubble and propagation of mechanical effects, such as stress and shock waves, occur near the focal point.[26-27]

Surely, the fs laser photoinjection has already been applied for introduction of macromolecules, such as genes and proteins, to mammalian cells efficiently.[30-35] Tirlapur and König demonstrated the transfection of Chinese hamster ovarian (CHO) cells with DNA plasmid encoding enhanced GFP using fs laser photoinjection for the first time in 2002.[30] Unlike plant cells, the animal cells were irradiated in normal culture medium without pre-treatment of hypertonic solution. Indeed, the vacuoles in animal cells are either absent or very few and small, so there is lower inner pressure in animal cells, compared to that in plant cells. Subsequent work in 2006 by Stevenson *et al.* reported that the transfection efficiency of 4000 CHO cells was about 50 ± 10%.[31] Then, the technique was used to transfect human pancreatic and salivary gland stem cells. The transfected cells were found to divide and the daughter cells also showed the gene expression.[32] Davis *et al.* compared the use of fs laser amplifier (two 12 nJ pulses) and fs laser oscillator (3.8×10^6 1.0-nJ pulses) for the transfection of CHO cells in 2013. It was found that the transfection efficiency was similar at about 25% and 30% for fs laser amplifier and oscillator, respectively. The resulting pore sizes were larger with fs laser amplifier at about 160 nm, compared to that with fs oscillator at about 77 nm. In addition, larger pores were resealed more quickly than smaller pores, ruling out passive resealing mechanism. Moreover, the DNA plasmids accumulated at the laser focal point in cell membrane when using the fs laser amplifier, before being translocated into the cells.[33] Our group also reported the injection of biomolecules and genes into animal cells and living vertebrate embrio.[34-35]

However, injection of large molecules into plant cells is significantly more difficult than that into animal cells. LeBlanc *et al.* used fs laser photoinjection to introduce cascade blue-labeled dextran of 10 kDa into an intact single cell of *Arabidopsis thaliana*. The increase of fluorescence intensity in the cells stopped at 90 s, indicating the pore on the cell membrane resealed at this time scale. The dye stayed in the injected cells for at least 72 hours.[24] The fs laser photoinjection efficiency of fluorescein isothiocyanate-conjugated dextran (FITC-

dextran) into a tobacco BY-2 cell (TBY-2) depending on osmolarity, laser power and the conjugated dextran size was studied by Mitchell *et al.*[25] Cytosol leakage occurred when the cells were irradiated in the hypotonic solution and the injection efficiency increased when the cells were treated with more hypertonic solutions by addition of up to 0.67 M sucrose to the medium. They also noted that increasing laser energy would increase the photoinjection efficiency, although the cell viability decreased. Uptake of fluorescent molecules seemed to be faster in a high molarity solution. The fluorescence intensity in the cells reached the maximum value at about 180 s. In addition, it was found that the introduction efficiency decreased with higher molecular weight, and the maximum value was 40 kDa under optimized parameters, even in the protoplasts. That was about 4.42 nm in diameter, calculated with formula SR [nm] = 0.81 x (MW [kDa])$^{0.46}$, with SR is the Stokes radius in nm and MW is the molecular weight in kDa.[25, 36-37]

Nevertheless, the injection of DNA-sized macromolecules with molecular weights over 1 MDa into intact plant cells using fs laser photoinjection has not been attained yet. Unlike animal cells, plant cells have cell wall that protects their cell membrane (Fig. 2).[38] Cell walls, which consist of cellulose fiber networks, are relatively thick and rigid, and block molecules larger than around 30 kDa with diameter size of 4 nm. In addition, the results of experiments above indicated that the effective formed pore is tiny in size or the perforation was only happened on the cell membrane. In those experiments, fs laser pulses with a low pulse energy (<1 nJ/pulse) and high repetition rate (>10 MHz) were used.[25] However, due to the high repetition rate, accumulation of thermal energy and formation of a long-lasting vapor bubble at a laser focal point could occur when the laser pulse energy is increased. The pore formation on the rigid cell wall would likely decrease the cell viability. Therefore, the cell wall would still be a barrier for macromolecule diffusion into a cytosol despite of a small pore formation on it by the fs laser irradiation.

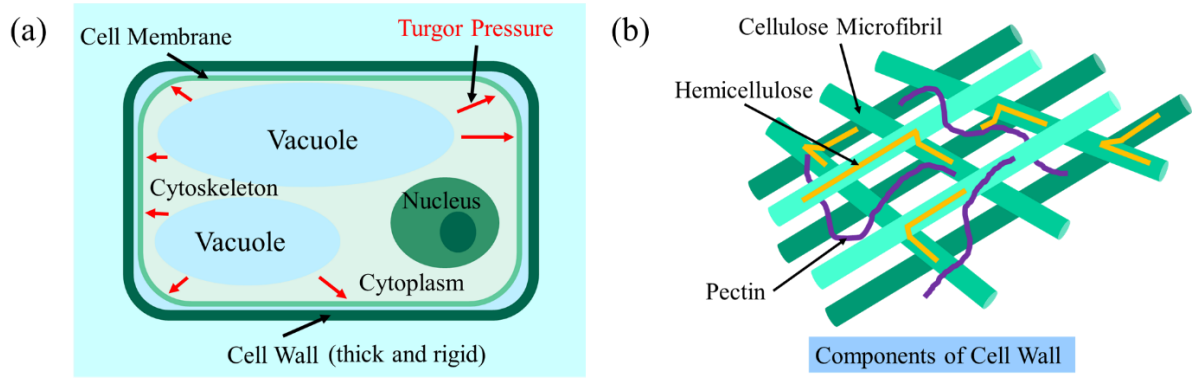

Figure 2. (a) Structure of plant cell. Unlike animal cells, plant cells have many large vacuoles that induce inner pressure, called turgor pressure, in the cell. In addition, plant cell membranes are protected by thick and rigid cell walls. (b) Components of cell wall. Cell walls mainly consist of cellulose microfibril (25%), hemicellulose (25%), and pectin (35%).[38]

1.2 Research objective

In this work, the research objective is to develop photoinjection technique for the introduction of macromolecules into single intact plant cells using femtosecond laser amplifier. First, the injection of FITC conjugated dextran of 20 kDa (FITC-20k) with diameter of 3.2 nm, as a comparison, and of 2 MDa (FITC-2M) with diameter of 26.7 nm, which is similar in size with DNA plasmid, into single TBY-2 cells with a fs Ti:sapphire laser amplifier would be attempted. A moderate enzyme treatment with cellulase and pectolyase would be applied to partially degrade the cell wall main components, without forming protoplasts. It is expected that the application of intense fs laser pulse in this experiment could perforate the cell wall efficiently and the enzyme treatment would enhance large molecule diffusion through the cell wall.

Next, the method would be applied to inject fluorescent polymer nanoparticles with diameter of 80 nm into single intact TBY-2 cells. The ultrabright green fluorescent nanoparticles (G-FNPs) made of copolymer of styrene and fluorescent BDPMA (boron-dipyrromethene (BODIPY) methacrylate) were used to obtain sensitive imaging of nanoparticle injection into TBY-2 cells. The shell consisted on carboxylic terminals enhancing the nanoparticle solubility

in water. Meanwhile, the core was a copolymer of styrene and the BODIPY monomer. BODIPY is a hydrophobic fluorophore that can be modified chemically to give green to red emission. The hydrophilic shell and hydrophobic core were linked covalently which ensure the stability and biocompatibility of the nanoparticles.[39-40] A successful photoinjection of nanoparticles would open a way for the utilization of nanoparticles, which are capable to contain functional molecules, for manipulation of single plant cells. In addition, the mechanism of photoinjection would also be elaborated, based on laser ablation and photomechanical effect induced by fs laser amplifier. Moreover, possible applications of this method would be attempted, including the investigation of nanoparticle diffusion process in plant cell cytoplasm.

1.3 Thesis outline

Chapter 1 General introduction: In this chapter, several techniques of molecular introduction into plant cells were described, including photoinjection and its shortcoming. The research objective and thesis outline were also presented.

Chapter 2 Methods: In this chapter, the preparation of TBY-2 cells as the plant samples was explained. Then, the experimental setup of NIR fs laser photoinjection was described. The fluorescent measurements to evaluate the injection efficiency was also presented. In addition, the cell viability assay to examine cell conditions after laser irradiation was described.

Chapter 3 Photoinjection of megadalton molecules: In this chapter, the effect of mannitol addition and enzyme treatment on cell structures, the molecular introduction in the hypertonic solution and with enzyme assistance, and the introduction efficiencies in those conditions for FITC-20k and FITC-2M were discussed.

Chapter 4 Photoinjection of fluorescent nanoparticles: In this chapter, the nanoparticle injection in the hypertonic solution and with enzyme assistance, and the injection efficiencies in those conditions were discussed.

Chapter 5 Mechanism of photoinjection: In this chapter, the mechanisms of photoinjection, based on the observation of the transient morphological change induced by the fs laser irradiation and photoinjection with various focal point position, were discussed.

Chapter 6 Application of photoinjection: In this chapter, the application of photoinjection for the observation of intracellular and intercellular diffusion was discussed.

Chapter 7 General conclusion: In this chapter, the general conclusion and perspective were presented.

Chapter 2

Methods

2.1 Preparation of tobacco BY-2 cells

Wild-type TBY-2 cells were cultured as described elsewhere with slight modifications.[41-42] The TBY-2 cells were grown in a suspension of 4.6% (w/v) of Murashige-Skoog (MS) basal medium (Ducheva Biochemie). The medium was supplemented with 3% (w/v) of sucrose (Sigma-Aldrich), 0.2 g/L of KH_2PO_4 (Sigma-Aldrich), 1 mg/L of thiamine-HCl (Sigma-Aldrich), 100 mg/L of myo-inositol (Sigma-Aldrich), and 0.1 mg/L of 2,4-dichlorophenoxyacetic acid (Sigma-Aldrich). The cell suspension was continuously shaken at 130 rpm in a dark place at 27 °C. The cells were sub-cultured at weekly intervals by transferring 2 mL of the suspension into 95 mL of the fresh medium.

TBY-2 cells have high growth rates and multiply 80- to 100-fold after 1 week of initial transfer, as presented at Fig. 3.[41] This type of tobacco cells does not contain chloroplast and nicotine. In 1 to 4 days after transfer, they have 5-8% mitotic index, which is the percentage of cells undergoing division. Thus, the cells have high homogeneity and are commonly used in plant researches. At 7 days after transfer, most cells stop dividing and enter stationary phase, therefore they need to be sub-cultured.[41] As the cells are not differentiated, TBY-2 cells only have primary cell walls which consist of cellulose microfibrils, hemicellulose, and pectin. Their cell walls do not contain lignin which is commonly found in secondary cell walls of more specialized cells, such as in epidermis, xylem, and floem tissues.[38]

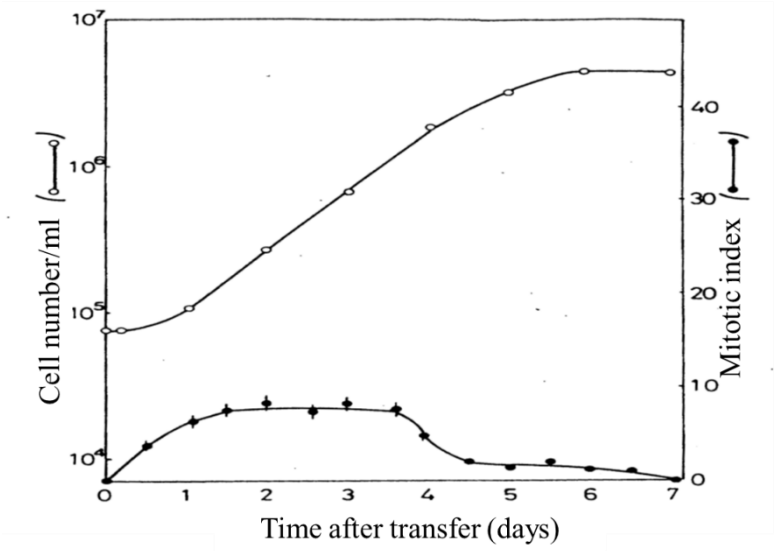

Figure 3. Growth curve and mitotic indices of TBY-2 cells.[41]

Two-day old cultured cells were used for the photoporation experiments (Fig. 4). First, 1 mL of the cell suspension was centrifuged at 1000 rpm for 1 min, and the TBY-2 cell pellet was re-suspended in 1 mL of the same culture medium. A mannitol treatment was applied to control osmotic pressure with addition of 0.5 M mannitol into the final culture medium.

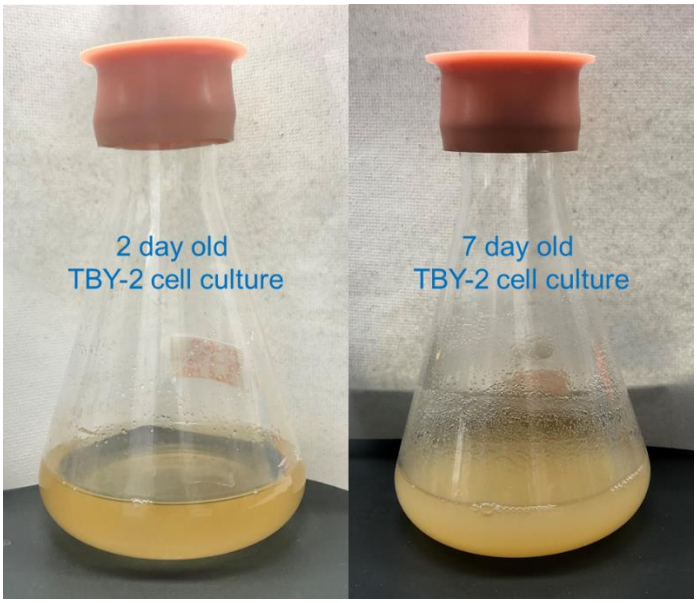

Figure 4. The TBY-2 cell cultures on 2 and 7 day old after sub-culturing.

The partial degradation of cell wall was done by enzyme treatment. After the centrifugation, the standard culture medium was substituted with 1 mL of an enzyme solution. The enzyme solution was prepared in 0.05 M of MES buffer (2-(*N*-morpholino)-ethane-sulfonic acid) (Sigma-Aldrich) with pH of 5.8. It contained 0.5% (w/v) of cellulase Onozuka RS (Serva Electrophoresis), 0.05% (w/v) of pectolyase Y-23 (Serva Electrophoresis), and 0.3 M of mannitol (Sigma-Aldrich). The cells were incubated in the enzyme solution in a dark place at 27 °C for 10 min, washed 5 times with 1 mL of 0.4 M of mannitol solution, and then re-suspended in 1 mL of the same culture medium containing 0.5 M mannitol.

Cellulase, comprises of a mixture of endocellulase, exocellulase, and cellobiase, is the enzyme that digest cellulose as a main component of cell walls (Fig. 5). Meanwhile, pectin, another component of cell walls, is degraded by pectolyase. Those enzymes are commonly applied for the protoplast preparation.[42-43] In the preparation procedure of protoplast, cell walls are usually removed about one hour after enzyme treatment. Generally, the enzyme concentrations for the protoplast preparation are 1.0% of cellulase and 0.1% of pectolyase. It was expected that with moderate 10 min enzyme treatment and half of enzyme concentration, the cell walls would be still intact and only partially degraded.

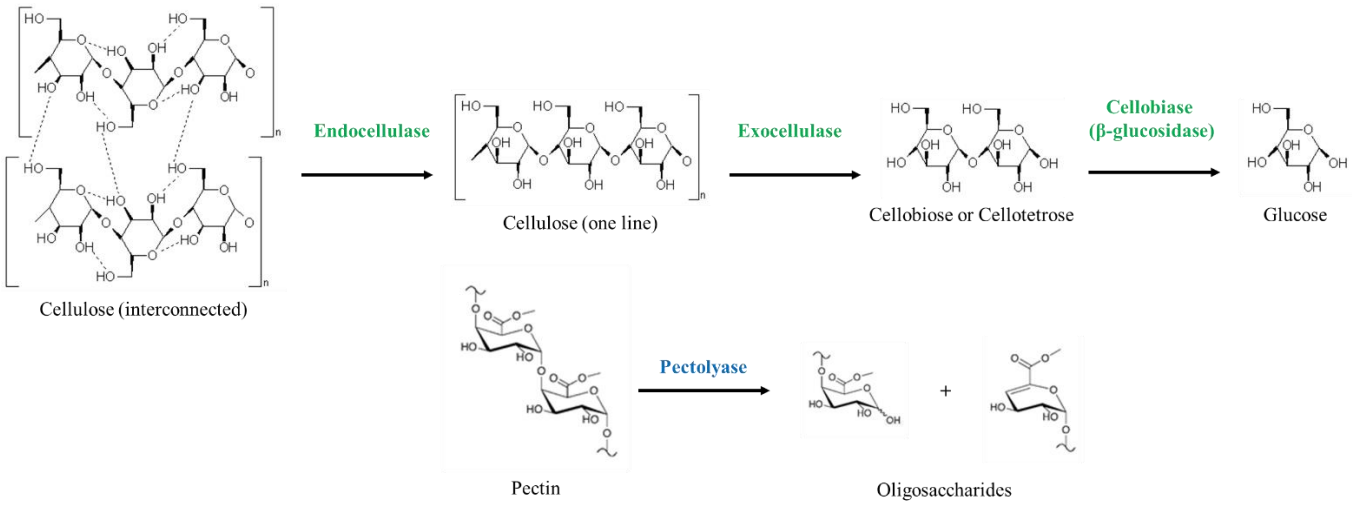

Figure 5. The digestion of cellulose (upper) and pectin (lower) in aqueous medium.[42-43]

Finally, 100 μL of the prepared cell suspensions in each treatment were placed in a glass-bottom dish (φ=12 mm, Iwaki). All the experiments were conducted within 6 hours after each treatment to maintain a healthy cell condition.

2.2 NIR fs laser photoinjection

The setup for the photoinjection is presented in Figs. 6 and 7. Amplified fs laser pulses from a regeneratively amplified fs Ti:sapphire laser system (Spectra-Physics, Solstice-Ref-MT5W, 800 nm, 150 fs) were led into a laser-scanning confocal microscope (Olympus, IX71FVSF-2) and focused on a TBY-2 cell through a 100x oil-immersion objective lens (Olympus; Plan N, NA = 1.25). A single laser pulse was obtained using a mechanical shutter with a gate time of 1/125 s from pulse trains of 125 Hz. The laser pulse energy was tuned by a half waveplate, polarizer, and neutral density filter. The laser beam was enlarged by a beam expander in order to fill the back aperture of the objective lens, and the laser focal plane was set to the image plane of the microscope. The laser pulse energy through the objective lens was measured with a laser power meter (Ophir, Nova Display-Rohr). A sample was put on a motorized microscope stage (Sigma Koki, E-65GR) equipped on the microscope.

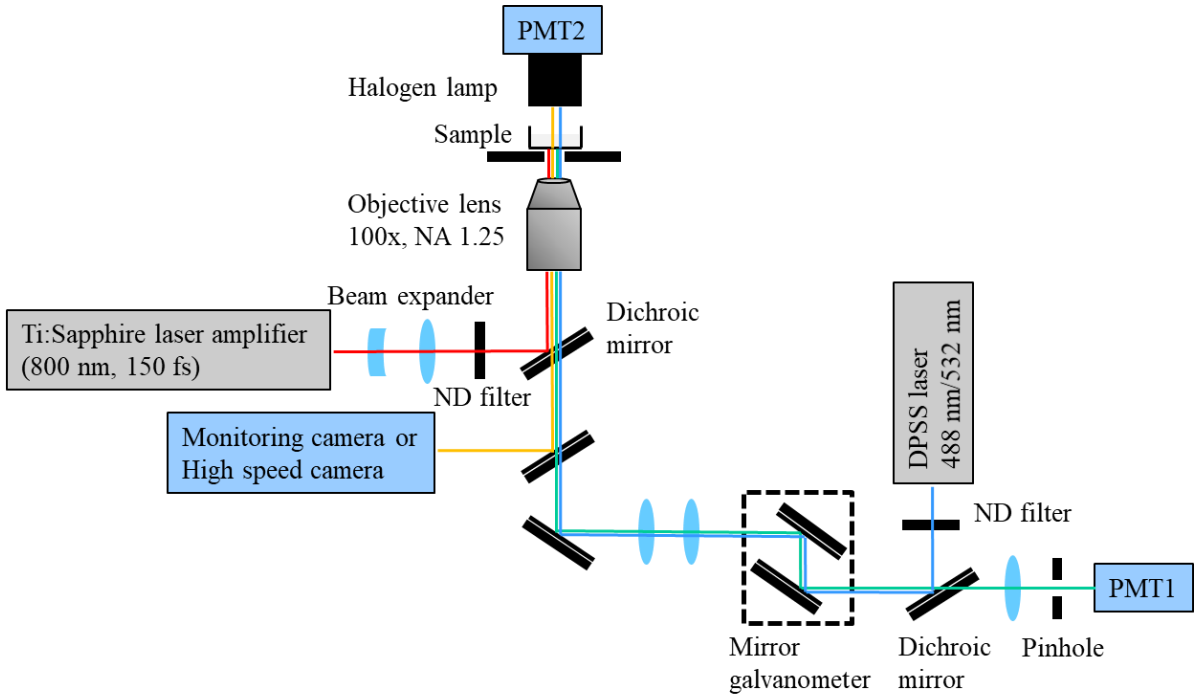

Figure 6. Schematic illustration of the NIR-femtosecond laser system coupled with a confocal laser scanning microscope.

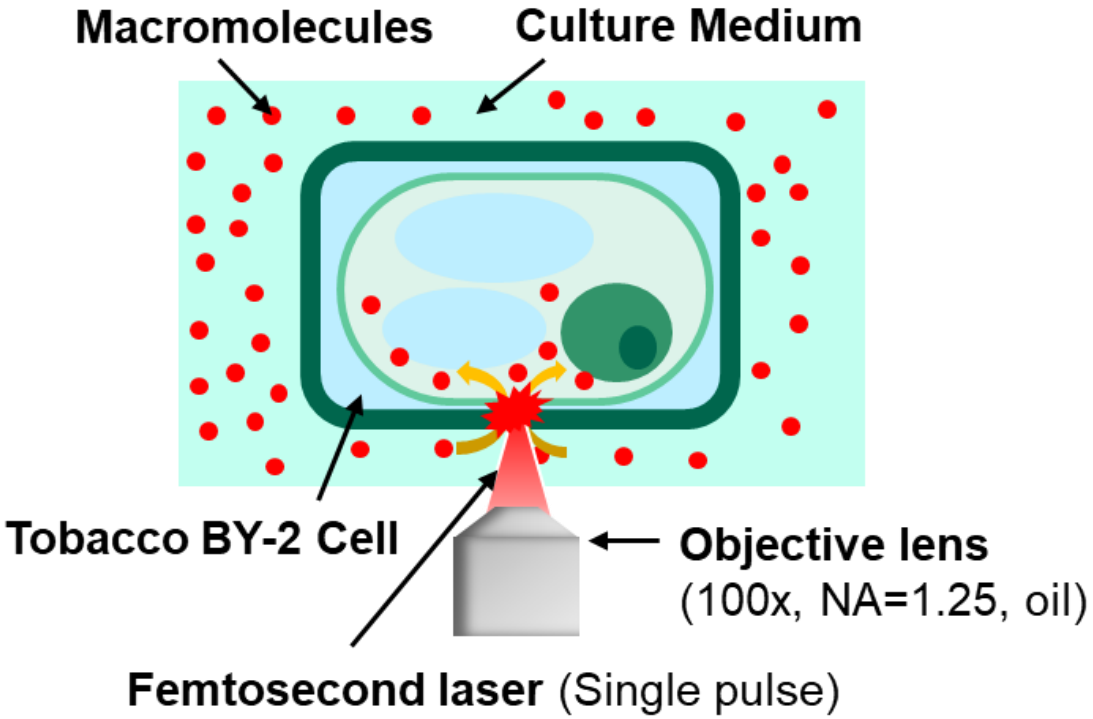

Figure 7. A model of the photoinjection of macromolecules into TBY-2 cell using single fs laser pulse focused by objective lens on the contact point of cell wall and membrane.

2.3 Fluorescence measurements

At first, fluorescein isothiocyanate (FITC-dextran, Sigma-Aldrich) conjugated with 20 kDa (FITC-20k) or 2 MDa (FITC-2M) dextran molecules were used as exogenous substances to be injected into TBY-2 cells. Dextran is a polysaccharide macromolecules while the FITC is a fluorescent dye. The FITC-20k was used as a comparison to observe the injection of smaller molecules. The FITC-2M is similar in size with typical DNA plasmid. FITC is grafted randomly to hydroxyl groups of dextran at a frequency of 0.003 to 0.02 moles of FITC per mole of glucose, as presented in Fig. 8. The dye solutions were prepared with concentrations of 0.5 mM for 20 kDa and 2 μM for 2 MDa. The maximum wavelengths of excitation and emission of FITC are 490 and 520 nm, respectively.

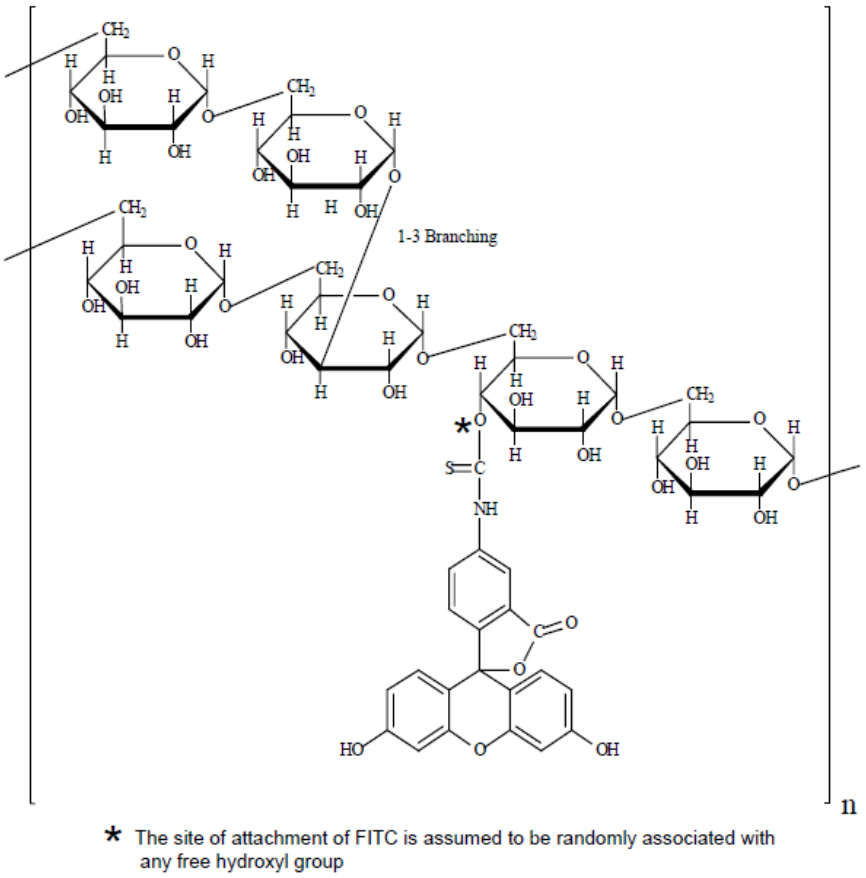

Figure 8. Chemical structure of FITC-conjugated dextran.[44]

Then, ultrabright green fluorescent nanoparticles (G-FNPs) made of copolymer of styrene and fluorescent BDPMA (boron-dipyrromethene (BODIPY) methacrylate) were used to get sensitive visualization of nanoparticle injection into TBY-2 cells. The G-FNP preparation would be described later.[39-40] The prepared G-FNPs have concentration of 7.3 ± 0.34 x 10^8 particles/mL and diameter of 80 ± 2.0 nm. The volume of this particles is about 20 times larger than typical DNA plasmids (2 MDa) and 400 times larger than average proteins (30 kDa) (Fig. 9).[45-47] The excitation and emission maxima were 529 and 547 nm, respectively.

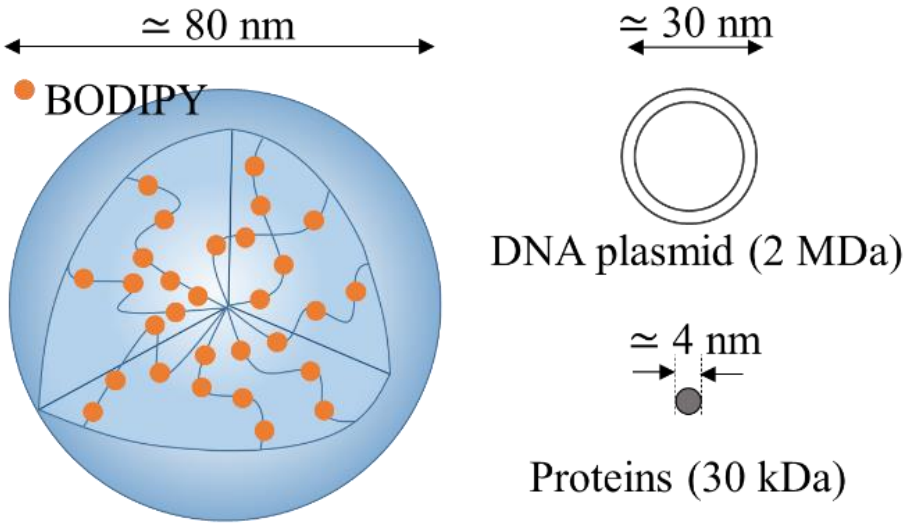

Figure 9. Comparison of hydrodynamic diameters among poly(styrene-*co*-BDPMA) nanoparticle, DNA plasmid with 2 MDa and an average protein (30 kDa).

The injections of FITC-dextran and G-FNPs were observed by confocal fluorescence imaging. A diode-pumped solid-state (DPSS) laser (Spectra-Physics, PC14763) at 488 nm wavelength was applied for the excitation. 1 μL of FITC-dextran or G-FNP solution was added to 100 μL of the TBY-2 cell suspension in the glass-bottom dish, and the sample was put on the microscope stage. All fluorescence images were captured with the same acquisition parameters for each substance.

2.4 Evaluation of injection level

The injection level was evaluated as a differential fluorescence intensity (ΔI) between before and after the photoporation. A TBY-2 cell cytoplasm was chosen as a region of interest with Image J software in the acquired fluorescence image, and the mean intensity value before photoporation (I_{before}) was subtracted from that of 2 min after photoporation (I_{after}). The calculation of ΔI is illustrated on Fig. 10. When cells were damaged by the fs laser irradiation, they were excluded from the data set and the histogram of ΔI was prepared using data of 20 viable cells.

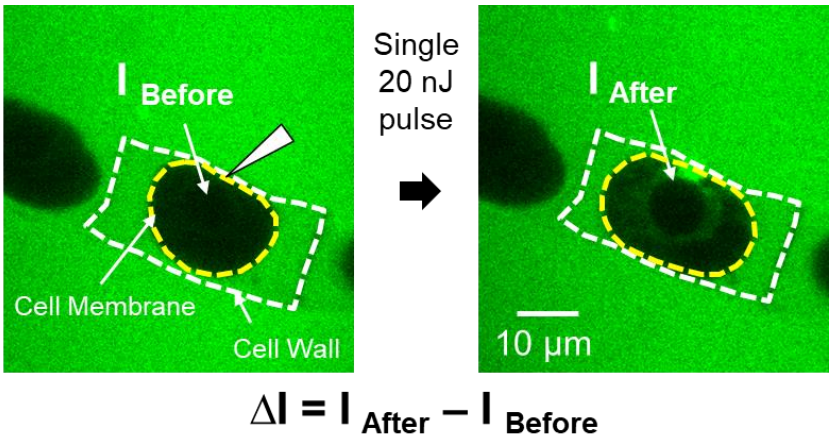

Figure 10. The calculation of differential fluorescence intensity (ΔI). A cytoplasm area, marked with yellow dashed lines, was selected using Image J software. The ΔI was calculated by substracting the average intensity value after photoporation (I_{after}) with the average intensity value before photoporation (I_{before}).

2.5 Preparation of green fluorescent nanoparticles

The G-FNPs were received from Institut des Sciences Moléculaires d'Orsay (ISMO, UMR 8214), CNRS, Université Paris-Saclay, Orsay, France. The G-FNP preparation, which include the reaction of polymerization between the BODIPY fluorophore and styrene, would be described in this section, as also reported elsewhere (Figs. 11 and 12).[39-40] First, in a 5 mL round bottom flask, the macro RAFT (reversible addition−fragmentation chain transfer) agent (PEOA-co-AA)-TTCA {([poly(ethylene oxide) acrylate]-co-poly(acrylic acid))-(2-methyl-2-

[(dodecyl-sulfanyl-thio-carbonyl)sulfanyl]propanoic acid)} (1 eq., 0.07 mmol, 0.42 g), the green-BDPMA (3.2 eq., 0.21 mmol, 0.097 g), and 2,2′-Azobisisobutyronitrile (AIBN, 0.5 eq., 0.03 mmol, 0.005 g) were dissolved in styrene (157 eq., 10.20 mmol, 1.06 g). Then, the mixture was placed in ice bath and degassed with argon (Ar) flux for 30 min. After that, the reaction was immediately placed in an oil bath at 80 °C and stirred for 70 min. The reaction was quenched in an ice bath and 5 mL of NaOH (0.1 M) solution was added. The reaction was placed in an ice bath, under ultrasounds at 120 W for 10 min. The miniemulsion was placed in an ice bath and degassed for 30 min with Ar flux. Next, the reaction was placed in an oil bath at 80 °C and stirred overnight to restart the polymerization. Finally, the G-FNPs were prepared and ready to be used. Another nanoparticles, the red fluorescent nanoparticles (R-FNPs), using similar preparation to the G-FNPs, except with a red BODIPY, would also be mentioned later.

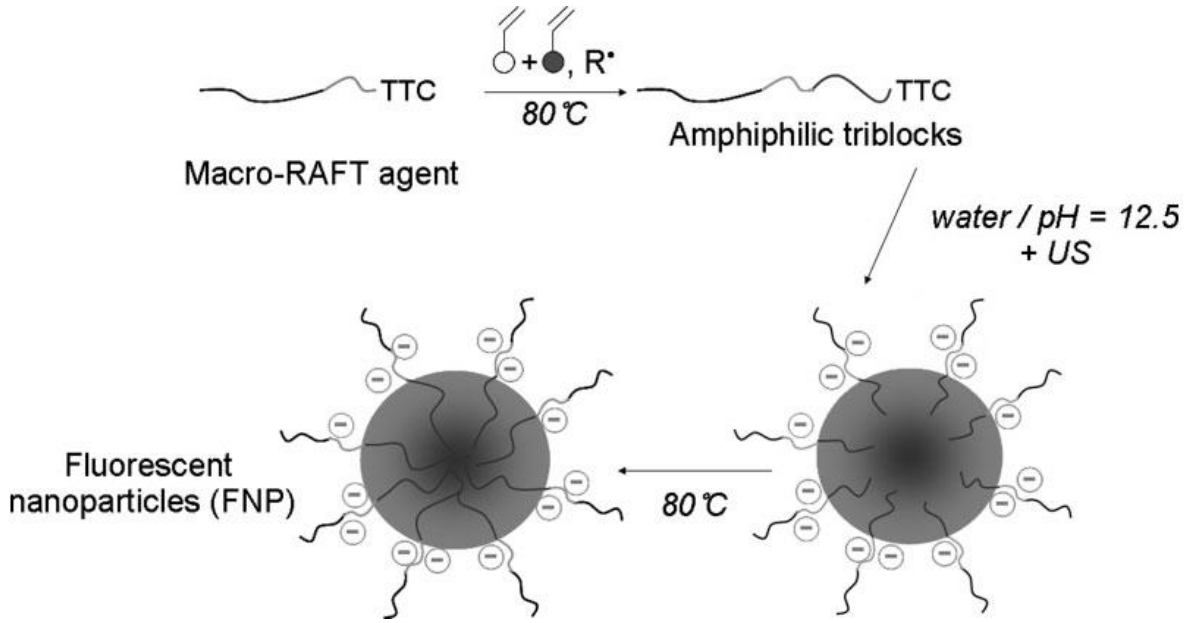

Figure 11. Synthesis of the G-FNPs using reaction of polymerization. The macro-RAFT agent was used to ensure the resulting polymer and nanoparticles would be homogenous in size.[39-40]

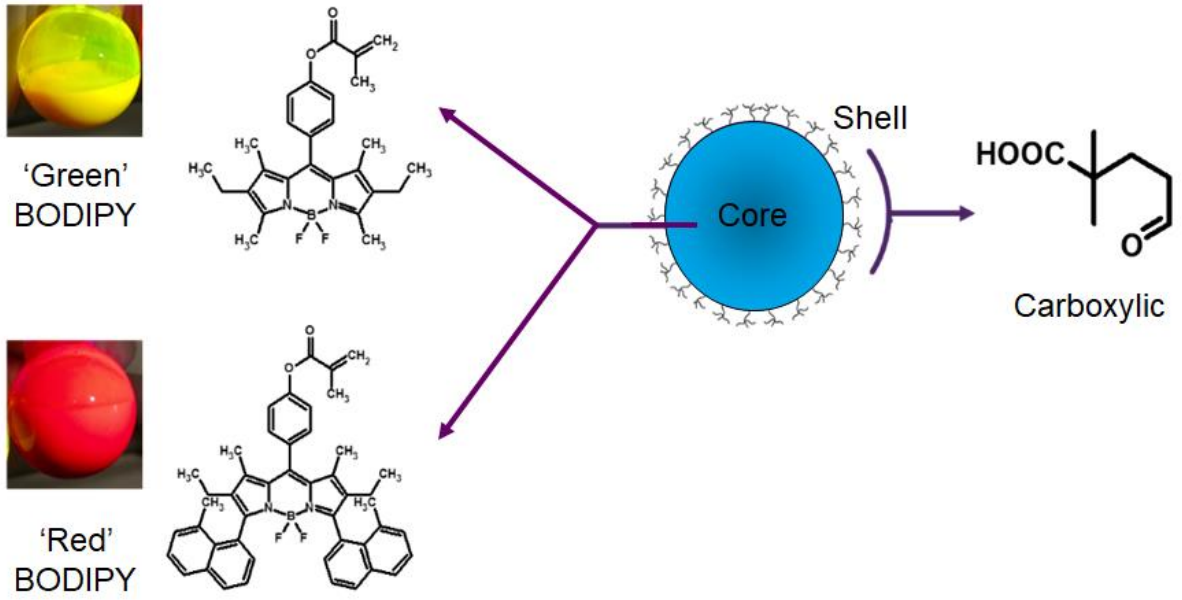

Figure 12. Structure of the G-FNPs and the R-FNPs. The hydrophobic green or red BODIPY fluorophore (BDPMA) was in the core of nanoparticles, linked covalently to the styrene polymer with carboxylic terminals that made up the hydrophilic nanoparticle shell.[39-40]

2.6 Cell viability assessment

The viability of TBY-2 cells after the fs laser irradiations was examined by observation of cytoplasmic streaming in transmission image, and fluorescein diacetate (FDA) assay. Cytoplasmic streaming is originated from the motion of cytoskeletal myosin on actin filaments. It transports nutrients within cytoplasm, therefore it is considered as an indicator for the viability of plant cells. FDA assay is a general test for plant cell viability based on the cell enzymatic activity.[48] In the case of viable plant cells, fluorescent fluorescein (λ_{ex} = 494 nm, λ_{em} = 521 nm) is produced from the hydrolysis of non-fluorescent FDA by intracellular esterase enzyme (Fig. 13). For FDA assay, 100 μL of TBY-2 culture medium was added with 2 μL of 0.36 mM FDA (Dojindo) aqueous solution and was subsequently incubated for 20 min. Its fluorescence signal was detected after the incubation, using the same confocal fluorescence imaging system as the macromolecule measurement.

In addition, propidium iodide (PI) assay was also conducted to examine non-viable cells.[48] Non-viable cells could be living or dead cells and distinguished from viable cells by their non-

intact or damaged cell membranes. PI (λ_{ex} = 535 nm, λ_{em} = 617 nm) can only enter cells when the cell membranes are damaged and will intercalate with nucleic acids in plant cells (Fig. 14). Non-viable cells will be stained in bright red, particularly in their nucleus. For PI assay, 100 µL of TBY-2 culture medium was added with 2 µL of 0.075 mM PI (Dojindo) aqueous solution and was subsequently incubated for 20 min in dark room. Its fluorescence signal was detected after the incubation, using the same confocal fluorescence imaging system as the macromolecule measurement, except that the excitation wavelength was 532 nm.

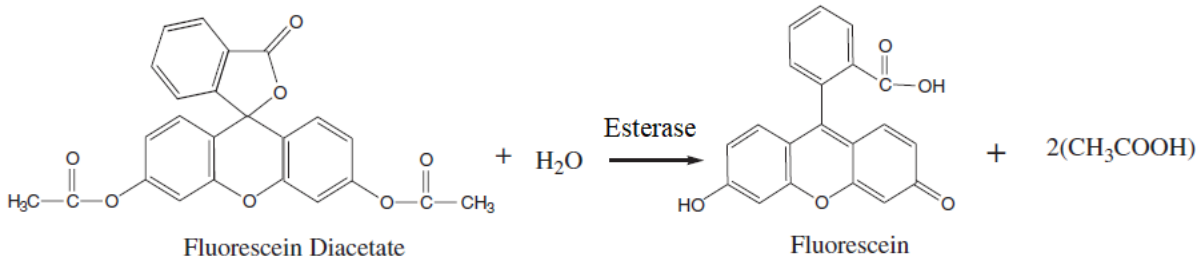

Figure 13. The hydrolysis of FDA into fluorescein by esterase in viable plant cells.[48-49]

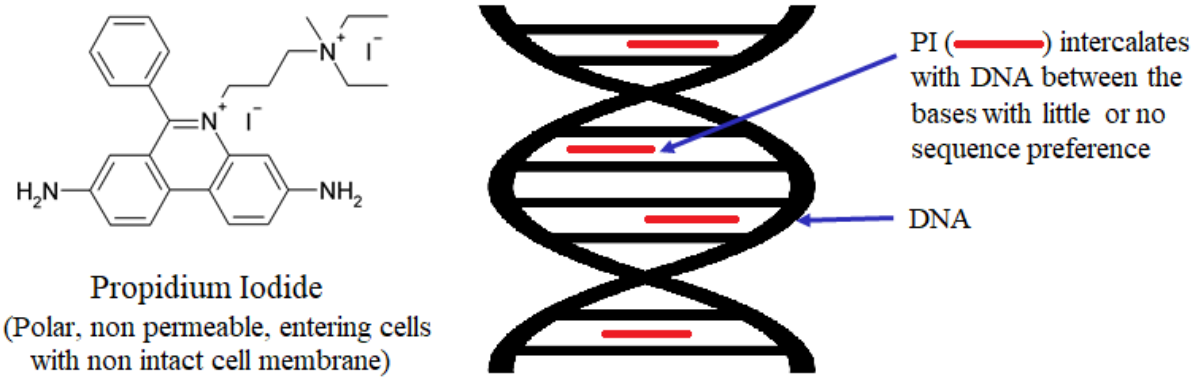

Figure 14. PI intercalating with DNA of non-viable plant cells.[48]

Chapter 3

Photoinjection of Megadalton Molecules

3.1 Introduction

The introduction of macromolecules with molecular weights over 1 MDa into intact plant cells using fs laser photoinjection has not been achieved. Plant cell vacuoles generate turgor pressure that prevent injection through molecular diffusion process. This has been overcome by treating plant cell in a hypertonic solution to suppress the inner pressure. However, there is another limitation, primarily because of the thick and rigid plant cell walls blocking molecules larger than 30 kDa or about 4 nm in diameter.[25] Therefore, it is still difficult to apply the photoinjection method in plants.

As described previously, TBY-2 cells would be treated in a hypertonic solution by adding 0.5 mannitol to the culture medium. A moderate enzyme treatment with cellulase and pectolyase was applied for 10 min to partially degrade the cell wall main components, without forming protoplasts. The changes in the cell morphology before and after those treatments would be described in this chapter.

Then, the injection of FITC-20k and -2M into single TBY-2 cells with a fs Ti:sapphire laser amplifier would be presented. It is expected that the application of intense fs laser pulses in this experiment could perforate the cell wall efficiently and the enzyme treatment would enhance macromolecule diffusion through the cell wall. In addition, the evaluation of photoinjection efficiency would be described, based on the difference of fluorescence intensity in cell cytoplasm between before and after laser irradiation. The cell viability after laser irradiation and the effects of laser energy, mannitol concentration, and enzyme reaction time to the photoinjection efficiency would be briefly mentioned.

3.2 Effect of mannitol addition and enzyme treatment on cell structures

Before the fs laser irradiation, the morphological changes in the TBY-2 cell intracellular structures (Fig. 15 (a)) after the mannitol addition and enzyme treatments were examined. After mannitol addition to the culture medium, the vacuoles shrank triggering cell membrane separation from the cell wall (Fig. 15 (b)), which meant that the cell was plasmolyzed in the hypertonic mannitol solution while the turgor pressure decreased. The enzyme treatment, adjunctively with the mannitol addition, was applied to enhance the cell wall permeability for macromolecules. Usually, cell wall is removed about one hour after enzyme treatment in the protoplast preparation procedure. Meanwhile, no noticeable change on the cell morphology was observed 10 min after the adjunctive enzyme treatment (Fig. 15 (c)). The cell wall cellulose fiber network would not be removed in this moderate process. Instead, it was only partially degraded. The fs laser photoinjection was conducted under these three cell conditions: untreated, mannitol treated (plasmolyzed) and adjunctive enzyme treated (enzyme and mannitol treated).

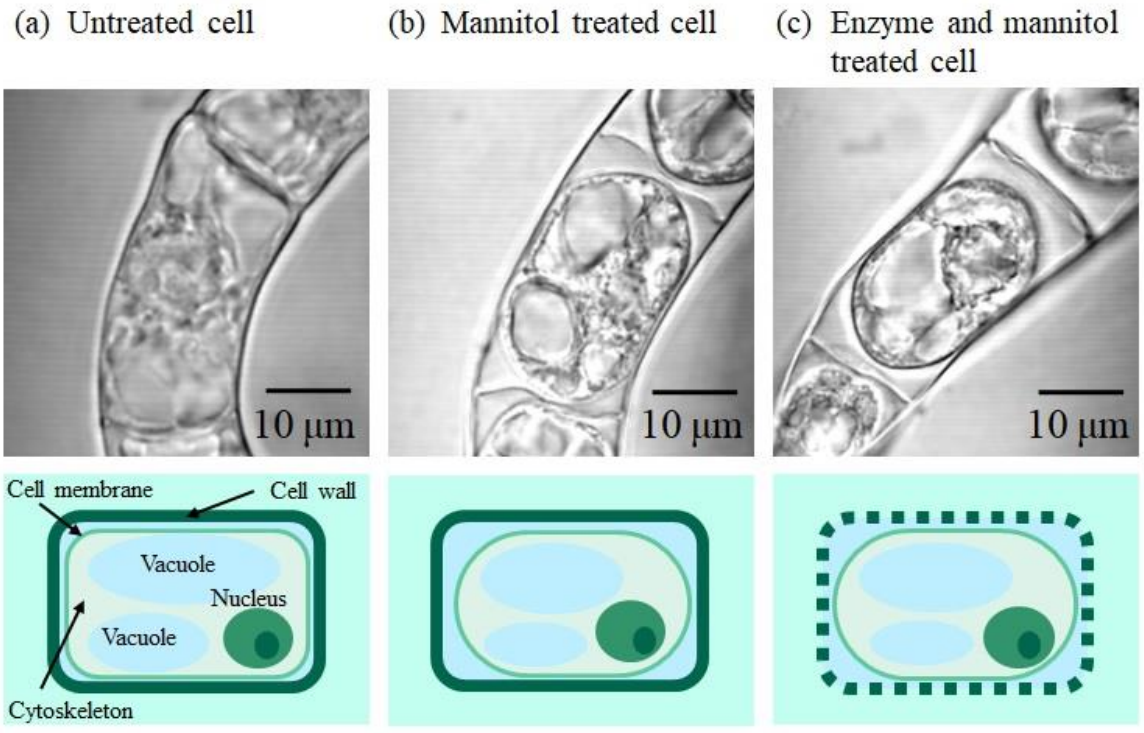

Figure 15. Transmission images and their schematic structures of TBY-2 cells; (a) untreated,

(b) mannitol treated (plasmolyzed) and (c) adjunctive enzyme treated (enzyme and mannitol treated). In an untreated TBY-2 cell, organelles such as a nucleus, plastids, vacuoles and cytoskeletons are inside the cell membrane. The cell membrane is covered with a cell wall consisting of polysaccharides such as cellulose and pectin. A turgor pressure, which is an inner pressure of the vacuoles observed at corners, presses the cell wall from inside to keep the cell structure and stiffness.

3.3 Molecular introduction in the hypertonic solution and with enzyme assistance

After examining the cell morphology, the photoinjection efficiencies of FITC-20k and of FITC-2M into untreated TBY-2 cells and into plasmolyzed TBY-2 cells in the hypertonic solution of 0.5 M mannitol in the culture medium were examined. Fluorescence images of the target cell cross section were acquired with a confocal fluorescence microscope before and 2 min after fs laser irradiation. Figures 16 (a, b) represent the fluorescence images of untreated TBY-2 cells before fs laser irradiation under the presence of FITC-20k and FITC-2M in the culture medium. Fluorescence was not seen inside the cell ensuring that both molecules did not spontaneously diffuse into the cell cytoplasm. Cell plasmolysis was clearly observed after the mannitol treatment for FITC-20k and FITC-2M from their transmission images in Fig. 16. The fluorescence signal was seen within apoplast, which is a region between the cell wall and membrane, only for FITC-20k, but not FITC-2M, as depicted in Figs. 16 (e, f). This result suggests that FITC-20k molecules are capable to cross the cell wall, but not the cell membrane, confirming the previous report that molecules less than 30 kDa with hydrodynamic diameter of about 4 nm can pass through the cell wall.[25] In contrast, FITC-2M molecules are too large and blocked by the cell wall.

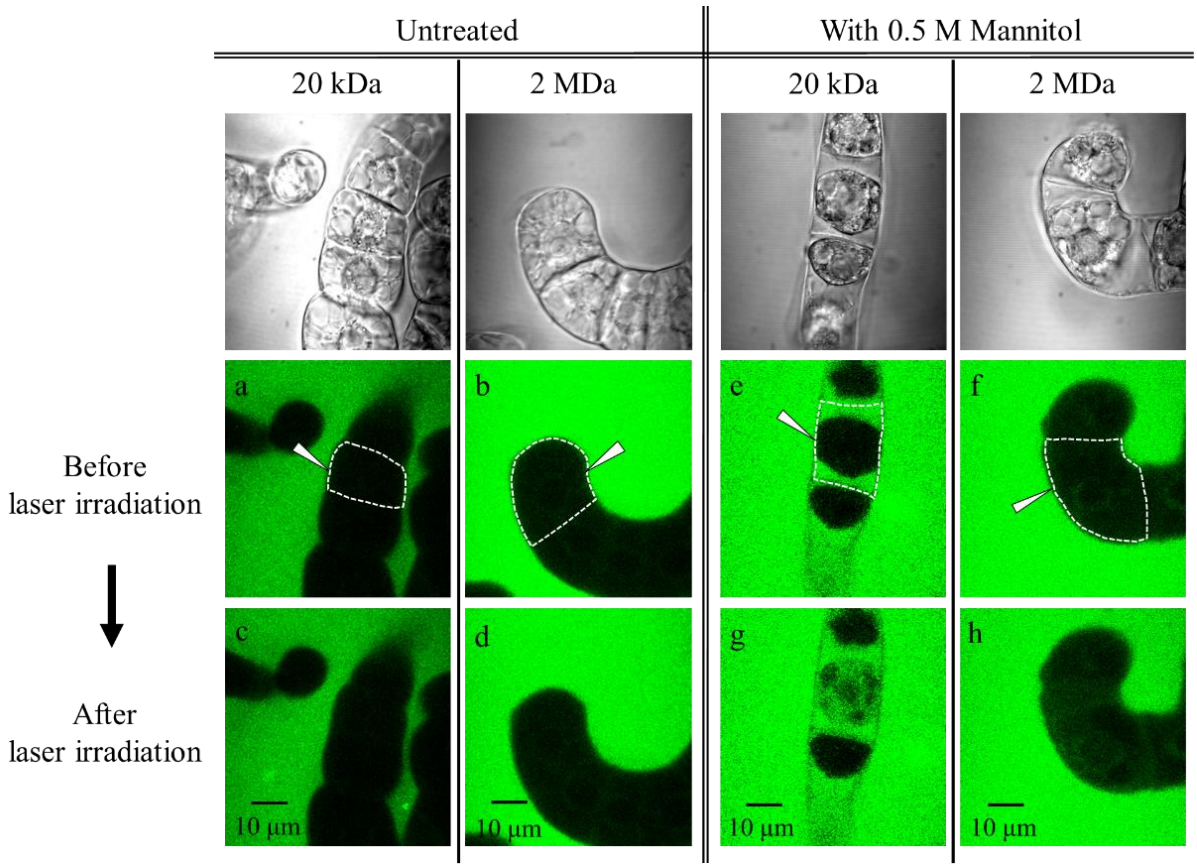

Figure 16. Confocal fluorescence images of (a-d) untreated and (e-h) mannitol added plasmolyzed TBY-2 cells before and after fs laser irradiation under the presence of FITC-20k and FITC-2M. Corresponding transmission images before laser irradiation were shown on the top row to identify each cell. The target single cells are surrounded by a dashed line, and the focal point is indicated with a white arrow. These images express the representative fluorescence intensity change that (a-d) no difference, (e, g) large increase and (f, h) slight increase in their appearance. The excitation and emission maxima of FITC are 490 and 520 nm, respectively. All fluorescence images were acquired with the excitation laser at 488 nm and same PMT gains.

After that, a single fs laser pulse was focused at a contact point of the cell membrane and cell wall in the presence of FITC-dextran molecules. Figures 16 (c, d, g, h) depict the typical fluorescence images of untreated and plasmolyzed cells 2 min after the laser irradiation. In the case of untreated cells, there was almost no change in the fluorescence images before and after laser irradiation. On the other hand, for the plasmolyzed cells, the increase of fluorescence intensity was noticed inside cytoplasm for both FITC-20k and FITC-2M. In addition, there was no increase of auto-fluorescence under the same photoporation condition without FITC molecules in the culture medium. Thus, it was concluded that the injection of FITC molecules

into cytoplasm succeeded.

Photoinjection was also performed by focusing the fs laser pulse specifically on the cell membrane, without irradiating the cell wall, for the plasmolyzed cells to verify the effect of fs laser irradiation on the cell membrane and cell wall. Fluorescence increases within the cytoplasm were seen only for FITC-20k (Fig. 17). This suggests that because of the presence of FITC-20k molecules within apoplast under the mannitol treatment, a pore formation on the cell membrane alone is necessary for a successful injection. In contrast, since FITC-2M cannot cross the cell wall, perforation on both the cell membrane and the cell wall is needed for the introduction of FITC-2M into the cell cytoplasm.

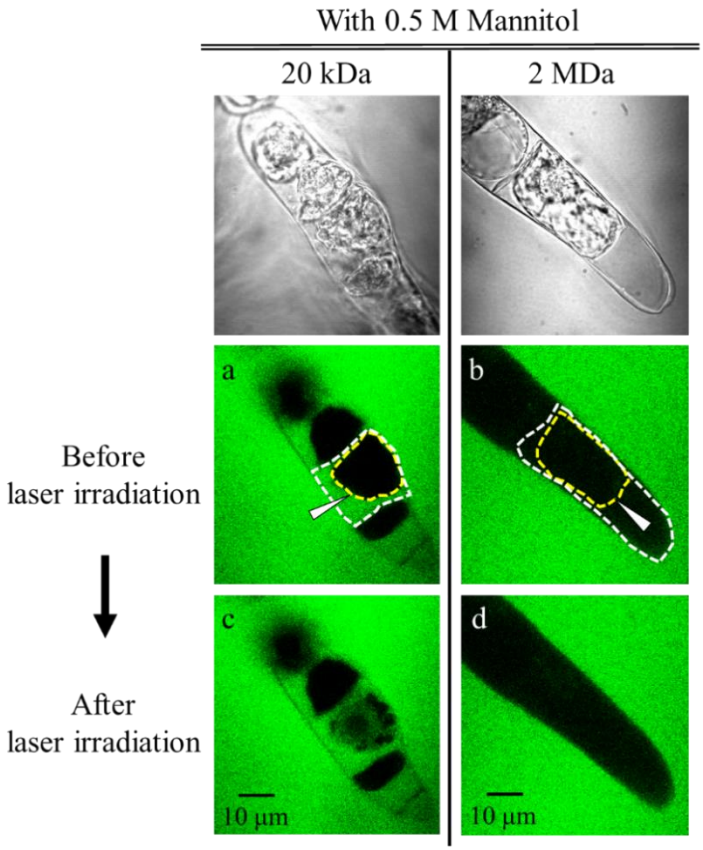

Figure 17. Confocal fluorescence images of mannitol added plasmolyzed TBY-2 cells before and after fs laser irradiation under presence of (a, c) FITC-20k and (b, d) FITC-2M. Corresponding transmission images before laser irradiation were shown on the top row to clarify each cell. The target single cells are surrounded by a white broken line and their cell membranes are surrounded by a yellow dashed line. The fs laser pulse was focused on the cell membrane indicated with the white arrow.

It was previously stated that the pore formation on the cell membrane at the presence of FITC-molecules inside apoplast was crucial for their injection into the cytoplasm. Nevertheless, for FITC-2M molecules, the increase of cell wall permeability by the fs laser perforation was not very efficient. Enzyme treatment using cellulase and pectolyase was performed for cell wall partial degradation to increase the cell wall permeability for large molecules with the minimum damage.

Fluorescence images of adjunctive enzyme treated TBY-2 cells before the photoporation under the presence of FITC molecules are represented in Figs. 18 (a, b). In contrast to the results depicted in Figs. 16 (b) and 16 (f), fluorescence was observed within apoplast even for FITC-2M. The permeability of the cell membrane seemed to be unchanged in this condition since it was always dark within cytoplasm.

The fluorescence images of the adjunctive enzyme treated TBY-2 cells 2 min after the laser irradiation are presented in Figs. 18 (c, d). The increase of fluorescence intensity was clearly seen within cytoplasm for both FITC-20k and FITC-2M. The fluorescence increase was notably enhanced compared with that of only mannitol addition, which would be described in detail later. Cytoplasmic streaming was observed, therefore the cell viability was not compromised.

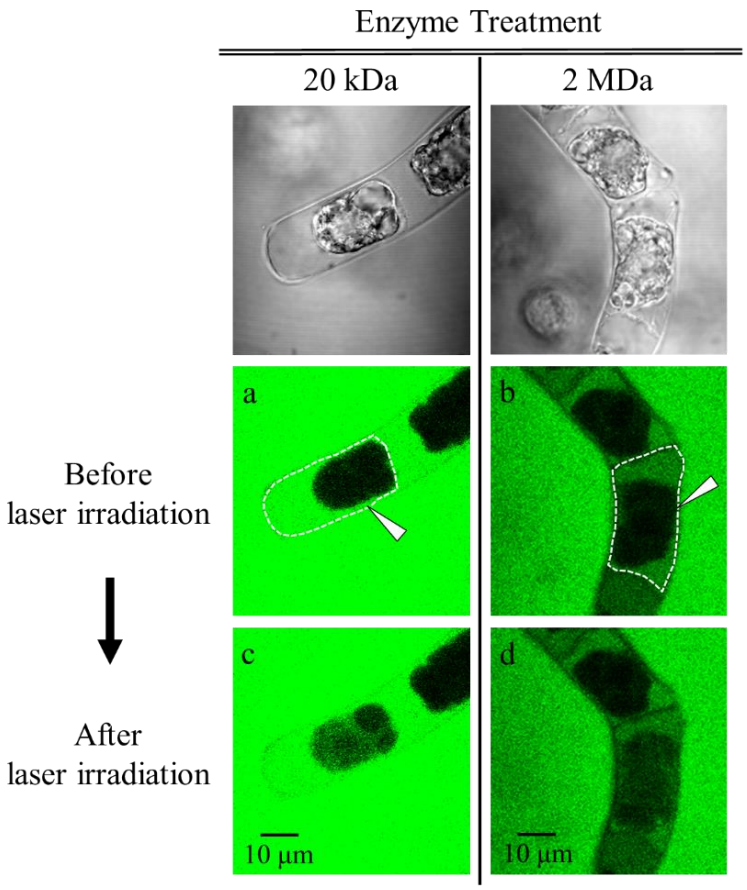

Figure 18. Confocal fluorescence images of adjunctive enzyme treated TBY-2 cells before and after fs laser irradiation under presence of FITC-20k and FITC-2M. Corresponding transmission images before laser irradiation were shown on the top row to clarify each cell. The target single cells are surrounded by a dashed line, and the focal point is indicated with a white arrow. The fluorescence images were acquired with the same conditions as those in Fig. 16.

3.4 Introduction efficiencies under three conditions

The introduction levels of FITC molecules, for the untreated, mannitol treated and adjunctive enzyme treated cells, were quantitatively analyzed by measuring differential fluorescence intensities in cytoplasm, between before and after the photoporation (ΔI). A small background fluorescence signal within the cytoplasm, that come from cell auto fluorescence and/or scattered fluorescence by cells, was detected even before laser irradiations. The changes of background fluorescence intensity during 2 min without laser irradiation are shown as a histogram in Fig. 19 (a). The fluctuations of background fluorescence for 40 cells over time varied from -3.45 to 1.30 with an average of -0.94. The negative values were caused by

fluorescence bleaching during the laser scanning. Regarding the estimation of background temporal fluctuations, ΔI was defined as molecular introduction level and the ΔI value of 2 was called the molecular introduction threshold. The ΔI values for 20 cells in each condition are presented as histograms in Figs. 19 (b, c). The observations in Figs. 16 and 18 are well represented in the histograms below.

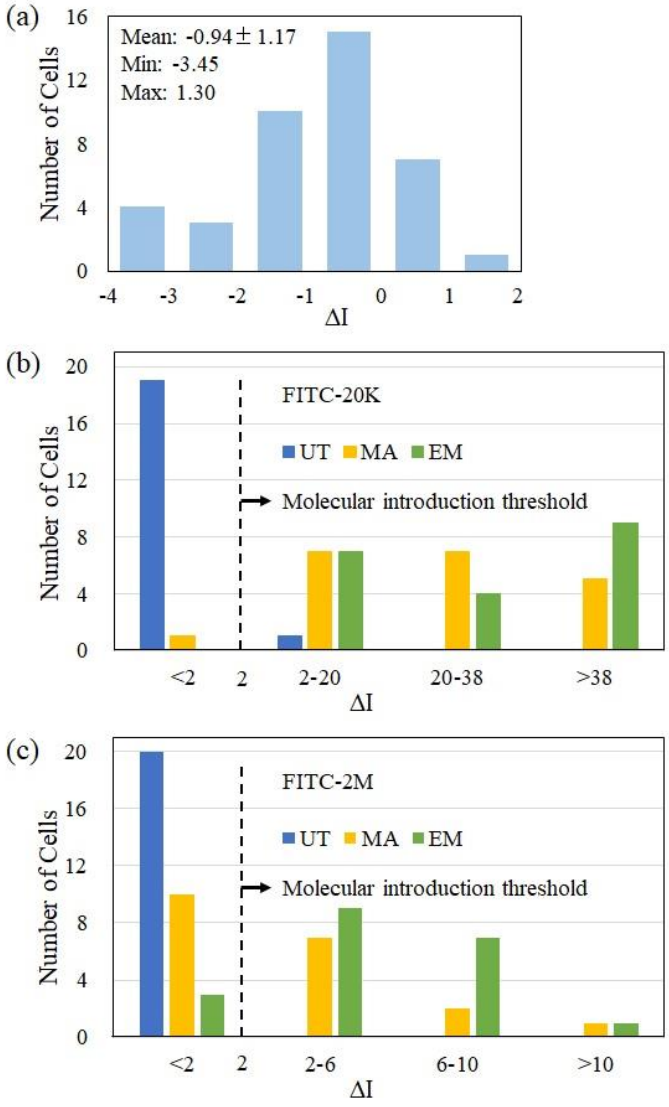

Figure 19. (a) The histograms of intensity fluctuations of the background signal inside the cytoplasm during 2 min without laser irradiation (N = 40). The histograms of differential fluorescence intensities (ΔI) between before and after laser irradiations of untreated (UT, blue), mannitol treated (MA, yellow) and adjunctive enzyme treatment (EM, green) cells: (b) for FITC-20k (N = 20) and (c) for FITC-2M (N = 20).

The average ΔI values increased in the order of untreated, mannitol treated and adjunctive enzyme treated cells. Most ΔI values were less than 2, the molecular introduction threshold, in untreated cells for both FITC-20k and FITC-2M, suggesting FITC molecules were not injected into the cells by the photoporation. In contrast, after the mannitol addition, the ΔI distribution of both FITC-20k and FITC-2M shifted to a higher level than the background fluctuations in the plasmolyzed cells. This result indicated that in the hypertonic condition, both FITC molecules were successfully introduced into the cytosol by the photoporation. However, as half the ΔI values were still close to the background level, the introduction efficiency for FITC-2M was not very high. In the adjunctive enzyme treated cells, the ΔI distribution of both FITC-20k and FITC-2M shifted further to a higher level than the plasmolyzed cells. The increase of ΔI was typically larger for FITC-2M than that for FITC-20k.

The temporal changes of ΔI after the photoporation was also measured. The ΔI reached to the maximum in about 30 s for FITC-20k, indicating its rapid diffusion in cytoplasm. From the time to reach maximum ΔI for FITC-2M, whose diffusion would be much slower than FITC-20k, it was estimated that the formed pore was resealed roughly in 100 to 150 s (Fig. 20).

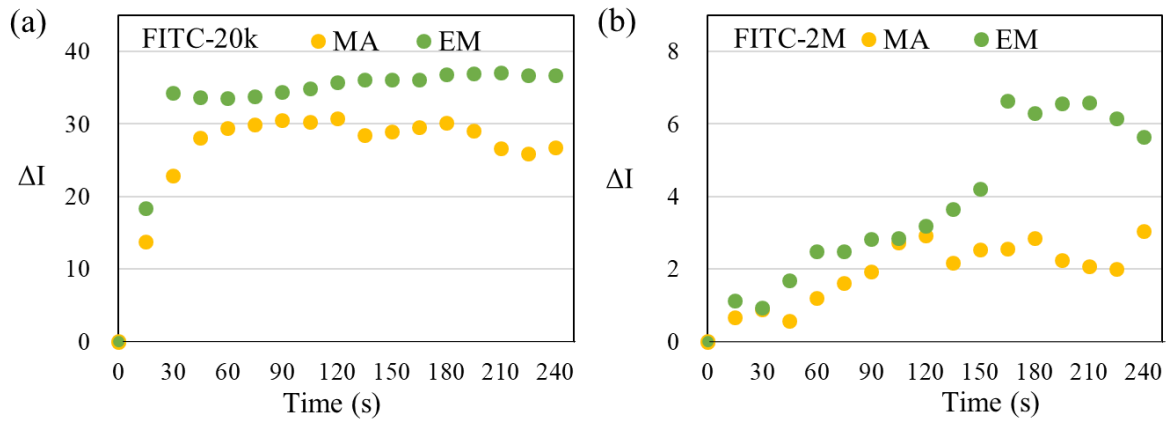

Figure 20. Representative of fluorescence intensity change in cytoplasm over time for mannitol treated (MA, yellow) and adjunctive enzyme treated (enzyme and mannitol treated) (EM, green) cells: (a) for FITC-20k and (b) for FITC-2M.

As a side note, a leakage of cell contents, as a sign of cell damage by the laser irradiation, was observed for 25% of the untreated cells in transmission images (Fig. 21). However, such outflow was not seen for any plasmolyzed cells. It seemed that the decrease of turgor pressure reduced the cell damage by preventing cytosol leakage. Indeed, cytoplasmic streaming was observed in the plasmolyzed cells even after the photoporation. These results indicated that the cell was still viable after the photoporation. The cytoplasmic streaming was also still observed in adjunctive enzyme treated cells after the photoporation. Thus, it was considered that the enzyme treatment was not augmenting damage of the photoinjection process. The number of damaged cells with laser treatment in each condition was summarized in Fig. 22.

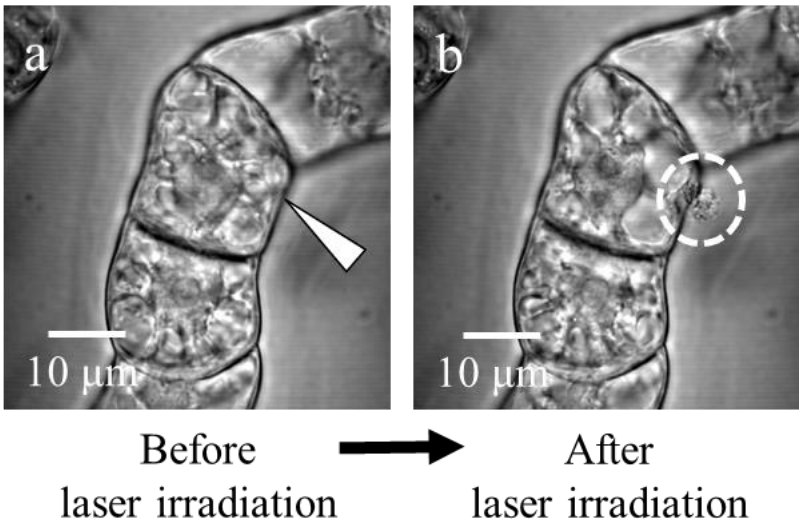

Figure 21. Transmission images of TBY-2 cells (a) before and (b) after the laser irradiation. Leakage from the cell was observed in a damaged cell as seen inside the broken line circle in (b).

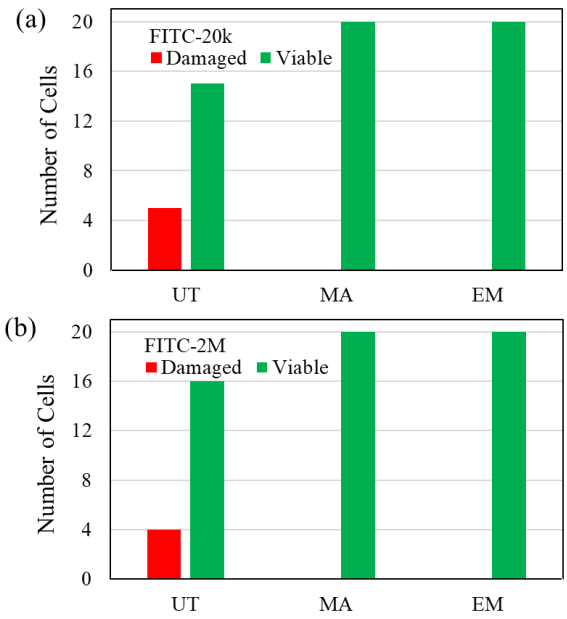

Figure 22. The number of damaged (red) and viable (green) cells after laser irradiation in untreated (UT), mannitol treatment (MA) and adjunctive enzyme treatment (EM) with laser energy of 20 nJ/pulse: (a) FITC-20k and (b) FITC-2M.

In this experiment, the photoinjection efficiencies with 10, 20 and 30 nJ pulse energies (Fig. 23) were also examined. The introduction efficiency was very low with 10 nJ/pulse. Meanwhile, the introduction efficiencies of 20 and 30 nJ/pulse were similar under the enzyme treated condition, but cells started to be damaged with 30 nJ/pulse. The photoinjection efficiencies with lower concentration of mannitol (Fig. 24) were also checked. The injection efficiency was lower in the enzyme treated cells without mannitol or with 0.1 M mannitol, compared to that with 0.5 M mannitol. In addition, the photoinjection efficiencies with longer time of enzyme treatment (Fig. 25) were analyzed. The photoinjection efficiencies were similar in the cells with partially degraded cell walls. Instead, some of the observed cells already became protoplasts with 20 min and 30 min enzyme treatment. Therefore, the pulse energy of 20 nJ, the mannitol concentration of 0.5 M, and the enzyme reaction of 10 min were selected for the experiment.

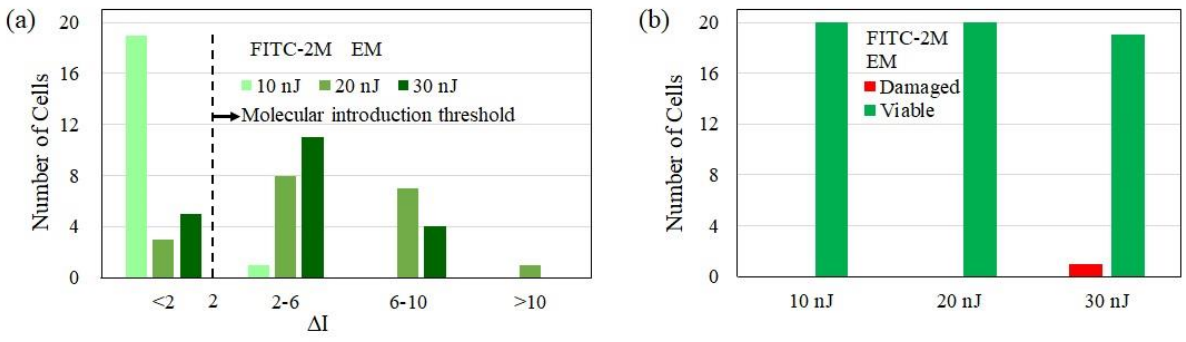

Figure 23. (a) The histograms of differential fluorescence intensities (ΔI) between before and after laser irradiations and (b) the number of damaged (red) and viable (green) cells after laser irradiation of adjunctive enzyme treatment (EM) cells for FITC-2M (N = 20) with laser energy of 10, 20 and 30 nJ/pulse.

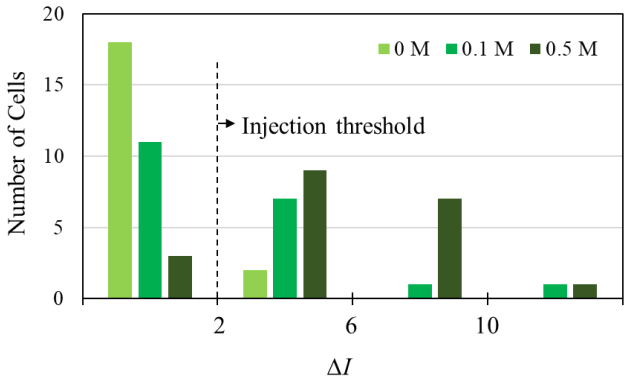

Figure 24. The histograms of differential fluorescence intensities (ΔI) between before and after laser irradiations for adjunctive enzyme treated cells (N = 20) with various concentration of mannitol (0, 0.1, and 0.5 M) under the presence of FITC-2M.

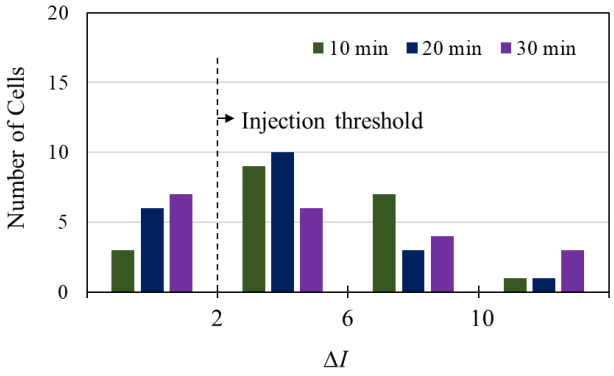

Figure 25. The histograms of differential fluorescence intensities (ΔI) between before and after laser irradiations for adjunctive enzyme treated cells (N = 20) with various reaction time (10, 20, and 30 min) under the presence of FITC-2M.

3.5 Discussion

The introduction of FITC-20k and -2M into TBY-2 cells was achieved by fs laser photoinjection in the hypertonic condition by mannitol addition (Fig. 16 and Fig. 19). The introduction efficiency was enhanced by the enzyme treatment, especially for FITC-2M (Fig. 18 and Fig. 19). The osmolarity effects are similar with previous reports on fs laser photoinjection into plant cells, which showed the injection of dye-conjugated dextran molecules was attained only in a hypertonic solution. Nevertheless, the introduced molecules' sizes were limited to only a few tens of kDa in these studies, in contrast to 2 MDa in this work.

The different type of fs laser system used for perforation in this experiment could be a factor for the successful introduction of the larger molecules. A single pulse from fs laser amplifier with higher energy was used here, compared to the previous reports which used multiple laser pulses with low energy and high repetition rate from fs laser oscillator. This would be explained later in the chapter discussing the mechanism of photoinjection.

After the adjunctive enzyme treatment, the ΔI values for both FITC-20k and -2M were increased further. From the transmission (Fig. 15) and fluorescence images (Fig. 18), the cell wall network is partially degraded without forming a protoplast. This contributes to the enhancement of the molecule diffusion rate through the cell wall. As FITC-20k can already diffuse into apoplast, the effect of the adjunctive enzyme treatment is more prominent for FITC-2M. The high concentration of FITC-2M molecules in apoplast after the enzyme treatment allows their efficient introduction into the cytoplasm.

In addition, the moderate enzyme treatment also softens the cell wall causing an increase in the level of deformation by the mechanical stress. The larger deformation of TBY-2 cells under adjunctive enzyme treatment might have a role to the increased photoinjection efficiency by the amplified fs laser pulse. Therefore, this treatment is useful to be applied in the future works for the photoinjection of macromolecules into single intact plant cells.

3.6 Conclusion

This study is the first report of the photoinjection of macromolecules with molecular weight of megadalton into an intact single plant cell cytoplasm by employing a femtosecond laser amplifier with moderate enzyme treatment. The results suggest that the photoinjection using the amplified fs laser pulse is promising and applicable for efficient injection of macromolecules, such as DNA plasmid, to intact plant cells. The specific targeting ability is the most significant benefit of the fs laser photoinjection.[50] The development of a transfection method into an intact single plant cells is expected to add new insights into plant systems being used in genetic manipulations.

Chapter 4

Photoinjection of Fluorescent Nanoparticles

4.1 Introduction

The nanoparticle introduction into intact plant cells is an encouraging method applied in the fields of agriculture and plant physiological study. Utilizing their unique properties such as accumulation tendency in a specific region and controlled release of contained substances, they become transporters for various functional materials ranging from small agrochemicals (herbicides, pesticides, fertilizers, etc.) to large DNA and proteins.[9-11]

The nanoparticles internalization into intact plant cells is usually administered either by diffusion via the plant cell wall or by active uptake managed by cellular processes.[12-14] The nanoparticles then reach to other parts of the plant through plant transportation system. Nevertheless, such passive method applicability is highly material dependent. Particle bombardment, as a physical approach, also permits the delivery of gold or tungsten nanoparticles coated with genetic substances (DNA, RNA, etc.) through cell walls.[14, 19] However, it has a low introduction efficiency and a risk of damaging target samples or transported substances. Thus, our thought is led to a laser-assisted introduction method called photoinjection.

In the previous chapter, an fs laser amplifier generating single pulse irradiation was used to inject 2 MDa macromolecules into a target tobacco BY-2 (TBY-2) cell. Moreover, additional enzyme treatment, which increased the cell wall permeability, enhanced the photoinjection efficiency. In this chapter, the fs laser amplifier would be applied for the photoinjection of nanoparticles into single TBY-2 cells. The nanoparticle photoinjection efficiency was examined in regard of cellular conditions and laser irradiation parameters.

4.2 Nanoparticles injection in the hypertonic solution and with enzyme assistance

First, the G-FNP photoinjection into untreated and mannitol treated TBY-2 cells was evaluated. Fluorescence images of the target cell cross section were captured before and 2 min after fs laser photoporation using confocal fluorescence microscopy. Fig. 26 (a) represents a fluorescence image of untreated TBY-2 cells before laser irradiation. There is no intracellular fluorescence observed suggesting that the G-FNPs did not diffuse into the cytoplasm instantaneously. From the transmission image in Fig. 26, cell plasmolysis can be seen after the mannitol treatment, while the fluorescence signal is not observed inside the apoplast, which is an area between the cell wall and membrane, as shown in Fig. 26 (c). This observation reveals that G-FNPs are too large to cross the cell wall.

The contact point of the cell wall and membrane was irradiated by a single 20 nJ fs laser pulse under the presence of the G-FNPs in the medium. This location was selected as the laser focusing position for simultaneous perforation on both the cell wall and membrane. Photoporations with different laser focal point positions are mentioned later. Fig. 26 (b, d) represents fluorescence images of untreated and mannitol treated cells 2 min after irradiation. For untreated cells, the fluorescence images before and after fs laser irradiation were almost similar. For mannitol treated cells, the change of fluorescence intensity inside the cytoplasm was also negligible. Therefore, the injection of G-FNPs into the cytoplasm of untreated and mannitol treated cells was not efficient. The single 20 nJ laser pulse could not generate a pore in the cell wall and membrane that was large enough for the G-FNP introduction into cytoplasm.

Next, the cell wall was partially degraded with cellulase and pectolyase to increase the permeability of cell wall for large particles with minimal damage. Fig. 26 (e) shows a representative fluorescence image of adjunctive enzyme treated TBY-2 cells before irradiation in the culture medium containing the G-FNPs. Different from the image depicted in Fig. 26 (c), fluorescence was clearly observed within apoplast. Nevertheless, it was always darker in the

cytoplasm, suggesting that the permeability of cell membrane was not compromised by the enzyme treatment.

The fluorescence image of enzyme treated TBY-2 cells 2 min after laser irradiation is shown in Fig. 26 (f). The increase of fluorescence intensity was clearly seen inside the cytoplasm. Meanwhile, increase of auto-fluorescence was not observed using the same photoinjection parameter without G-FNPs in the culture medium. Thus, it was concluded that the injection of G-FNPs into the cytoplasm was achieved.

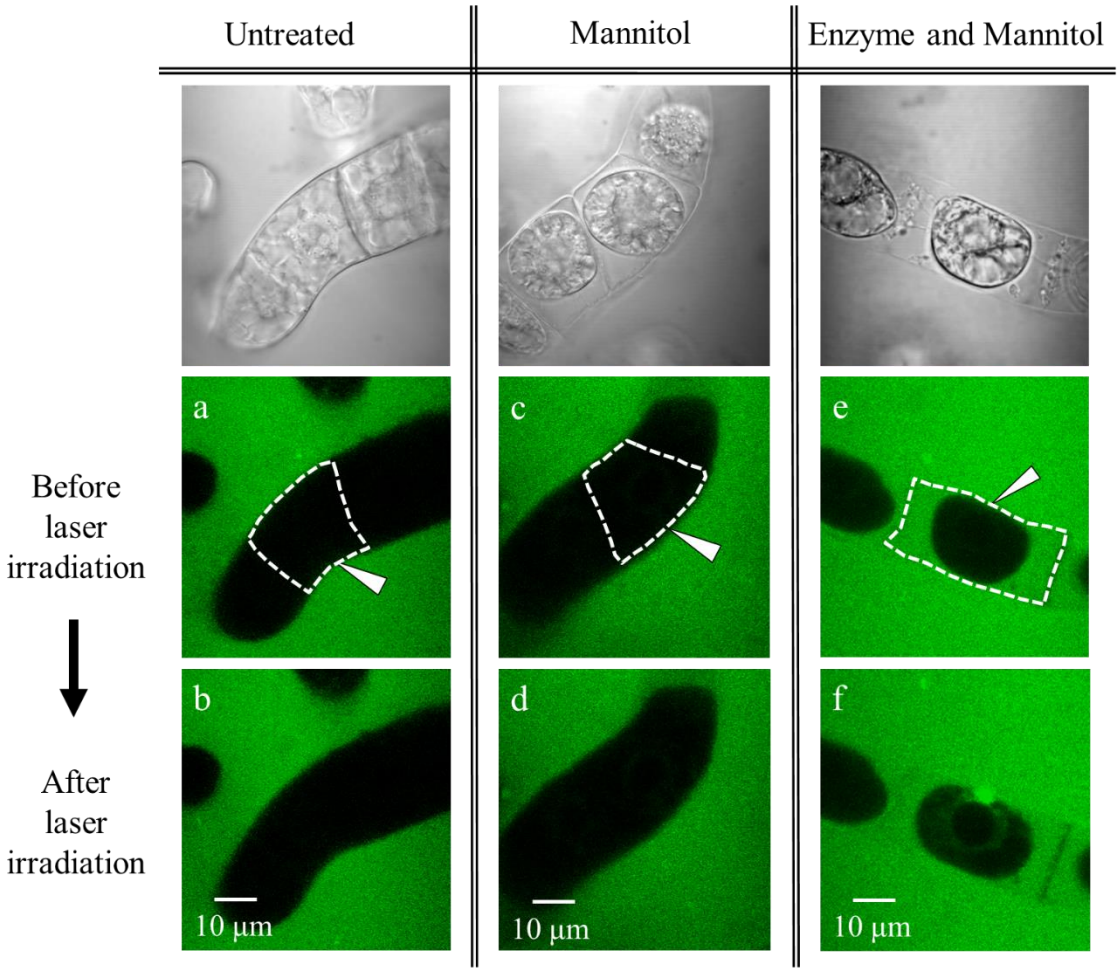

Figure 26. Confocal fluorescence images of (a, b) untreated, (c, d) mannitol treated and (e, f) enzyme and mannitol treated TBY-2 cells before and after fs laser irradiation under the presence of G-FNPs. The top row shows corresponding transmission images before laser irradiation. The dashed line indicates the outline of a target single cell and the white arrowheads indicate the laser focal point. These images represent the change of fluorescence intensity: (b, d) have no differences from (a, c), and (f) has a clear intensity increase compared to (e).

4.3 Injection efficiencies under three conditions

The levels of the G-FNP injection under untreated, mannitol treated and adjunctive enzyme treated conditions were evaluated using differential fluorescence intensities between before and after laser irradiation (ΔI). There was a background fluorescence signal within the cytoplasm even without laser irradiation. This was originated from cell's auto fluorescence and/or scattered fluorescence by cells. The histogram in Fig. 27 (a) shows the differential intensity of background fluorescence during 2 min without laser irradiation. The fluctuations of background fluorescence over time for 20 cells ranged from -2.25 to 1.25. The negative values were caused by fluorescence bleaching during the laser scanning. The level of particle injection is described as ΔI, and the ΔI value of 2 is determined as injection threshold. The ΔI values for 20 cells in the three conditions is summarized as histograms in Fig. 27 (b). The findings in Figs. 26 were suitably reflected in the histograms as mentioned below.

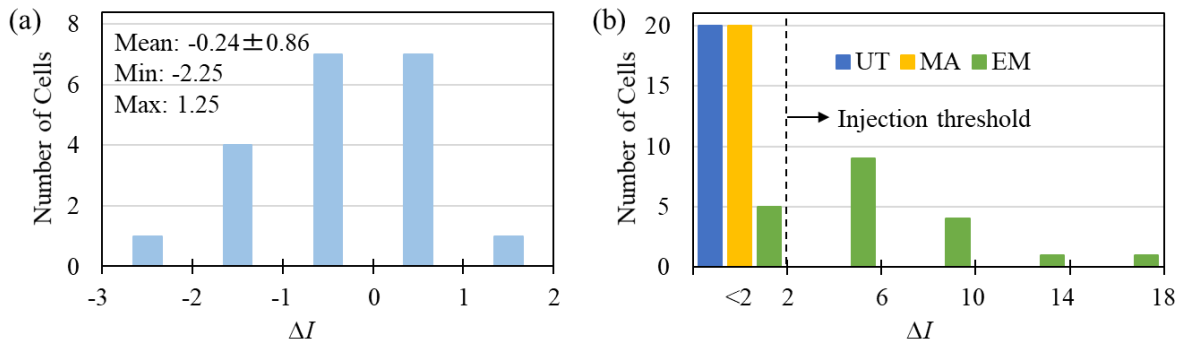

Figure 27. The histograms of (a) intensity changes of the background signal inside the cytoplasm in 2 min without laser irradiation, and (b) differential fluorescence intensities (ΔI) between before and after laser irradiations. Untreated (UT, blue), mannitol treated (MA, yellow) and adjunctive enzyme treated (EM, green) cells (N = 20).

The values of ΔI both for untreated and mannitol treated cells were all smaller than the injection threshold, indicating that the G-FNPs were not introduced into cytoplasm in these conditions. After adjunctive enzyme treatment, the distribution of ΔI values was shifted to a higher level than the injection threshold, confirming the successful injection of the G-FNPs into

cytoplasm. Even though cell content leakage was seen for 30% of untreated cells, such outflow was not found for any mannitol and adjunctive enzyme treated cells. Moreover, cytoplasmic streaming was observed, thus the cells could be considered as viable. It was assumed that the decrease of turgor pressure reduced the cell damage by preventing cytosol outflow.

It is noteworthy that the G-FNP injection into the cytoplasm could also be seen for the mannitol treated cells when over 30 nJ laser pulse was applied. Thus, the enzyme treatment is not crucial for this method. However, the injection was still less efficient compared to that with adjunctive enzyme treated cells. Instead, higher pulse energy caused the cells to be damaged (Fig. 28 (a, b)). Furthermore, the addition of enzyme treatment is not a big disadvantage as such enzyme treatment is commonly used in plant biotechnology. The efficiencies of photoinjection under the adjunctive enzyme treatment with 10, 15, 20, 25 and 30 nJ pulse energies were also examined (Fig. 28 (c, d)). The introduction efficiencies with 10 and 15 nJ were very low, and they become higher with increasing the pulse energy from 20 to 30 nJ/pulse. However, adjunctive enzyme treated cells started showing outflow of cytosol with 25 and 30 nJ/pulse.

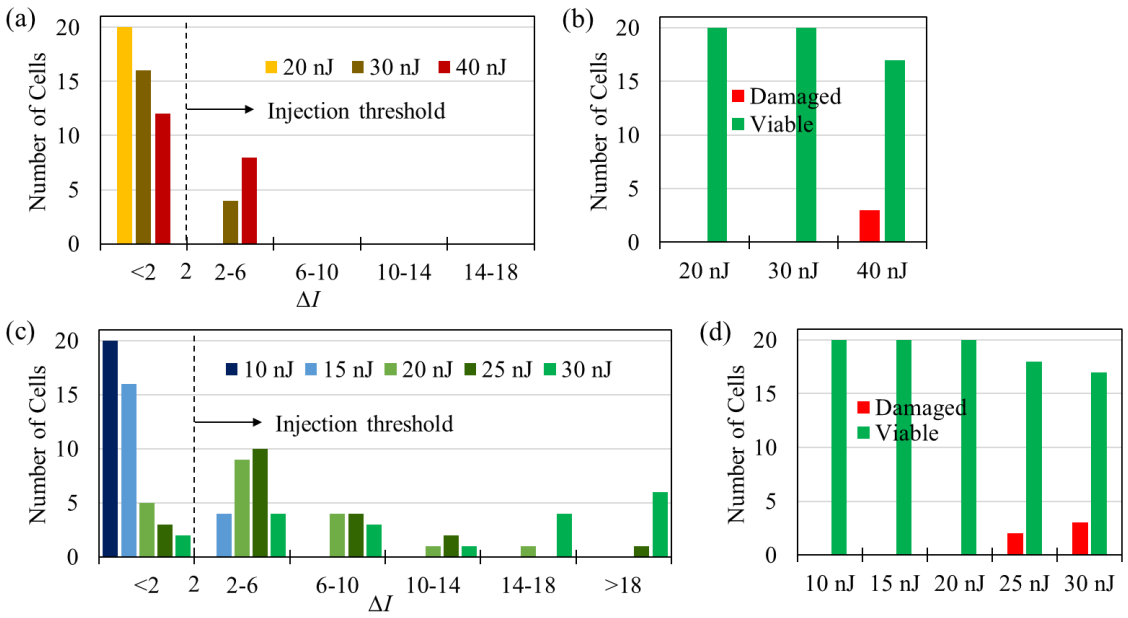

Figure 28. The laser pulse energy dependent injection efficiency of G-FNPs and damaged rate based on cytosol leakage. The histograms of differential fluorescence intensities (ΔI) between

before and after laser irradiations and the number of damaged cells after laser irradiation under (a, b) mannitol, and (c, d) adjunctive enzyme treatments. The used laser pulse energies were indicated in figures.

In addition, the photoinjection efficiency in 1 day old cultured cells was examined. The photoinjection efficiency was lower than that of 2 day old cultured cells, as shown in Fig. 29. In 1 day old cultured cells, probably some cells were still not dividing yet and might retain the morphology of 7 day old cultured cells, from previous week sub-culture, with thick cell wall. On the other hand, most of 2 day old cultured cells would have divided, so they were new cells with thinner cell wall. Therefore, the photoinjection efficiency in 2 day old cultured cells was higher than 1 day old cultured cells.

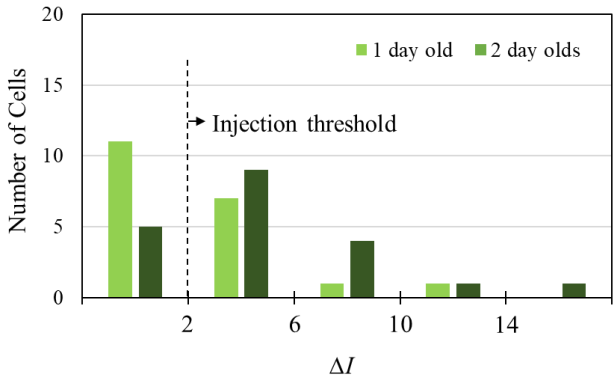

Figure 29. The histograms of differential fluorescence intensities (ΔI) between before and after laser irradiations for 1 day and 2 day old cultured adjunctive-enzyme-treated cells (N = 20) under the presence of G-FNPs.

The changes of ΔI over time for adjunctive enzyme treated cells that were exposed with 20 nJ fs laser pulse were also shown in Fig. 30. The ΔI started to increase about 15 s after laser irradiation, suggesting that G-FNPs are accumulated near the laser focal point, as seen in Fig. 26 (f). In average, the ΔI increased to the maximum value in about 240 s, indicating that the formed pore was closed again roughly in this period.

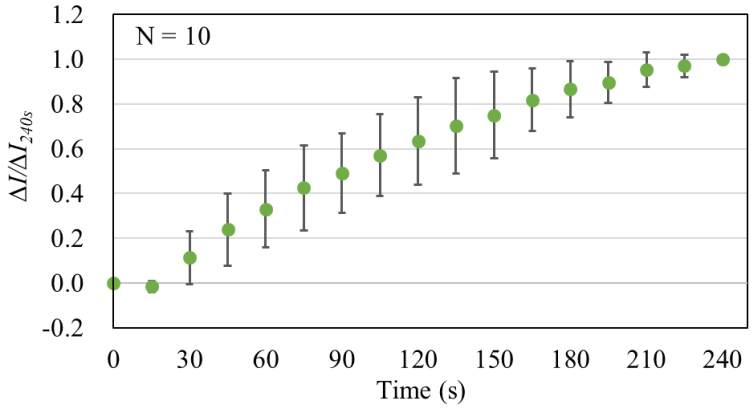

Figure 30. Temporal evolution of fluorescence intensity in the cytoplasm for enzyme treated cells. The graph is averaged for 10 cells and normalized by the ΔI at 240 s. The error bar indicates standard deviation.

The size of molecules was reported to affect the photoinjection efficiency into mannitol treated cell and protoplast.[25] Generally, smaller molecules have been injected more efficiently into cell cytoplasm. To get a better idea for macromolecules, the effect of macromolecule size to the photoinjection efficiency was also examined, as summarized in Fig. 31, combining all previous data in this experiment with a larger nanoparticles. The larger polymer nanoparticles were the red fluorescent nanoparticles (R-FNPs) with diameter of 110 ± 2 nm and concentration of 10.0 ± 0.36 x 10^8 particles/mL, and made of similar components with the G-FNPs, except using red bodipy molecules with the maximum wavelengths of excitation and emission of 559 and 605, respectively. A DPSS laser at 532 nm wavelength was applied for the excitation of the R-FNPs.

In the case of plasmolyzed cells without enzyme treatment (Fig. 31 (a)), macromolecules with diameter up to 26.7 nm (FITC-2M) could be injected by single 20 nJ pulse fs laser irradiation. However, the photoinjection efficiency is low, only about 50%. When 80 nm and 110 nanoparticles were used, there was no photoinjection confirmed. The maximum size of injected particles in this condition was estimated between 26.7 nm and 80 nm in diameter.

The photoinjection efficiencies were increased in the adjunctive enzyme treated cells (Fig. 31 (b)). The 80 nm nanoparticles now could be injected, but the injection of 110 nm

nanoparticles could not still be confirmed, as depicted in Figs. 32 and 33. It was suggested that nanoparticles with diameter of 110 nm was too large to pass through the pore on cell membrane and they diffused even slower than 80 nm nanoparticles. The maximum size of injected particles in this condition was estimated between 80 nm and 110 nm in diameter. When a higher laser energy was used, the injection of 110 nm nanoparticles were still not confirmed, instead, the cell would be damaged. Thus, the unsuccessful injection of larger nanoparticles may correlate with the cell limitation.

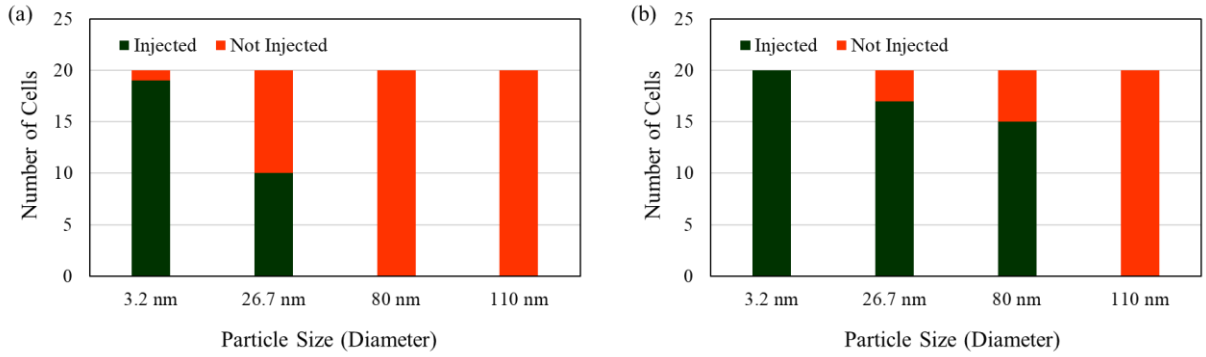

Figure 31. Photoinjection efficiencies into (a) plasmolyzed and (b) adjunctive enzyme treated tobacco BY-2 cells after irradiation with single 20 nJ pulse fs laser amplifier under presence of objects with different particle sizes: FITC-20k (d = 3.2 nm), FITC-2M (d = 26.7 nm), G-FNPs (d = 80 nm) and R-FNPs (d = 110 nm).

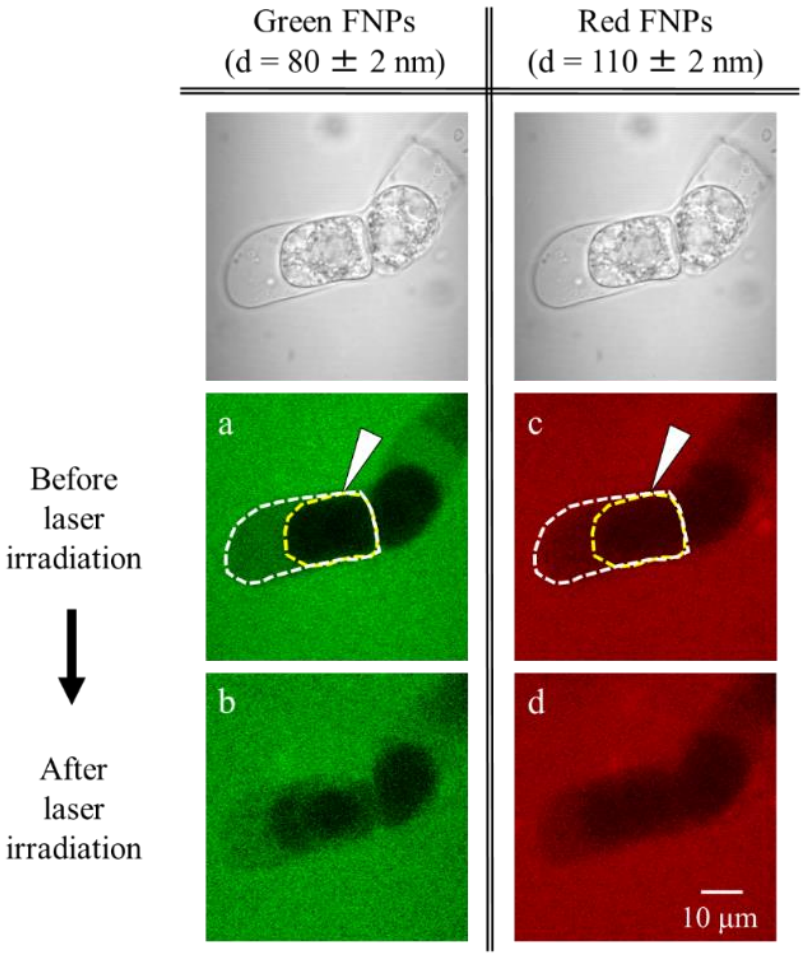

Figure 32. Confocal fluorescence images of enzyme and mannitol treated TBY-2 cells before and after fs laser irradiation under the presence of G-FNPs (a, b) and R-FNPs (c, d). The top row shows corresponding transmission images before laser irradiation. The dashed line indicates the outline of a target single cell and the white arrowheads indicate the laser focal point. These images represent the change of fluorescence intensity: (b) has a clear intensity increase compared to (a), while (d) have no noticeable differences from (c).

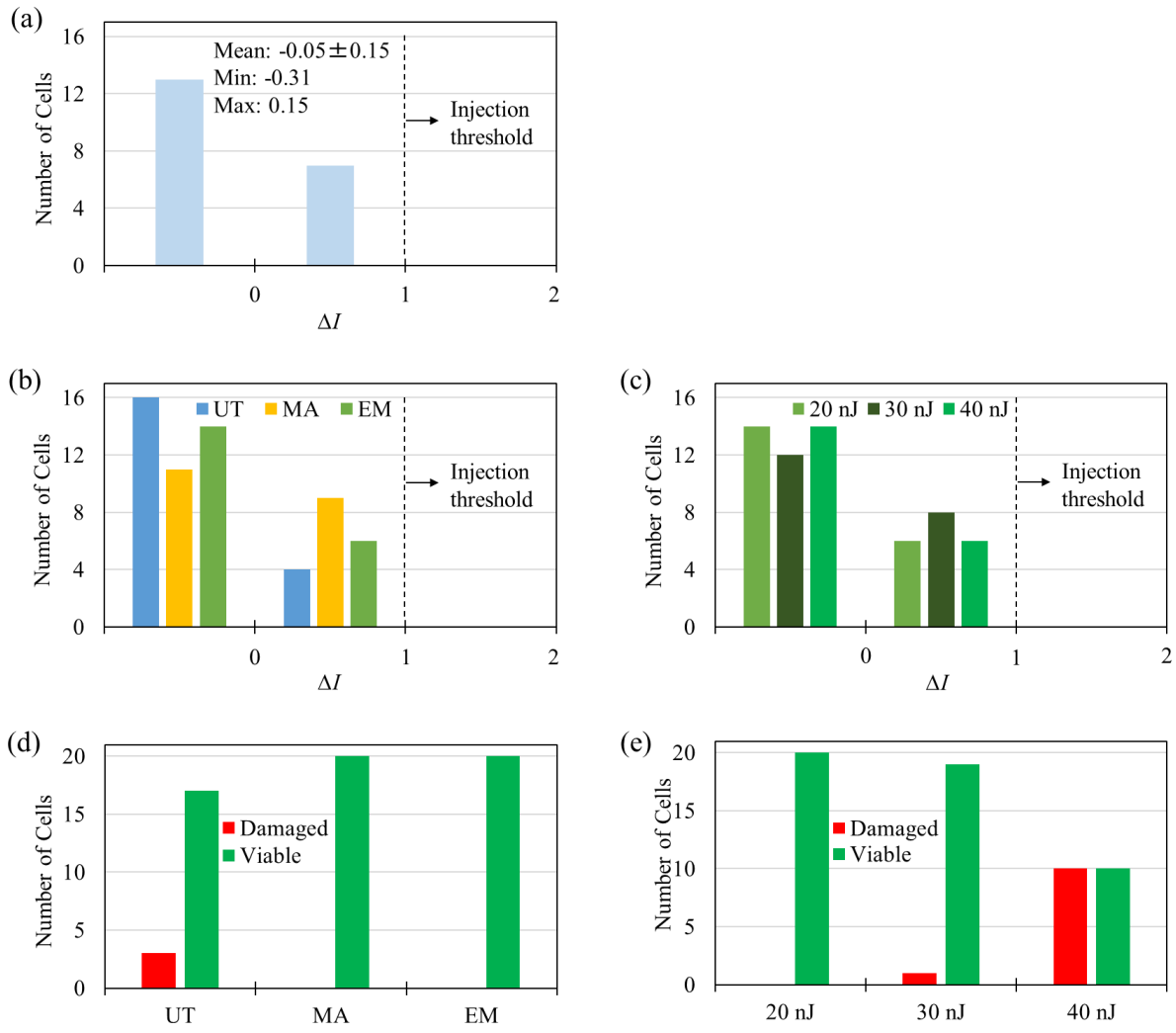

Figure 33. The histograms of (a) intensity changes of the background signal inside the cytoplasm in 2 min without laser irradiation, (b) differential fluorescence intensities (ΔI) between before and after laser irradiations: untreated (UT, blue), mannitol treated (MA, yellow) and adjunctive enzyme treated (EM, green) cells (N = 20) with single 20 nJ pulse, and (c) the laser pulse energy dependent injection efficiency of R-FNPs: the used laser pulse energies were indicated in figures. The damaged rate based on cytosol leakage (d, e).

As a side note, the correlations between the ΔI value and the size of cell cytoplasm, apoplast, and whole cell, were also examined. The results for the G-FNPs, and FITC-2M as a comparison, are presented in Fig. 34. There was no significant relationship between the cell sizes, either cell cytoplasm, apoplast, or whole cell, and the injection level of fluorescent molecules. Thus, although the cell size might affect the injection level, probably there are other factors that also contribute to the difference of injection level in individual cells, including the pore size, the

strength of cell wall and cell membrane, and the cytoplasmic streaming, among others. The effect of such factors could not be examined at present, but the important thing is the macromolecules were injected into individual cells, even though at different level of injection.

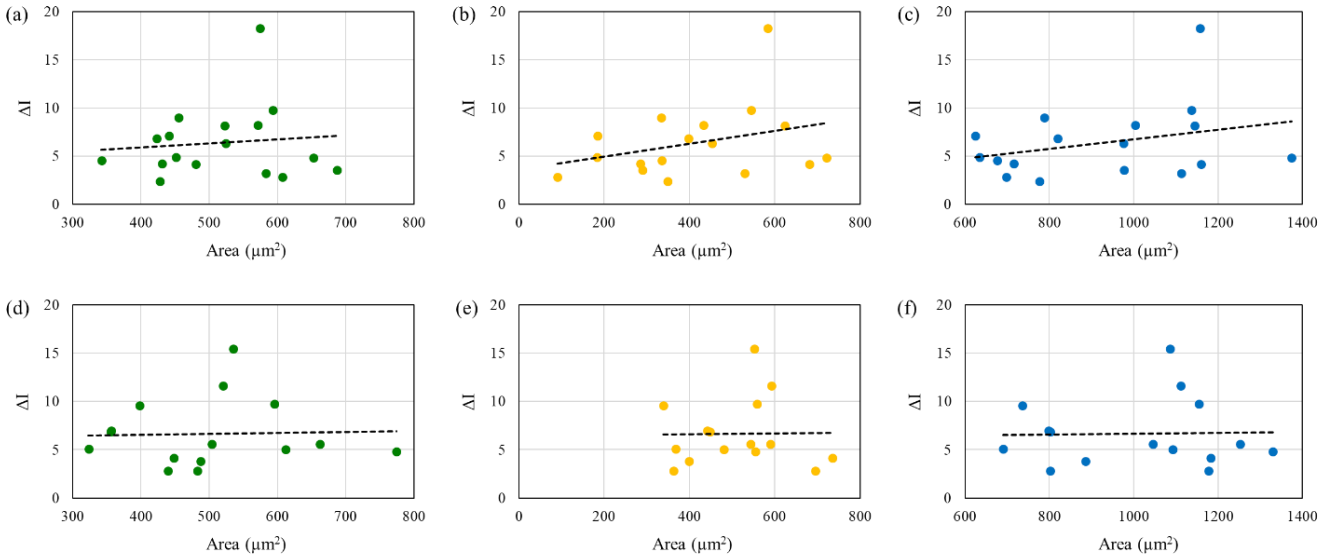

Figure 34. Differential fluorescence intensities in cell cytoplasm after single 20 nJ fs laser irradiation for adjunctive enzyme treated cells under presence of FITC-2M (a, b, c) and G-FNPs (d, e, f) were plotted against the size of cytoplasm area (a, d), apoplast area (b, e), and cell area (c, f).

The FDA assay was conducted to evaluate the cell viability after laser irradiation in a long term. Single 20 nJ laser pulse was focused on every TBY-2 cells in a cell culture dish. Then, the irradiated cells were incubated at 27 °C for 12 h in a dark room. After FDA addition to the cell culture medium, fluorescence signals from fluorescein were detected in 95.7% of enzyme treated cells as observed in Fig. 35 (a). The staining rate between laser irradiated and un-irradiated cells were similar, suggesting that after laser irradiation, the cells still had their physiological activity. Therefore, photoinjection of adjunctive enzyme treated cells with laser energy of 20 nJ was used as standard condition. Meanwhile, a few cells (20.69%) were stained by PI, in addition to FDA, so it was assumed that the cells were viable, but their cell membranes were still permeable for small molecules. It is recommended to verify how fast the cell

membrane recover in future experiment by conducting FDA and PI staining in a shorter time period.

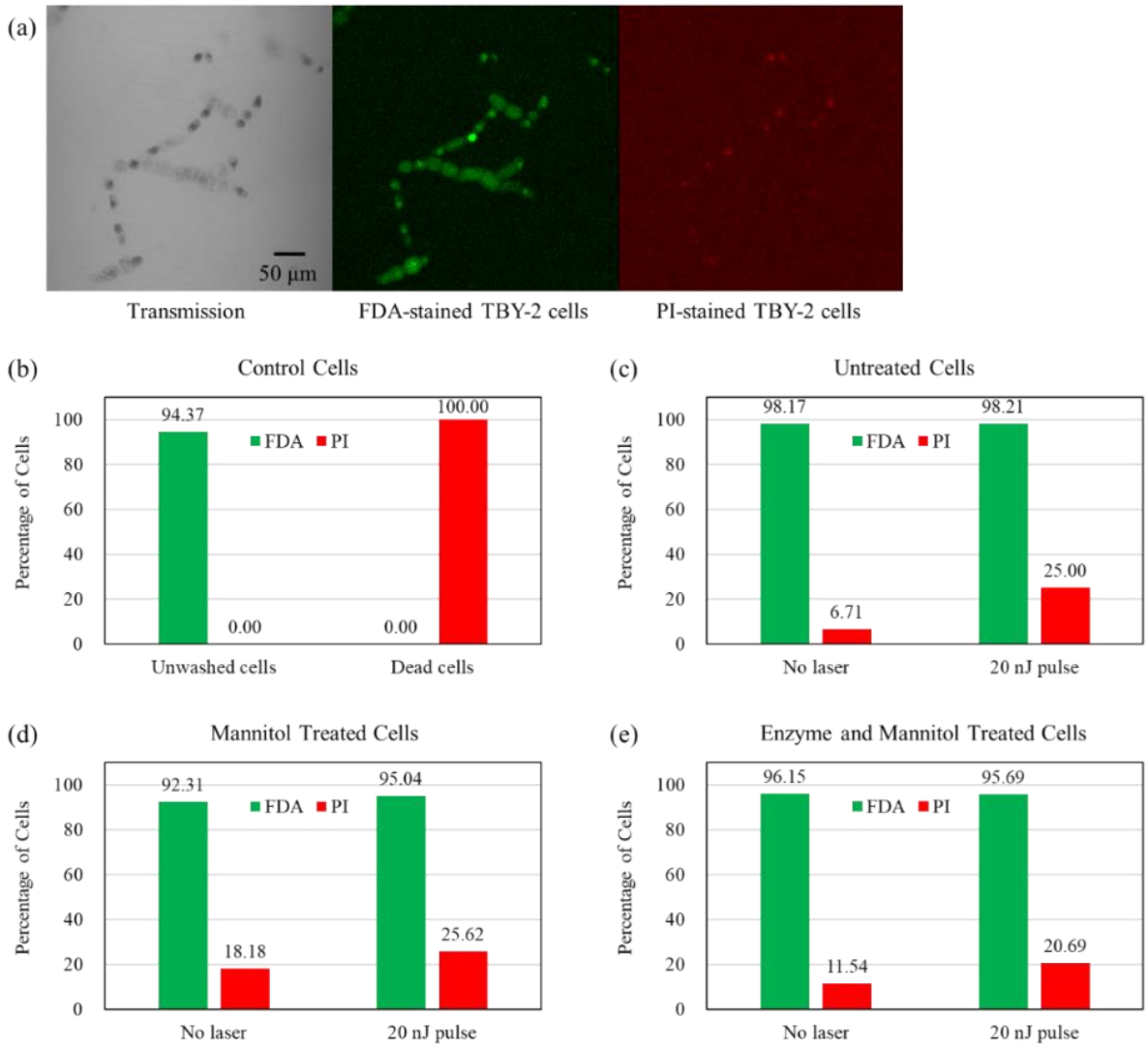

Figure 35. (a) Confocal fluorescence and transmission images of enzyme treated TBY-2 cells stained by FDA and PI 12 h after irradiation of a single 20 nJ laser pulse. The percentage of FDA (green) and PI (red) stained tobacco BY-2 cells; (b) Control cells: living cells without washing by centrifugation (N = 142) and dead cells with addition of ethanol 70% (N = 108); (c) Untreated cells: without laser irradiation (N = 164) and 12 hour after single 20 nJ pulse laser irradiation (N = 112); (d) Mannitol treated cells: without laser irradiation (N = 143) and 12 hour after single 20 nJ pulse laser irradiation (N = 121); and (e) Enzyme and mannitol treated cells: without laser irradiation (N = 104) and 12 hour after single 20 nJ pulse laser irradiation (N = 116).

4.4 Discussion

The G-FNP photoinjection into TBY-2 cells was accomplished by applying a single intense fs laser pulse of 20 nJ efficiently in the hypertonic condition with adjunctive enzyme treatment. The partial degradation of cellulose fiber network of the cell wall by the enzyme treatment enhanced the particle diffusion rate crossing the cell wall without producing a protoplast, as shown in the transmission and fluorescence images (Fig. 26). The high concentration of G-FNPs in the apoplast permits the efficient photoinjection of the nanoparticles into the cytoplasm. Nevertheless, the introduction of G-FNPs into the cytoplasm was not occurred by enzyme treatment alone, rather the perforation of the cell membrane by the fs laser photoporation was critical for the nanoparticle injection.

In addition, the photoinjection of G-FNPs into TBY-2 cells was also achieved in the hypertonic condition without adjunctive enzyme treatment, albeit with a higher laser energy (Fig. 28). The photoinjection efficiency of G-FNPs seems lower than expected when the 40 nJ fs laser pulse was used for perforation of the cell wall and membrane in the hypertonic condition without the enzyme treatment, although it can cause a cytoplasm leakage. It is regarded that the enzymatically softened cell wall would have a role to increase the mechanically propagated deformation that enhances the G-FNP injection through a small pore. In absence of the enzyme treatment, generation of the tensile stress at the laser focusing position and deformation of the cell membrane might be limited by the rigid cell wall.

The G-FNPs were injected when the fs laser pulse was focused on the contact point of the cell wall and membrane. It was assumed that laser ablation at the laser focal point would generate a pore on the cell wall and cell membrane. However, following the ablation, there would be mechanical effects that occur near the focal point, such as propagation of stress and shock waves. To understand the role of those mechanical effects in the photoinjection process, photoinjection experiment would be conducted by focusing laser beside the cell in the culture

medium. The contribution of the photo-mechanical effects would be described in the following chapter that would discuss the mechanism of photoinjection.

4.5 Conclusion

The photoinjection of fluorescent polymer nanoparticles with diameter of 80 nm into the cytoplasm of single plant cells was achieved by employing fs laser amplifier. The nanoparticle injection is valuable because nanoparticles can possess unique surface characteristics or functional molecule delivery capability. The combination of the precise fs laser photoinjection targeting ability and smart nanoparticles would be an important breakthrough that brings through a broad opportunity for the study of plant biology and genetic manipulation.

Chapter 5

Mechanism of Photoinjection

5.1 Introduction

In previous reports, fs laser pulses with a low pulse energy (<1 nJ/pulse) and high repetition rate (>10 MHz) were used, but only molecules smaller than 30 kDa with diameter of 4 nm could be injected.[25] Meanwhile, a single 20 nJ pulse from fs laser amplifier was employed in this work and macromolecules over 1 MDa were injected. The photoinjections of macromolecules, such as megadalton polysaccharides and polymer nanoparticles, into single plant cells with single pulse from fs laser amplifier were described in the previous chapters. The photoinjection occurred on both plasmolyzed cells with mannitol treatment and adjunctive enzyme treated cells, and the enzyme treatment enhanced the photoinjection efficiency.

It was thought that the ablation induced by multiphoton absorption at laser focal point generated by intense amplified fs laser pulse would induce a pore formation on the cell wall and membrane. Indeed, a pore was formed as proven by a leakage of cell cytoplasm in a damaged cell through the pore. However, the propagation of shock and stress waves around laser focal point might also have a role that contribute to the efficient photoinjection of macromolecules. In this chapter, in order to get a comprehensive understanding, transient morphological changes induced by fs laser irradiation were observed to ascertain the cell condition at the time of photoinjection. The photoinjection of macromolecules with various laser focal point position would also be described, including laser irradiation beside the cell in the culture medium to assess the role of photo-mechanical effects, such as shock and stress waves, in the photoinjection process. Then, the photoinjection mechanism would also be discussed, based on the experiment results and phenomena that occurred when NIR fs laser was focused by objective lens.

5.2 Transient morphological change induced by the fs laser irradiation

When a near-infra-red (NIR) fs laser pulse is focused through a high numerical aperture (NA) objective lens on the TBY-2 cell wall and membrane, efficient non-linear processes demonstrated by the multiphoton absorption lead to an ablation at the laser focal point. In addition, the ablation generates rapid expansion of a cavitation bubble and a tensile stress wave propagates to the periphery.[24, 51] These phenomena mechanically act on the cell wall and membrane. These mechanical phenomena are particularly prominent in amplified intense laser pulses: the higher energy density at the laser focal point causes the higher stress increase. Thus, the mechanical effects on TBY-2 morphology in the photoinjection process with the fs laser amplifier is valuable to be verified in this context.

The transient morphological change of TBY-2 cells that was obtained with a high-speed camera are represented in Fig. 36. Cavitation bubble generation was noticed when a single 20 nJ fs laser pulse was focused on the cell wall. Differential images showed instantaneous deformation of the TBY-2 cell membrane and wall around the laser focal point, and that deformation returned to the initial state in about 8 μs. A gas bubble was also observed at the laser focal point for only a few milliseconds.

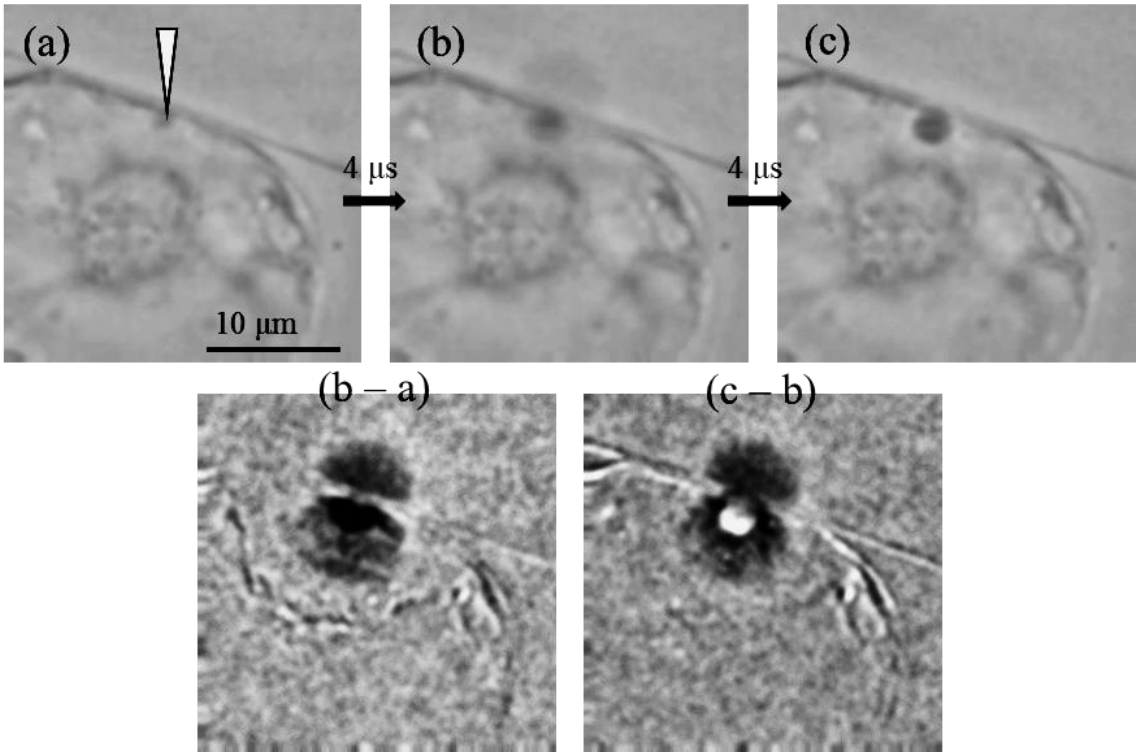

Figure 36. A series of high-speed images (frame rate, 4 µs) taken for the fs laser photoporation experiment. The images (a) before laser irradiation, (b) 4 µs after irradiation and (c) 8 µs after it. The laser focal point is indicated with the white arrow. The differential images were obtained by image calculation of Image J.

In addition, the experiment with the fs laser focal point nearby TBY-2 cells, without directly focusing on the cell wall and membrane was also conducted. In this situation, a fast expansion of a cavitation bubble escorted by an impulsive hydrodynamic force extending to the periphery can bring mechanical force to the TBY-2 cells. Likewise, the cavitation bubble also spread when the fs laser pulse was focused in the culture medium at the distance of 10 µm from the cell wall (Fig. 37 (a, b, c)). It then hit the cells and caused an instantaneous deformation. This finding confirmed that the cells got a mechanical force that came from the cavitation bubble.

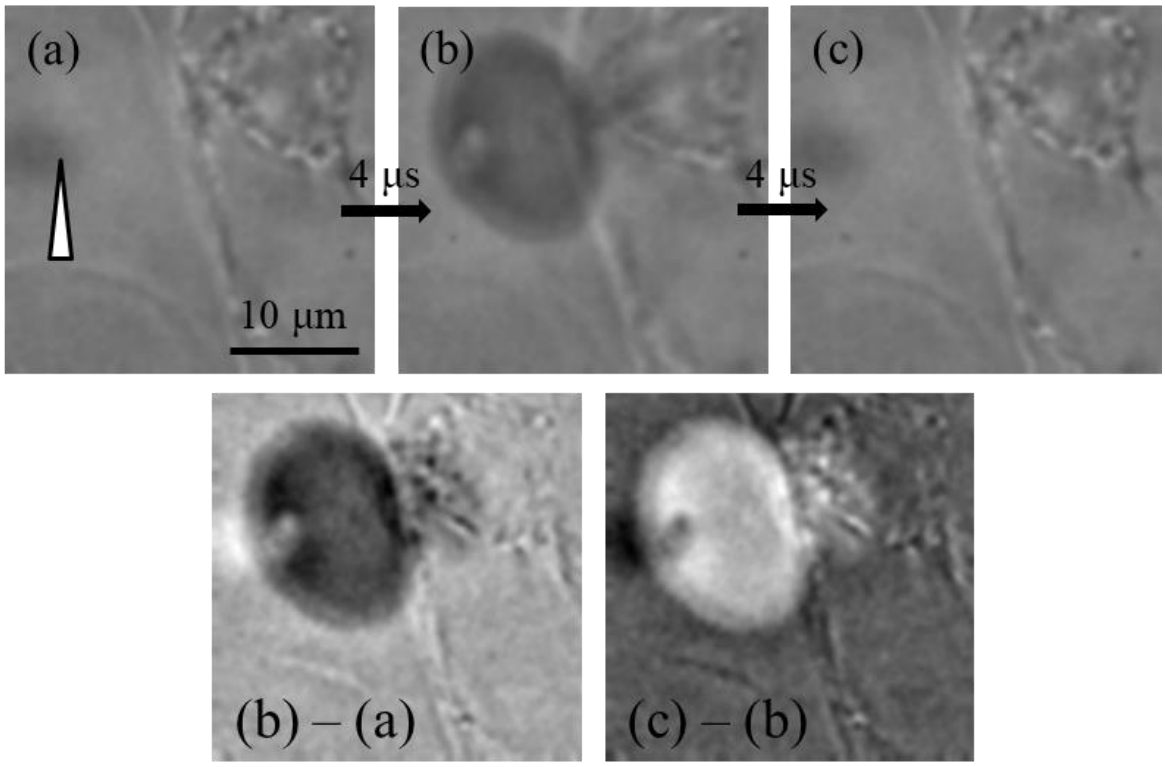

Figure 37. A series of high-speed images at 4 μs intervals. White arrowheads indicate the laser focal points at 10 μm distance from the cell. The differential images were acquired by image calculation using Image J.

5.3 Photoinjection with various focal point position

Interestingly, the G-FNP injection could be seen even when the fs laser pulse was focused beside a cell in culture medium, not directly on the cell. Fluorescence images of the TBY-2 cell before and after fs laser irradiation at 10 μm distance from the cell wall are displayed in Fig. 38 (a). The increase of fluorescence intensity is observed in the image, even though the injection efficiency was less than that of the direct fs laser irradiation as shown in Fig. 38 (b). For other positions of laser focal points, the photoinjection at 10 μm distance from the cell membrane in the apoplast (Fig. 39 (a, b)) was also conducted. The G-FNP photoinjection efficiency was similar with the case when the laser was focused 10 μm outside the cell wall. The accumulation of the G-FNPs was noticed on the cell membrane nearest to the laser focal point. The laser irradiation in the cytoplasm was even examined, even though cells could be damaged and not appropriate as an injection technique. The G-FNP injection was very efficient and the

nanoparticles were accumulated at a large area on the cell membrane (Fig. 39 (e, f)). The photoinjection efficiencies of the G-FNPs and of FITC-2M, as a comparison, for various laser focusing positions are summarized in Fig. 40.

The photoinjection efficiency of G-FNPs with irradiation only on cell membrane was lower than that of irradiation on the contact point of cell wall and membrane. The nanoparticles that would enter into cytoplasm were probably limited to the nanoparticles that were already in apoplast. Even though cell wall permeability was increased by partial degradation with enzyme, the nanoparticles still needed to diffuse into the apoplast. In some cases, the fluorescence in apoplast was less bright if compared to that of the medium outside cell, indicating that the amount of nanoparticles in apoplast was less than in the medium. In the case of irradiation in cytoplasm, the photo-mechanical effects, such as stress and shock waves, might propagate to various direction from inside cell. It was assumed that several pore would be produced in many spots on cell membrane and wall. Therefore, the nanoparticles from apoplast and also from medium outside cells could enter into cytoplasm through those pores, resulting in the relatively high photoinjection efficiency when the cell was irradiated in cytoplasm.

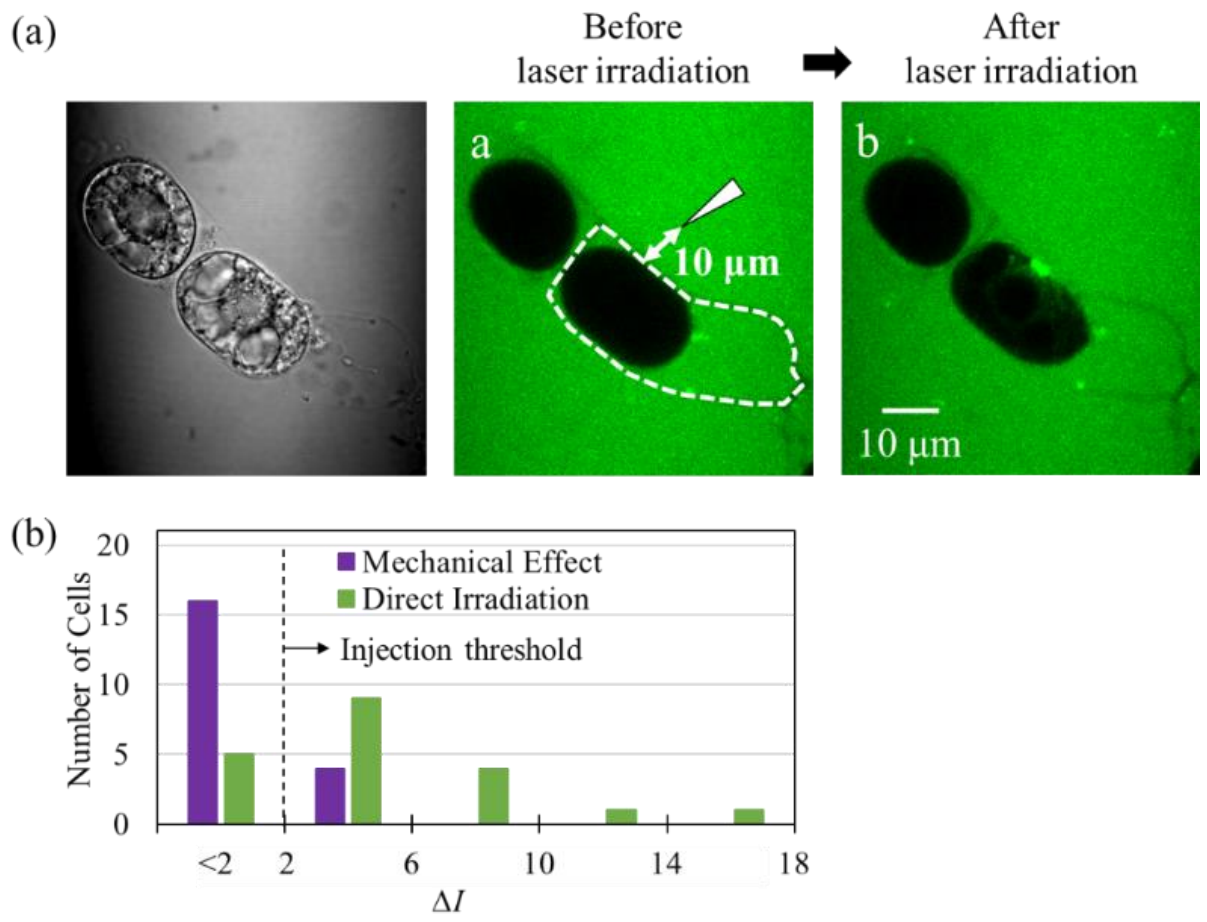

Figure 38. (a) Transmission and confocal fluorescence images of the enzyme treated TBY-2 cell before and after the fs laser irradiation at 10 µm distance from the cell under the presence of G-FNPs. The 20 nJ laser pulse energy was used. The dashed line indicates the outline of target single cell and the white arrowhead indicates the laser focal point. The same conditions as those in Fig. 26 were used for acquiring the fluorescence images. (b) The histogram of ΔI between before and after laser irradiations in medium beside enzyme treated cells (purple, N = 20). The case of direct irradiation is also shown as a reference (green).

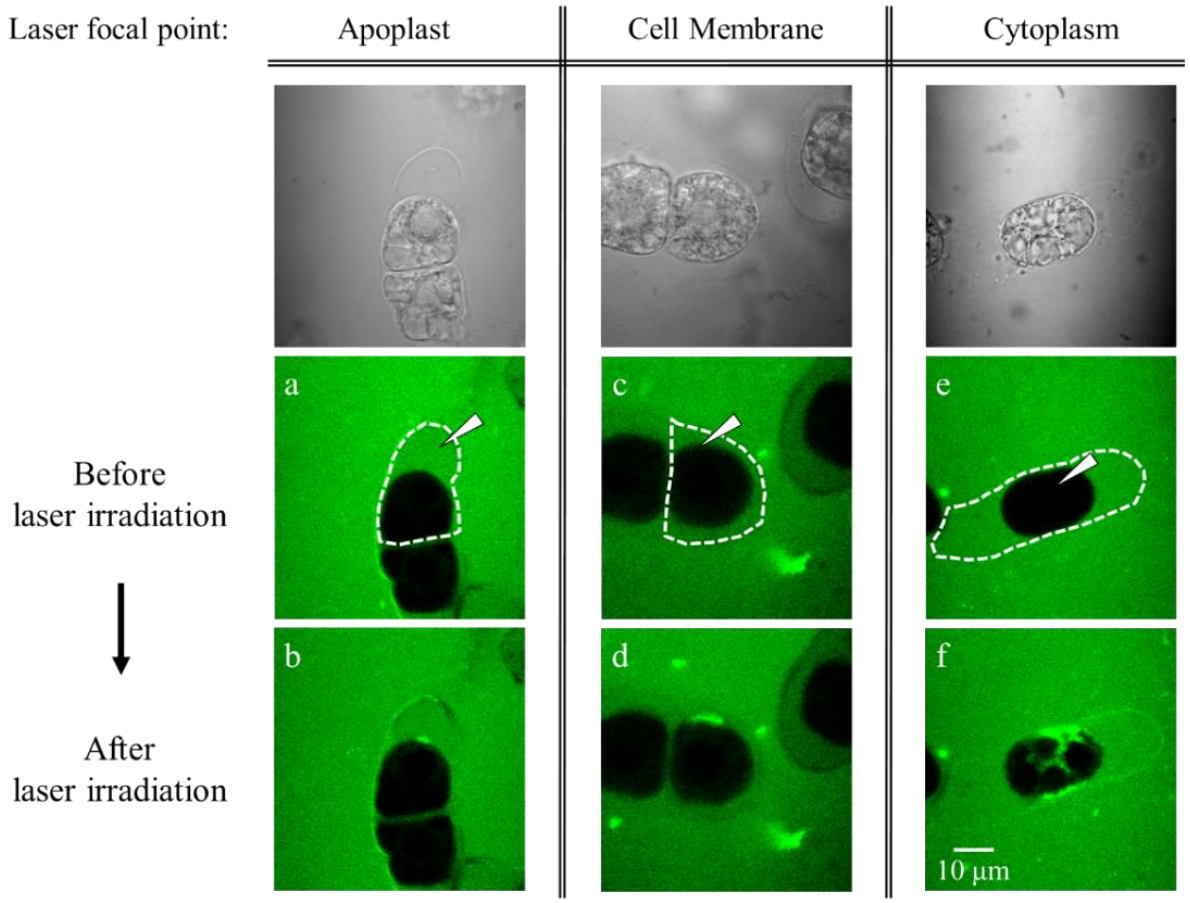

Figure 39. Laser focusing position dependent photoinjection behaviors of G-FNPs. Confocal fluorescence images of TBY-2 cells before and after 20 nJ fs laser pulse irradiation under the enzyme treatment. The white arrowheads indicate the laser focal points: (a) in the apoplast at 10 µm distance from the cell membrane, (b) on the cell membrane, (c) in the cytoplasm. The white dashed lines indicate the target single cells. The same conditions as those in Fig. 26 were used for acquiring the fluorescence images. The top row shows corresponding transmission images before laser irradiation to clarify individual cell shape.

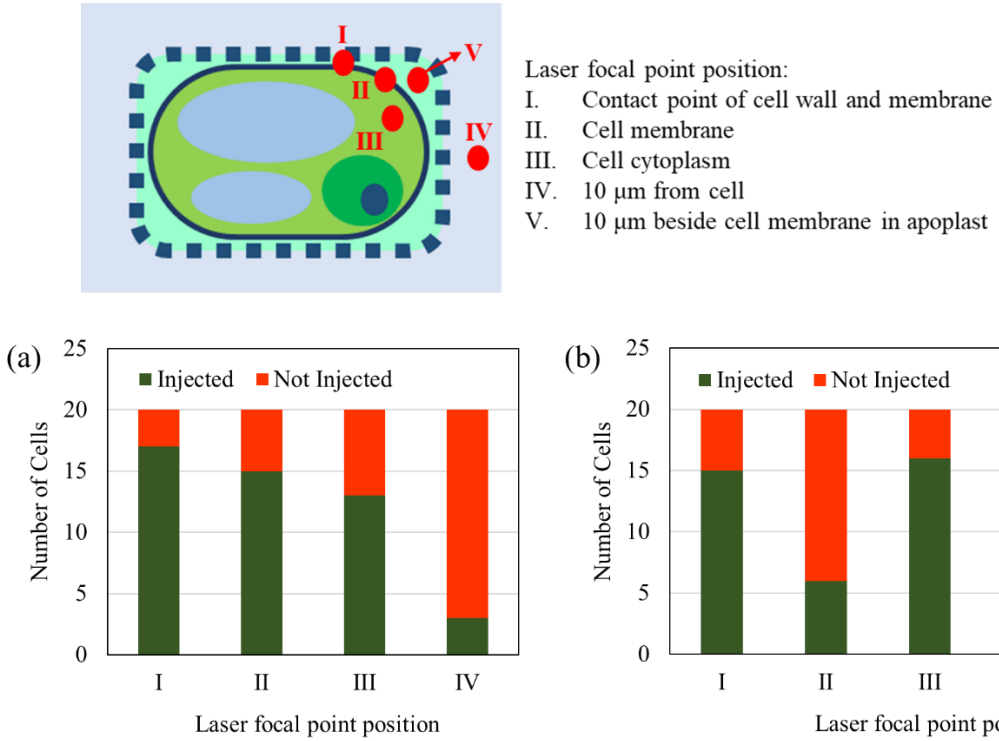

Figure 40. Photoinjection efficiencies of (a) FITC-2M and (b) G-FNPs into adjunctive enzyme treated tobacco BY-2 cells after irradiation with single 20 nJ pulse fs laser amplifier. The laser focal point position were indicated in figures. The injected cells mean that they had ΔI value higher than the injection threshold.

5.4. Discussion

The different type of fs laser system used for perforation in this experiment could be a factor for the successful introduction of the macromolecules with molecular weight over 1 MDa. In this work, a single-shot 20 nJ laser pulse from the fs laser amplifier was used while the previous reports used low-energy and high-repetition rate pulses from an fs laser oscillator. The much higher laser fluence in this experiment would produce an efficient perforation of the cell wall and membrane at the laser focal point with less thermal accumulation. This suggestion is also supported by the study for mammalian cells. A single higher energy fs laser pulse can form a twice-larger pore compared with trains of low energy pulses. These are in optimal conditions on photoinjection efficiency and cell viability for the irradiation parameters.[33] Furthermore, induced tensile stress around the pore should be stronger for the fs laser amplifier than the fs laser oscillator.[51] A transient morphological change by the laser-induced mechanical stress was

seen for the TBY-2 cell in Figs. 36 and 37. Thus, it is regarded that the generation of strong tensile stress correlated with the fs laser photoporation could possess a significant role to increase the cell membrane permeability simultaneously.

As already described, macromolecules were injected by focusing the fs laser pulse on the contact point of the cell wall and membrane in the hypertonic condition. Following enzyme treatment, the injection of macromolecules was observed even when the fs laser pulse was directed beside TBY-2 cells in the culture medium. As an interpretation of these two injection arrangements, and also from previous studies about phenomena that occurred when NIR fs laser was focused by objective lens, there might be primarily two mechanisms that have a role on the perforation of the cell membrane, as presented on Fig. 41.

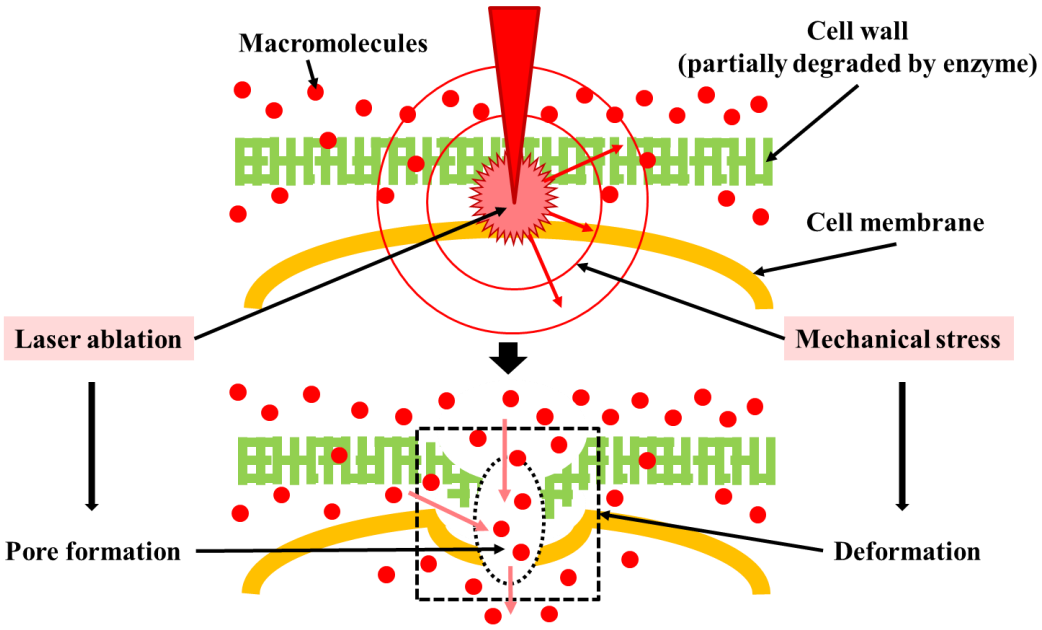

Figure 41. A proposed model of mechanism of photoinjection. Laser ablation and mechanical stress would generate pore formation and deformation in cell membrane and cell wall. In enzyme-and-mannitol treatment, the cell wall is partially degraded and softened by enzymes. In addition, macromolecules are present in the apoplast through diffusion so they could enter into cytoplasm easily when the pore is formed.

The first mechanism is that the photochemical ablation of the cell membrane induces a pore formation. Precisely, this mechanism is not proven directly. However, the laser irradiation

induces the breakdown of water and generates the cavitation bubble as confirmed in Fig. 37. Thus, it is tough to regard the breakdown alone happens without the cell membrane dissociation via multiphoton absorption, as the absorbance of cell membrane components, such as lipids and proteins, at 800 nm is usually higher than that of water. On the other hand, the pore formation with low energy and high repetition rate of fs laser pulses in the previous studies could inject only a few nm sized objects into plant protoplasts.[25] Thus, it is considered that the pore formation induced by photochemical ablation alone was not enough for the macromolecule injection.

The second mechanism is that the photo-mechanically induced tensile stresses, such as stress and shock waves, cause the cell membrane rupture. This photo-mechanical effect is especially significant using amplified intense laser pulses. The higher density of laser energy at the focusing point generates a higher stress elevation and its fast relaxation to the periphery.[51] Cell deformations were induced instantaneously in both injection schemes near the laser focal point and the cavitation bubble impact area, as observed in Figs. 36 and 37. Generally, the plant cell membrane has less flexibility compared to animal cell membrane. Therefore, the cell membrane would be ruptured by a tensile stress induced by the deformation. This process becomes more obvious with laser focal point in the cytoplasm. The cavitation bubble enlarges almost isotropically in the cytoplasm within the cell. The pressure would cause the stretching of the cell membrane. Then, several breaks would occur in various directions.

Finally, the photoinjection efficiency of macromolecules is still low in cells without enzyme treatment, even when a higher laser energy is used. The tensile stress generation at the laser focal point and the cell membrane deformation might be limited by the rigid cell wall. It is suggested that the mechanically propagated deformation is increased in the enzymatically softened cell wall, thus enhances the macromolecule injection through a small pore.

5.5 Conclusion

It is suggested that there are two mechanisms that contribute to an efficient photoinjection of macromolecules. The first mechanism is a pore formation that was induced by the laser ablation at the focal point. The second mechanism is the contribution from the mechanical effects of the intense fs laser pulse, such as the propagation of shock and stress waves near the laser focal point, which cause a rupture on the cell membrane. Ascertaining of the precise photomechanical action of amplified fs laser pulses on biological membrane would bring new point of view in its utilization in biophotonics.

Chapter 6

Application of Photoinjection

6.1 Introduction

In previous chapters, the photoinjection technique of macromolecules into intact plant cells under hypertonic condition with fs laser amplifier was developed. Macromolecules, such as megadalton polysaccharide molecules and polymer nanoparticles, were injected through a pore on cell wall and membrane generated by laser ablation at the laser focal point. The mechanical effects induced by amplified fs laser pulse, such as stress and shock waves, also had a role on causing a rupture on cell membrane. The adjunctive enzyme treatment partially degraded the cell wall and enhanced the photoinjection efficiency. Considering those achievements, the photoinjection of functional macromolecules into plant cells for the study of plant physiology and genetic engineering would be possible.

In this chapter, the photoinjection technique would be applied for the observation of macromolecule diffusion behavior in cell cytoplasm. The polymer nanoparticles from chapter 4 was used for that purpose. The investigation of intracellular and intercellular diffusion could be useful in the plant physiological study, particularly to examine cytoplasmic streaming and molecular transport, biological phase separation in cytoplasm, and cell-to-cell communication.[52]

6.2 Observation of intracellular and intercellular diffusion

A possible application of this photoinjection technique is the investigation of diffusion behavior in plant cell cytoplasm. After laser irradiation, macromolecules would diffuse through a pore on cell membrane into the cytoplasm. Then, the intracellular diffusion of the injected molecules could be observed in the cell cytoplasm. Such diffusion behavior of macromolecules

in cell cytoplasm is useful to be studied, especially to get information of the macromolecule interaction with cytoplasm and other plant organelles, and biological phase separation. In addition, intercellular diffusion could also be seen when the molecules move to other cell adjacent to the target cell. It would be useful for examining molecular transport and cell-to-cell communication.[52]

In this section, the observation of diffusion behavior of polymer nanoparticles in a single plant cell cytoplasm after fs laser photoinjection was demonstrated. The nanoparticles used here were the same with the nanoparticles used in chapter 4, the G-FNPs with diameter of 80 nm. The evaluation was based on the differential fluorescence intensity in various parts of the cells in a period of time after injection. The regions on the cytoplasm chosen were: near the laser focal point (0 μm), at 10 μm distance from the laser focal point, and at 20 μm from the laser focal point, as presented on Fig. 42. The temporal evolution of fluorescence intensity at those area were presented on Fig. 43.

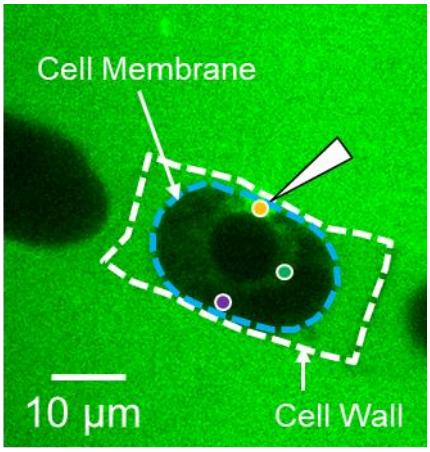

Figure 42. The regions of cytoplasm selected as the sites of measurement. Upper yellow dot is near the laser focal point. Middle green dot is at 10 μm distance from the laser focal point. Lower purple dot is at 20 μm distance from the laser focal point.

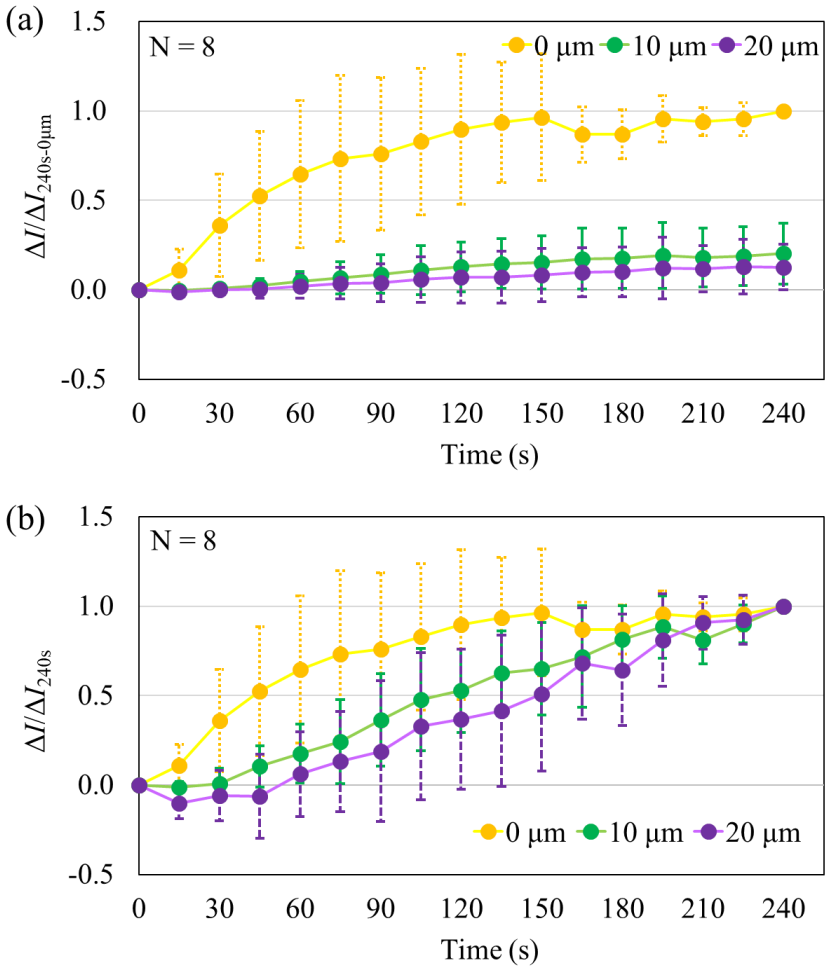

Figure 43. Temporal evolution of fluorescence intensity in the cytoplasm for enzyme treated cells on various distance from the laser focal point (0 µm, 10 µm, and 20 µm). The graphs are averaged for 8 cells and normalized by the ΔI at 240 s of 0 µm value (a) and of each distance value (b). The error bar indicates standard deviation.

As indicated on Fig. 43 (a), on the laser focal point (0 µm), fluorescence intensity started to increase immediately after laser irradiation, meanwhile at the distance of 10 µm and 20 µm, the fluorescence intensity started to increase at about 45 s and 60 s after laser irradiation, respectively. The ΔI value was highest on the laser focal point, far higher than the other position in the cell cytoplasm. The further distance from the laser focal point, the ΔI value would be lower. It was suggested that the fluorescent nanoparticles were accumulated on the laser focal point before diffusing to the other location in the cell cytoplasm. Indeed, the area nearby laser focusing position was the brightest part.

The particle diffusion patterns could be observed on Fig. 43 (b). The fluorescence intensity increased to the half of maximum value at about 45 s, 105 s and 150 s after laser irradiation on the laser focal point (0 μm), and at the distance of 10 μm and 20 μm from the laser focal point, respectively. As the nanoparticles were first accumulated on the laser focal point, the initial diffusion to other part of the cells was rather slow. It was probably due to cytoplasmic streaming into the focal point, responding the pore formation on the cell membrane and wall by fs laser irradiation. Then, once the nanoparticles enter the cytoplasm, they began to diffuse to the other position in the cytoplasm. The accumulation was clearly visible as a bright spot on the laser focal point as shown on Fig. 44.

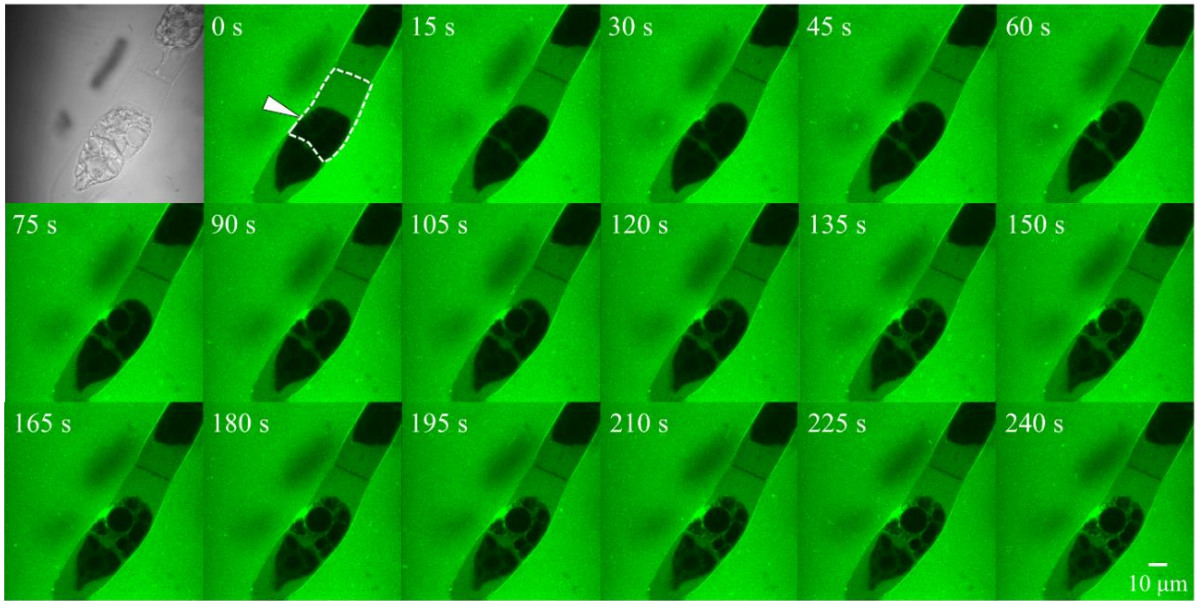

Figure 44. Confocal fluorescence images of enzyme and mannitol treated TBY-2 cells before (0 s) and after fs laser irradiation (15-240 s) under the presence of G-FNPs. The top left image shows the transmission image before laser irradiation. The dashed line indicates the outline of a target single cell and the white arrowheads indicate the laser focal point. These images represent the change of fluorescence intensity overtime. Interestingly, the G-FNPs also diffused into the adjacent cell that was connected the target cell.

Interestingly, from Fig. 44, the nanoparticles were also found to diffuse into the adjacent cell which was attached to the target cell. To ascertain this, the differential fluorescence intensity in the neighboring cell was also measured, as shown on Fig. 45. The fluorescence intensity also

increased in the adjacent cell, even though it was lower than that of the target cell. There are many tunnels that connect the cytoplasm between plant cells called plasmodesmata. The plasmodesmata typically have diameter about 50 to 60 nm, and in tobacco, it could be as wide as 500 nm.[53] The plasmodesmata could be closed or enlarged in response to cell conditions, such as turgor pressure.[54] In this case, turgor pressure decreased and the plasmodesmata might be enlarged. In addition, enzyme treatment might have some effects to the structure of plasmodesmata, the pore size might be enlarged.[55] However, those effects are not clearly understood for now. Nevertheless, the gradual diffusion of 80 nm nanoparticles through this tunnel into the adjacent cell was observed. With this knowledge, the photoinjection with fs laser amplifier has a great potential to be used for studying plant physiology, especially molecular transport and cell-to-cell communication. This was a significant finding since it was the first time an intercellular diffusion of macromolecules was directly observed over a period of time.

It needs to be mentioned that in the observation of intracellular diffusion, the measurement of fluorescence intensity was conducted in a small portion of cytoplasm area of a cell, namely at the distance of 0, 10 and 20 μm from the laser focal point. On the other hand, in the observation of intercellular diffusion, the measurement of fluorescence intensity was conducted in whole cytoplasm area of each cells, the target cell and the adjacent cell. Therefore, it seemed that there was no delay of fluorescence intensity increase in adjacent cell. It could be because the measurement of fluorescence intensity was in whole cytoplasm area, so the difference of fluorescence intensity increase in different spots of adjacent cell was not observed. Thus, the results of the observations of intracellular diffusion and intercellular diffusion could not be directly compared since the area of measurement was different in each case.

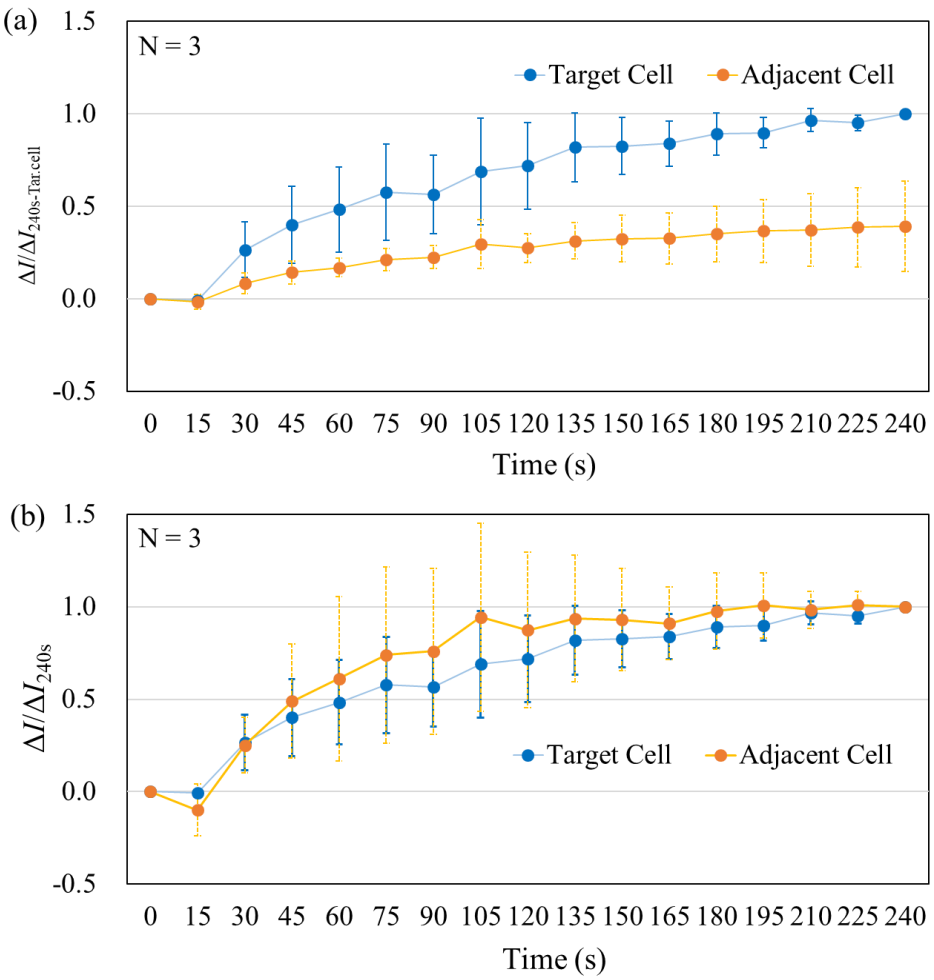

Figure 45. Temporal evolution of fluorescence intensity in the cytoplasm for target cells and their adjacent cells. The graphs are averaged for 3 cells and normalized by the ΔI at 240 s of target cell value (a) and of each cell value (b). The error bar indicates standard deviation.

In above experiment, the adjunctive enzyme treated cells were used. Hence, the cell wall was partially degraded and the nanoparticles were already present in cell apoplast. As stated previously, the photoinjection of the G-FNPs was efficient in this condition, but it was not successful without enzyme treatment, when single 20 nJ fs laser pulse was used. Instead, for cell without enzyme treatment, a higher laser energy needed to be used to inject nanoparticles into plant cells, even though the efficiency was still low. A possible cause of this would be the pore on cell wall was not large enough for the diffusion of nanoparticles. To ascertain this, the photoinjection of nanoparticles into apoplast in mannitol treated cells, without enzyme treatment, was also examined, with laser focal point only on cell wall, as demonstrated on Fig.

46.

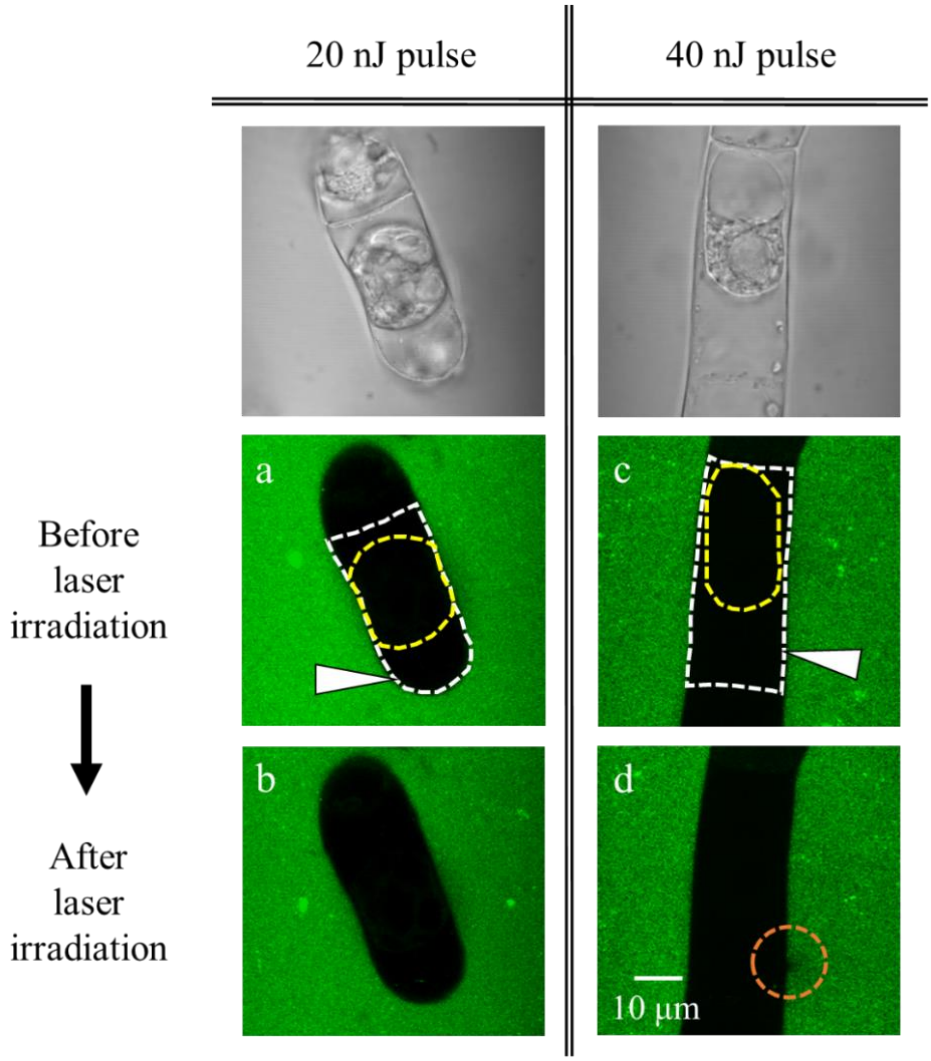

Figure 46. Confocal fluorescence images of mannitol treated TBY-2 cells before and after fs laser irradiation on cell wall under the presence of G-FNPs. The top row shows corresponding transmission images before laser irradiation. The white and yellow dashed lines indicate cell wall and membrane of a target single cell respectively and the white arrowheads indicate the laser focal point. A cell wall breakdown could be observed on laser focal point with irradiation of single 40 nJ pulse (d) indicated by orange dashed line, while not in single 20 nJ pulse (c).

As can be seen on Fig. 46 (b), there was no observable change on the cell, especially cell wall, 2 min after single 20 nJ pulse fs laser irradiation. Meanwhile, a small breakdown was visible on the cell wall with single 40 nJ pulse (Fig. 46 (d)) at the laser focal point. The breakdown of cell wall was more intense with higher laser energy, even though the nanoparticles had not yet diffuse into the cell apoplast. It turned out that the diffusion of the G-

FNPs into the apoplast through the cell wall happened slowly. Fig. 47 (b) shows that at first, the ΔI value in apoplast increased slowly, and only reached to higher than 2, the injection threshold, at 10 min after single 40 nJ pulse laser irradiation on cell wall. Then, the ΔI continued to increase until 60 min after laser irradiation, almost at the same level of fluorescence intensity with the surrounding area outside the cell (Fig. 47 (a)).

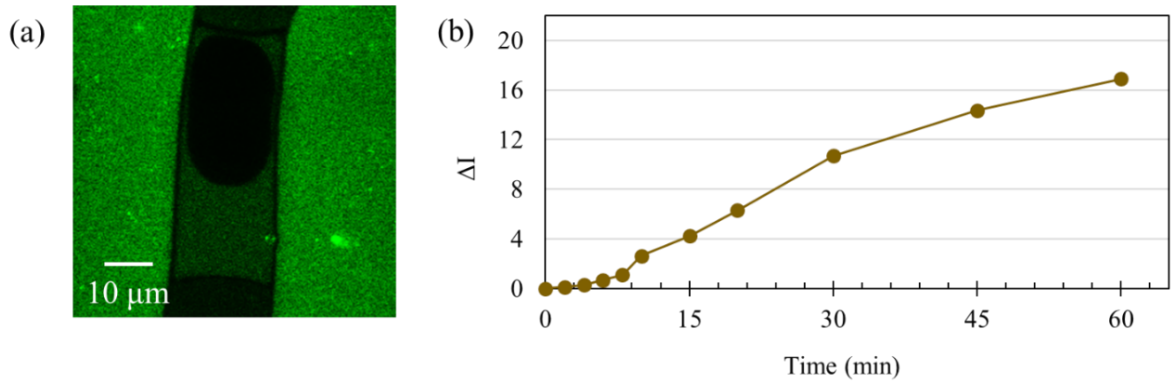

Figure 47. (a) Confocal fluorescence image of mannitol treated TBY-2 cells 60 min after single 40 nJ pulse fs laser irradiation on cell wall under the presence of G-FNPs. (b) Temporal evolution of fluorescence intensity in the apoplast for mannitol treated cell.

It was described that when the cell wall and cell membrane were irradiated with single 40 nJ pulse simultaneously, a pore was formed on both of them, thus enabled the nanoparticles to diffuse directly into cell cytoplasm. The differential fluorescence intensity was already higher than 2, the injection threshold, in cytoplasm at 2 min after laser irradiation even though the possibility is still low (Fig. 28 (a)), in contrast to 10 min in apoplast (Fig. 47 (b)). This could be due to higher osmotic pressure in the hypertonic medium than in cytoplasm. Meanwhile, the pressure in the medium and apoplast might be similar, so the nanoparticles only diffused because of the concentration differences. In the case of 20 nJ pulse, it was assumed that the photoinjection of the G-FNPs with this lower energy was not efficient into both cytoplasm and apoplast because the nanoparticles diffused even slower through a smaller pore on the cell wall. Hence, when the cell membrane was closed again, the nanoparticles could not reach sufficient

concentration in cytoplasm to be detected above the injection threshold at 2 min after laser irradiation. When a smaller molecule, such as FITC-2M (26.7 nm) was used, the molecules could be injected at 2 min after 20 nJ pulse irradiation in mannitol treated cell (Fig. 19 (c)), suggesting that the molecular size had also affected the diffusion through the pore and subsequently the photoinjection efficiency.

6.4 Discussion

An application for this method to observe macromolecule diffusion in plant cell cytoplasm was demonstrated. The diffusion of polymer nanoparticles, the G-FNPs, in the cytoplasm after photoinjection was investigated by measuring the increase of fluorescence intensity at different points in the cytoplasm (Figs. 42 and 43). The G-FNPs tend to accumulate near the laser focal point before diffusing to other part of the cells. This could be due to cytoplasmic streaming into the pore formed by fs laser irradiation. Indeed, when the pore was large enough when a higher laser energy was used, the cytosol leakage occurred. The nanoparticle size probably also has a role for the slower initial diffusion, compared to that of smaller molecules, such as FITC-2M. The diffusion through a similar sized pore may become slower with increasing particle size. In addition, the nanoparticle surface properties, such as zeta potential and affinity, might also affect the diffusion in the cytoplasm, although it is still need to be ascertained. Understanding nanoparticle diffusion in plant cell cytoplasm could be useful for the design of future nanoparticles with faster or slower diffusion, including controlled release of contained molecules. Moreover, as the photoinjection method has been developed, it becomes possible to observe real-time molecular diffusion in single plant cells.

An interesting result in this work was the possibility of direct observation of intercellular diffusion of macromolecules. For the first time, the nanoparticle diffusion from one cell to another cell through plasmodesmata was directly observed over a period of time. Usually, the

movement of nanoparticles in plant organs is analyzed indirectly, such as measuring the concentration of nanoparticles in leaves and stems after submerging the root in a nanoparticle suspension or spraying the leaves.[13, 56-57] Thus, the photoinjection method would open a way to directly monitor the diffusion of macromolecules between cells, and this is promising for plant physiological study, especially to examine molecular transport and cell-to-cell communication.

6.5 Conclusion

The direct observation of intracellular and intercellular diffusion of macromolecules, as an application of this photoinjection method, was demonstrated for the first time. The ability to observe such processes would be very useful in the study of plant physiology, including cytoplasmic streaming and molecular transport, biological phase separation in cytoplasm, and cell-to-cell communication.[52]

Chapter 7

General Conclusion

7.1 Conclusion

The research objective to develop a photoinjection technique for the introduction of macromolecules into single intact plant cells using femtosecond laser amplifier was achieved. Large 2 MDa molecules with diameter of 26.7 nm, whose size is similar to DNA plasmid, were injected with irradiation of single 20 nJ pulse from fs Ti:sapphire laser amplifier into single TBY-2 cells under hypertonic condition. Polymer nanoparticles with diameter of 80 nm containing fluorescent dye were also injected into single intact TBY-2 cells using this method. The intense fs laser pulse in this experiment perforated the cell wall and membrane efficiently. A moderate enzyme treatment with cellulase and pectolyase was applied to partially degrade the cell wall. The enzyme treatment enhanced the macromolecule diffusion through the cell wall and increased the photoinjection efficiency. The photoinjection mechanism, through laser ablation and photomechanical effect induced by fs laser amplifier, was elaborated. In addition, an application of this method for the investigation of nanoparticle diffusion in plant cell cytoplasm was described. Those findings would be summarized chapter by chapter below.

Chapter 1 described several techniques of molecular introduction into plant cells, including photoinjection and its shortcomings. Previous photoinjection methods could not introduce molecules larger than 30 kDa into single intact plant cells, mainly because of rigid and thick cell walls. The research objective was presented with a strategy of using fs laser amplifier and enzyme treatment for the cell wall partial degradation. Then, the research outline was stated.

Chapter 2 described the preparation of TBY-2 cells as the plant samples, including their treatments, such as the cell plasmolysis in a hypertonic condition with addition of mannitol to the culture medium and the partial degradation of cell wall by cellulase and pectolyase enzymes.

Then, the experimental setup of NIR fs laser photoinjection was described, utilizing laser pulses from a regeneratively amplified fs Ti:sapphire laser system that were led into a laser-scanning confocal microscope and focused on a TBY-2 cell through a 100x oil-immersion objective lens. The fluorescent measurements to evaluate the injection efficiency and the cell viability assay to examine cell conditions after laser irradiation were also described.

Chapter 3 reported the photoinjection of macromolecules, the FITC conjugated dextran, with molecular weight of megadalton into an intact single plant cells for the first time. This was achieved by employing single 20 nJ pulse from an fs laser amplifier into TBY-2 cells under hypertonic condition. An adjunctive enzyme treatment to partially degrade the cell wall enhanced the photoinjection efficiency. The results suggest that the photoinjection using the amplified fs laser pulse is promising and applicable for efficient injection of macromolecules, such as DNA plasmid, to intact plant cells.

Chapter 4 reported the photoinjection of fluorescent polymer nanoparticles, the G-FNPs, with diameter of 80 nm into the cytoplasm of TBY-2 cells using the above method. Nanoparticles have unique surface properties and can contain functional molecules, thus photoinjection of nanoparticles would open a wide opportunity for the study of plant biology and genetic engineering.

Chapter 5 showed an interesting result that beside direct irradiation on the contact point of cell wall and membrane, the injection also occurred even when the laser pulse was focused beside the cell in the culture medium. It suggests that there are two mechanisms contributing to an efficient photoinjection of macromolecules. The first mechanism is a pore formation induced by the laser ablation at the focal point. The second mechanism is that the mechanical effects of the intense fs laser pulse, such as stress and shock waves, generate a rupture on the cell membrane. Understanding the precise photomechanical action of amplified fs laser pulses on biological membrane would offer a new perspective in biophotonics.

Chapter 6 presented an application of the photoinjection technique for the observation of diffusion in plant cell cytoplasm. The direct observation of intracellular and intercellular diffusion was demonstrated for the first time. It is potentially useful in plant physiological study, especially for understanding molecular transport, biological phase separation, and cell-to-cell communication.[52]

Chapter 7, as the general conclusion, described that the research objective to develop a photoinjection technique for the introduction of macromolecules into single intact plant cells using femtosecond laser amplifier was achieved. The research findings was summarized chapter by chapter. Some perspectives for the future works, such as gene transfection into plant cells and the design of nanoparticles containing functional molecules, were also presented.

The photoinjection of macromolecules into single plant cells was achieved by employing fs laser amplifier under osmotic pressure control in a hypertonic condition. The partial degradation of cell wall by enzyme treatment increased the injection efficiency. As the specific targeting ability is the most significant benefit of the fs laser photoinjection, this injection method has a great potential to be applied for plant physiological study and genetic engineering, especially at single cell level.[42, 45]

7.2 Perspectives

7.2.1 Gene transfection into plant cells

This photoinjection technique was applied for the injection of macromolecules, whose size is similar with DNA plasmid into plant cells. Thus, it is potential to be used for the introduction of DNA plasmid into single intact plant cells. Usually, to observe whether such genes are injected or not, the genes must produce observable substances, such as fluorescent proteins. The genes that encode the production of green fluorescent protein (GFP) or its relatives are commonly used for this purpose.[58] However, the plant cells need to survive for a period of time

after the injection until the genetic manipulation is expressed. The foreign genes are expected to merge with the host genes in nucleus during the division of cells. Thus, ensuring a long term cell viability after injection is necessary for a successful transfection. It could be 3 to 24 hours, but it depends on the cell growth and the gene type.

The cell viability for 12 hours after injection was observed in this work with FDA and PI assay. The majority of cells, about 95%, were stained by FDA, indicating that the cells were viable as the cell enzymes still worked. However, about 20% of the cells were stained by PI, suggesting that their cell membranes were not intact. It could be that for the PI-stained cells, the pore was not resealed or the integrity of cell membrane could not recover after laser irradiation. It was recommended to verify how fast the cell membrane recover in future experiment by conducting FDA and PI staining in a shorter time period. In addition, avoiding to focus the laser near vacuoles was suggested to keep the cell integrity. Moreover, it looked like the number of cells after 12 hours in the medium with mannitol addition were similar, or in other word, the cells had not divided yet during this time period in the hypertonic condition. So, that would be another factor to consider for the injection of DNA plasmid into plant cells. Probably, the gene expression need more than 12 hours until the cells divided or the cell condition need to be changed. In addition, the expressed genes should be able to be distinguished for the cell auto-fluorescence to verify that the observed fluorescence would be from the successful transfection.

Following those observations, suggestions to improve the cell condition after injection are proposed. The enzyme concentration and its reaction time for partial degradation of cell wall and the centrifugation for washing the cells could be optimized. Then, the laser energy to be used in the optimized treatment also need to be verified again in order to get an efficient injection with most number of viable cells. After the injection, the cells need to be put back to normal culture medium to ensure the cells could grow and divide normally. This would be

challenging as the TBY-2 cells are suspended in the medium, so tracking the irradiated cells is almost impossible. Thus, it would be better to irradiate all cells in the bottom dish, applying a way to stick the cells to the dish, or using other plant species that could be attached to the dish. If irradiation of all cells in the bottom dish would be conducted, since there would be too many cells, it is recommended to decrease the number of cells by diluting the cells or taking a fewer volume of the cells. As for the observation of the transfected cells, it is suggested that a proper filter for specific emission wavelength of the fluorescent proteins would be used.

In addition, the method was used for the observation of diffusion in cell cytoplasm and to another cell. This would open a way for observation of other cellular process, such as interaction of the injected molecules with other plant organelles, molecular transports, biological phase separation, and cell-to-cell communication.[52] In this work, TBY-2 cells were used as the plant sample. Since the characteristics between species could vary, in order to be applied to another plant species, the parameters in this methods should also be optimized, such as laser energy, and enzyme concentration and reaction time, among others. Nevertheless, this work is a significant development in the plant research as it is the first report that demonstrated the photoinjection of macromolecules into intact plant cells. Thus, the application of this method for plant physiological study and genetic engineering is very promising.

7.2.2 Design of nanoparticles containing functional molecules

One of the main advantages of fs laser photoinjection is its ability for single cell manipulations, as the laser pulse could be directed at specific point of interest in the cells or tissues.[50] Now that the method is able to inject large-sized molecules into plant cells, it is potentially used for the injection of various macromolecules, such as proteins, DNA plasmid, and other organic polymers. Thus, the application of photoinjection for functional macromolecules introduction into plant cells is encouraging, particularly when the

macromolecules need to be injected in a specific part of the plants.

Nanoparticles have unique characteristics, such as surface properties and controlled release of contained molecules. Nanoparticles could be synthesized to contain functional molecules, from small-sized dyes, chemical agents, hormones and drugs, to large-sized molecules, such as proteins and genes.[9-11, 59-60] The functional molecules would take the benefit of the nanoparticle characteristics and be transported to intended part of the cells. Combining the photoinjection advantage with unique properties of nanoparticles containing functional molecules would be a promising alternative in the plant researches.

With those in mind, the design of polymer nanoparticles that could contain wide range of functional molecules was attempted. The nanoparticles described here has a great potential as a general platform of molecular delivery for future researches. The polymer to be used was PEG-PLGA (poly (ethylene glycol) methyl ether-block-poly (lactic-co-glycolide)), which is a copolymer of PEG (poly (ethylene glycol)) and PLGA (poly (lactic-co-glycolide)). PLGA itself is a copolymer of lactide and glycolide. The use of PEG-PLGA for nanoparticle synthesis offers many advantages. PLGA-based nanoparticles are able to encapsulate various kinds of functional molecules, from small drugs and dyes to large proteins and genes. In addition, both PEG and PLGA are biodegradable and biocompatible to be introduced into cell as they can be metabolized by esterase enzyme in the cell, thus PEG-PLGA is commonly used for controlled release in the drug delivery system. PEG is hydrophilic, meanwhile PLGA tends to be hydrophobic. However, as the content of lactide and glycolide in PLGA can be varied, the hydrophobicity of PLGA also varies. PLGA with more lactide content would be more hydrophobic with longer degradation time and PLGA with more gycolide would be more hydrophilic with faster degradation time. Depending on those properties, PLGA-based nanoparticles could release the contained molecules immediately or over a period of time, ranging from hours or even weeks.[61-65]

At this stage, the preparation of biodegradable polymer nanoparticles containing a fluorescent dye would be described. The nanoparticles were prepared using emulsification-solvent evaporation method (EEM) (Fig. 48) in Institut Galien Paris Sud, France.[61-66] For the organic phase, 2 mL CH_2Cl_2 (dichloromethane) containing PEG-PLGA 2.5% w/v (PEG average monomer 5000 and PLGA average monomer 55000 [lactide:glycolide 50:50]) was used. Then, 2 mg of specially synthesized BODIPY molecules were added to the organic phase as the fluorescence molecule. For the aqueous phase, 10 mL solution of sodium cholate in water (1.5% w/v) was used. Sodium cholate was put under stirring to dissolve it in water and then filtered using PVDF (polyvinylidene fluoride) filter 0.22 μm. The solution was kept at 4 °C and prepared at least a day before used. Next, pre-emulsification was conducted with mixing the organic phase and the aqueous phase in a vortex for 1 minutes. Then, emulsification was carried out using sonication with ultrasound for 1 minutes (amplitude 30%, power 300 W) in a cup filled with ice. After that, the emulsified solution was put under magnetic stirring 500 rpm for 3 hours at room temperature until the organic solvent (CH_2Cl_2) was evaporated. Finally, the suspension of nanoparticles in water was ready. The structure of biodegradable nanoparticles is shown in Fig. 49.

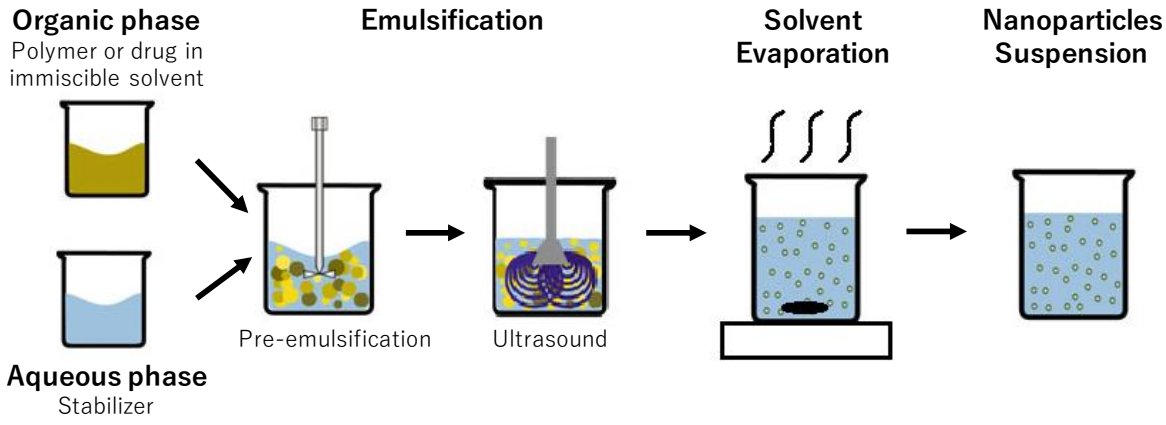

Figure 48. Schematic representation of the steps involved in the preparation of nanoparticles using emulsification-solvent evaporation method (EEM).[66]

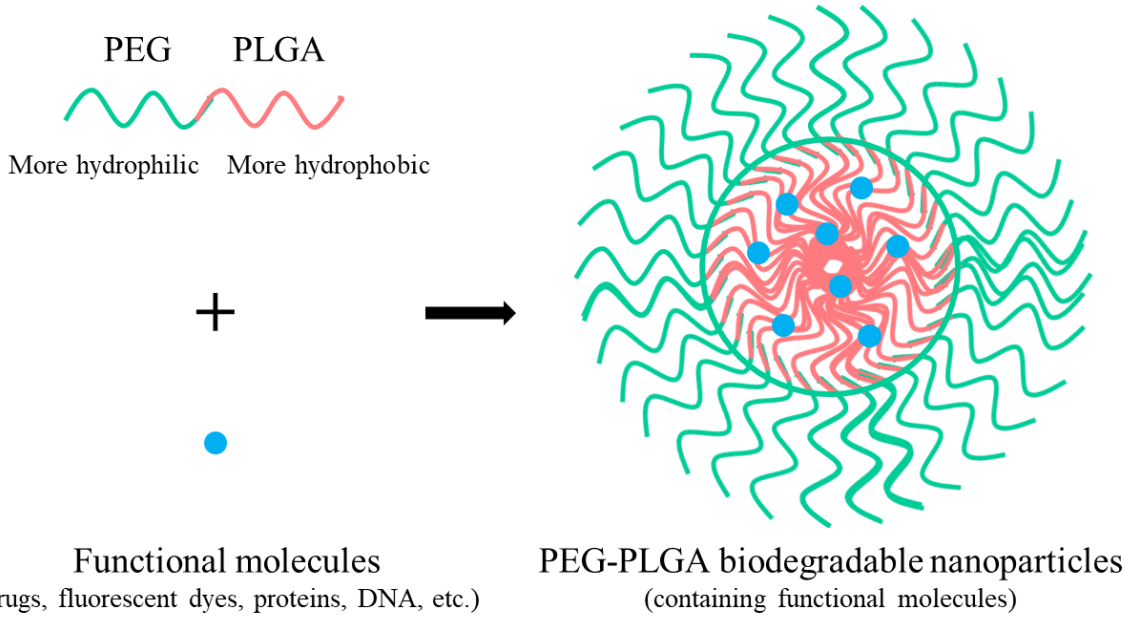

Figure 49. Structure of PEG-PLGA biodegradable nanoparticles containing functional molecules. The functional molecules are trapped, but not covalently bound to PLGA and gradually released as the nanoparticles degraded.[61, 63, 66]

An additional step could be applied after emulsification and solvent evaporation processes were conducted. The nanoparticles were put under centrifugation at 20000 rpm 4 ˚C for 1 hour. The supernatant was separated and the nanoparticles was suspended again in 10 ml water. This step was applied to remove the free dye, which was not contained in the nanoparticle, from the aqueous phase.

The prepared nanoparticles was about 132 nm ± 1 nm in size with zeta potential of -3.0 ± 0.2 mV, indicating that the nanoparticles were negatively charged. However, the injection of the nanoparticles into plant cells could not be conducted because nanoparticles did not give visible fluorescence. It turned out that the BODIPY molecules (Fig. 50) used here were not designed for this purpose. Instead, the molecules were synthesized specially for a photo-acoustic system in France. The prepared nanoparticles have maximum wavelengths of excitation and emission at about 780 nm and 800 nm, respectively.

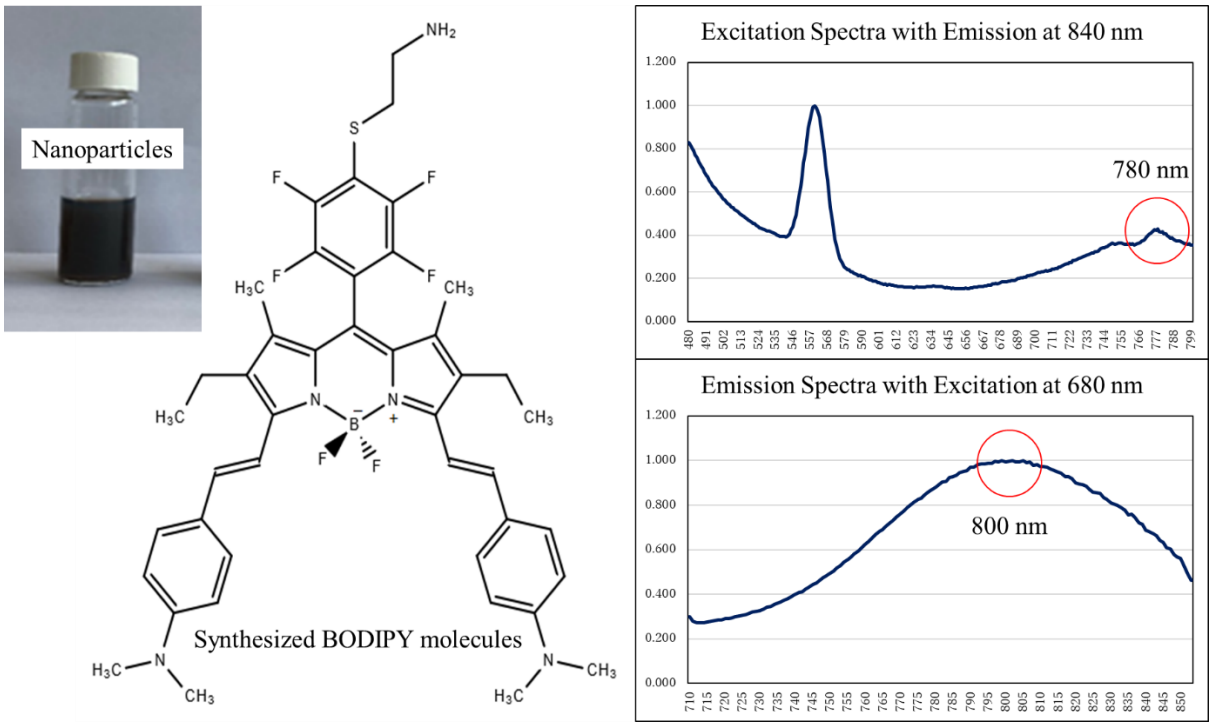

Figure 50. Chemical structure of a synthesized BODIPY molecule and its nanoparticles with their excitation and emission spectra.

Then, the preparations of biodegradable nanoparticles containing fluorescent dyes using similar method with minor modifications were attempted in NAIST. In the first experiment, the fluorescent dye used was 3 mg of perylene-diimide (PDI) with maximum excitation and emission wavelengths of 527 and 537 nm, respectively. For aqueous phase, polyvinyl alcohol (PVA) solution (1% w/w) was used, instead of sodium cholate solution. The emulsification process was carried out for 8 min (amplitude 16%, power 125 W) because of using a different sonication instrument. The additional step for removing free dye could not be conducted because the instrument was not available here. The prepared nanoparticles was about 177.5 nm in diameter. This time, the fluorescence was not observed either, probably because the concentration of PDI was not optimized. In the second experiment, the fluorescent dye used was 8 µg of Nile red with maximum excitation and emission wavelengths of 554 and 638 nm, respectively. The preparation step were similar with those of the previous nanoparticles containing PDI, except that the emulsification was for total 8 min (4 min sonication, 4 min stop,

every 30 s) with amplitude 70% and power 125 W. As the fluorescence was also not observed for the similar reason, the nanoparticle size was not measured this time.

As previously described, the injection of larger nanoparticles with diameter of 110 nm was also attempted, even though the injection could not be confirmed. Considering that, the biodegradable nanoparticles containing fluorescent dyes prepared in this work were over 130 nm in diameter, so if a smaller size nanoparticles are desired, the amplitude and power of the sonication instrument during emulsification process should be optimized.

Although the photoinjection of the nanoparticles prepared above was not conducted yet because of lack of observable fluorescence, even in the medium, at least the biodegradable nanoparticles could be prepared at NAIST. The fluorescent dye concentration needs to be optimized in order to get a bright fluorescent nanoparticles that can be used for photoinjection visualization. Nevertheless, the photoinjection of biodegradable polymer nanoparticles containing functional molecules into plant cells would be useful for future researches, especially in the study of plant physiology and genetic engineering.

References

1. Rivera, A. L., Gomez-Lim, M., Fernandez, F. & Loske, A. M. Physical methods for genetic plant transformation. *Phys. Life Rev.* **9,** 308-345 (2012).
2. Rao, A. Q. *et al*. The myth of plant transformation. *Biotechnol. Adv.* 27: 753-763 (2009).
3. Saito, Y. *et al*. A green fluorescent protein fused to rice prolamin forms protein body-like structures in transgenic rice. *J. Exp. Bot.* **60 (2),** 615-627 (2009).
4. Kim, S. Y., Sivaguru, M. & Stacey G. Extracellular ATP in plants. Visualization, localization, and analysis of physiological significance in growth and signaling. *Plant Physiol.* **142,** 984-992 (2006).
5. Yamaguchi, N. *et al*. A molecular framework for auxin-mediated initiation of flower primordia. *Dev. Cell* **24,** 271–282 (2013).
6. Donmez, D., Simsek, O. & Aka Kacar, Y. Genetic engineering techniques in fruit sciences. *Int. J. Envir. Agri. Res.* **2(12)**, 115-128 (2016).
7. Fuentes, P. *et al*. A new synthetic biology approach allows transfer of an entire metabolic pathway from a medicinal plant to a biomass crop. *eLife* **5,** e13664; 10.7554/eLife.13664 (2016).
8. Buyel, J. F., Twyman, R. M. & Fischer, R. Very-large-scale production of antibodies in plants: The biologization of manufacturing. *Biotechnol. Adv.* 35, 458-465 (2017).
9. Wang, P., Lombi, E., Zhao, F.-J., & Kopittke, P. M., Nanotechnology: A new opportunity in plant sciences. *Trends Plant Sci.* **21(8)**, 699-712 (2016).
10. Siddiqui, M. H., Al-Whaibi, M. H., Firoz, M., & Al-Khaishany, M. Y. Role of nanoparticles in plants in *Nanotechnology and Plant Sciences*, (eds. Siddiqui, M. H., Al-Whaibi, M. H., & Mohammad, F.) 19-35 (Springer, Cham, 2015).

11. Sanzari, I., Leone, A., Ambrosone, A. Nanotechnology in plant science: To make a long story short. *Front. Bioeng. Biotechnol.* **7**, 120 (2019).
12. Tripathi, D. K. *et al*. An overview on manufactured nanoparticles in plants: Uptake, translocation, accumulation and phytotoxicity. *Plant Physiol. Biochem.* **110**, 2-12 (2017).
13. Corredor, E. *et al*. Nanoparticle penetration and transport in living pumpkin plants: in situ subcellular identification. *BMC Plant Biol.* **9**, 45 (2009).
14. Cunningham, F. J., Goh, N. S., Demirer, G. S., Matos, J. L., & Landry, M. P. Nanoparticle-mediated delivery towards advancing plant genetic engineering. *Trends Biotechnol.* **36(9)**, 882-897 (2018).
15. Hayashimoto, A., Li, Z. & Murai, N. A polyethylene glycol-mediated protoplast transformation system for production of fertile transgenic rice plants. *Plant Physiol.* **93**, 857-863 (1990).
16. Bates, G. W. Genetic transformation of plants by protoplast electroporation. *Mol. Biotechnol.* **2**, 135-145 (1994).
17. Tzfira, T. & Citovsky, V. Agrobacterium-mediated genetic transformation of plants: biology and biotechnology. *Curr. Opin. Biotechnol.* **17**, 147–154 (2006).
18. Vanegas, P. E., Valdez-Morales, M., Valverde, M. E., Cruz-Hernandez, A. & Paredes-Lopez, O. Particle bombardment, a method for gene transfer in marigold. *Plant Cell Tissue Organ Cult.* **84**, 359–363 (2006).
19. Martin-Ortigosa, S., Valenstein, J. S., Lin, V. S.-Y., Trewyn, B. G., & Wang, K. Gold functionalized mesoporous silica nanoparticle mediated protein and DNA codelivery to plant cells via the biolistic method. *Adv. Funct. Mater.* **22**, 3576- 3582 (2012).
20. Weber, G., Monajembashi, S., Greulich, K. O. & Wolfrum, J. Genetic manipulation of plant cells and organelles with a laser microbeam. *Plant Cell Tissue Organ Cult.* **12,** 219-222 (1988).

21. Weber, G., Monajembashi, S., Greulich, K. O. & Wolfrum J. Microperforation of plant tissue with a UV laser microbeam and injection of DNA into cells. *Naturwissenschaften* **75,** 35-36 (1988).

22. Guo, Y., Liang, H. & Berns, M. W. Laser-mediated gene transfer in rice. *Physiol. Plant.* **93,** 19-24 (1995).

23. Tirlapur, U. K. & König, K. Femtosecond near-infrared laser pulses as a versatile non-invasive tool for intra-tissue nanoprocessing in plants without compromising viability. *Plant J.* **31(3)**, 365-374 (2002).

24. LeBlanc, M. L., Merritt, T. R., McMillan, J., Westwood, J. H. & Khodaparast, G. A. Optoperforation of single, intact Arabidopsis cells for uptake of extracellular dye-conjugated dextran. *Opt. Express* **21(12),** 14662-14673 (2013).

25. Mitchell, C. A. *et al*. Femtosecond optoinjection of intact tobacco BY-2 cells using a reconfigurable photoporation platform. *PLoS ONE* **8(11),** e79235; 10.1371/journal.pone.0079235 (2013).

26. Hosokawa, Y. Applications of the femtosecond laser-induced impulse to cell research. *Jpn. J. Appl. Phys.* **58**, 110102 (2019).

27. Iino, T. & Hosokawa, Y. Direct measurement of femtosecond laser impulse in water by atomic force microscopy. *Appl. Phys. Express* **3**, 107002 (2010).

28. Jacques, S. L. Optical properties of biological tissues: a review. *Phys. Med. Biol.* **58**, R37 (2013).

29. Kawakami, R. *et al*. In vivo two-photon imaging of mouse hippocampal neurons in dentate gyrus using a light source based on a high-peak power gain-switched laser diode. *Biomed. Opt. Express* **6**, 891 (2015).

30. Tirlapur, U. K. & König, K. Targeted transfection by femtosecond laser. *Nature* **418**, 290-291 (2002).

31. Stevenson, D. *et al.* Femtosecond optical transfection of cells: Viability and efficiency. *Opt. Express* **14(16)**, 7125-7133 (2006).

32. Uchugonova, A., König, K., Bueckle, R., Isemann, A. & Tempea, G. Targeted transfection of stem cells with sub-20 femtosecond laser pulses. *Opt. Express* **16(13)**, 9357-9364 (2008).

33. Davis, A. A., Farrar, M. J., Nishimura, N., Jin, M. M. & Schaffer, C. B. Optoporation and genetic manipulation of cells using femtosecond laser pulses. *Biophys. J.* **105(4)**, 862-871 (2013).

34. Hosokawa, Y. *et al*. Gene delivery process in a single animal cell after femtosecond laser microinjection. *Appl. Surf. Sci.* **255,** 9880-9884 (2009).

35. Hosokawa, Y., Ochi, H., Iino, T., Hiraoka, A. & Tanaka, M. Photoporation of biomolecules into single cells in living vertebrate embryos induced by a femtosecond laser amplifier. *PLoS ONE* **6(11),** e27677; 10.1371/journal.pone.0027677 (2011).

36. Granath, K. A. Solution properties of branched dextrans. *J. Colloid Sci.* **13**, 308–328 (1958).

37. Smit, J. A. M., Van Dijk, J. A. P. P., Mennen, M. G., & Daoud, M. Polymer size exponents of branched dextrans. *Macromolecules* **25**, 3585–3590; doi:10.1021/ma00039a044 (1992).

38. Taiz, L. & Zeiger, E. Cell walls: structure, biogenesis, and expansion in *Plant Physiology*, (eds. Taiz, L. & Zeiger, E.) 313-338 (Sinauer Associates, Sunderland, MA, 2006).

39. Grazon, C., Rieger, J., Méallet-Renault, R., Clavier, G., & Charleux, B., One-pot synthesis of pegylated fluorescent nanoparticles by RAFT miniemulsion polymerization using a phase inversion process. *Macromol. Rapid Commun.* **32**, 699-705 (2011).

40. Grazon, C., Rieger, J., Méallet-Renault, R., Charleux, B., & Clavier, G. Ultrabright fluorescent polymeric nanoparticles made from a new family of BODIPY monomers. *Macromolecules* **46**, 5167-5176 (2013).

41. Nagata, T., Nemoto, Y. & Hasezawa, S. Tobacco BY-2 cell line as the “HeLa” cell in the cell biology of higher plants. *Int. Rev. Cytol.* **132,** 1-30 (1992).

42. Schinkel, H., Jacobs, P., Schillberg, S. & Wehner, M. Infrared picosecond laser for perforation of single plant cells. *Biotechnol. Bioeng.* **99(1),** 244-248 (2008).

43. Tamaru, Y. *et al*. Formation of protoplasts from cultured tobacco cells and *Arabidopsis thaliana* by the action of cellulosomes and pectate lyase from *Clostridium cellulovorans*. *Appl. Environ. Microbiol.* **68(5)**, 2614–2618 (2002).

44. Dunlap, D. D., Maggi, A., Soria, M. R., & Monaco, L. Nanoscopic structure of DNA condensed for gene delivery. *Nucleic Acids Res.* **25(15)**, 3095-3101 (1997).

45. Sigma-Aldrich. Fluorescein isothiocyanate-dextran. *Product Information* **FD-4**, 1-3 (1997).

46. Dauty, E., Behr, J. P., & Remy, J. S. Development of plasmid and oligonucleotide nanometric particles. *Gene Ther.* **9**, 743-749 (2002).

47. Bhise, N. S., Shmueli, R. B., Gonzalez, J., & Green, J. J. A novel assay for quantifying the number of plasmids encapsulated by polymer nanoparticles. *Small* **8(3)**, 367-373 (2012).

48. Jones, K. H. & Senft, J. A. An improved method to determine cell viability by simultaneous staining with fluorescein diacetate-propidium iodide. *J. Histochem. Cytochem.* **33(1)**, 77-79 (1985).

49. Green, V. S., Stott, D. E., & Diack, M. Assay for fluorescein diacetate hydrolytic activity: Optimization for soil samples. *Soil Biol. Biochem.* **38**, 693–701 (2006).

50. Maeno, T. *et al*. Targeted delivery of fluorogenic peptide aptamers into live microalgae by femtosecond laser photoporation at single-cell resolution. *Sci. Rep.* **8**, 8271; 10.1038/s41598-018-26565-4 (2018).

51. Vogel, A., Noack, J., Huttman, G. & Paltauf, G. Mechanisms of femtosecond laser nanosurgery. *Appl. Phys. B* **81**, 1015–1047 (2005).

52. Libault, M., Pingault, L., Zogli, P., & Schiefelbein, J. Plant systems biology at the single-cell level. *Trends Plant Sci.* **22(11)**, 949-960 (2017).

53. Robards, A. W. Plasmodesmata. *Annu. Rev. Plant. Physiol.* **26**, 13-29 (1975).

54. Hernández-Hernández, V., Benitez, M. & Boudaoud, A. Interplay between turgor pressure and plasmodesmata during plant development. *J. Exp. Bot.* **71(3)**, 768-777 (2020).

55. Faulkner, C. Plasmodesmata and the symplast. *Curr. Microbiol.* **28(24)**, R1374-R1378 (2018).

56. Raliya, R. *et al*. Quantitative understanding of nanoparticle uptake in watermelon plants. *Front. Plant Sci.***7**, 1288; 10.3389/fpls.2016.0128 (2016).

57. Zhai, G., Walters, K. S., Peate, D. W., Alvarez, P. J. J. & Schnoor, J. L. Transport of gold nanoparticles through plasmodesmata and precipitation of gold ions in woody poplar. *Environ. Sci. Technol. Lett.* **1**, 146-151 (2014).

58. Tsien, R. Y. The green fluorescent protein. *Annu. Rev. Biochem.* **67**, 509-544 (1998).

59. Schomaker, M. *et al*. Characterization of nanoparticle mediated laser transfection by femtosecond laser pulses for applications in molecular medicine. *J. Nanobiotechnology* **13(10)**, 1-15 (2015).

60. Li, M., Lohmüller, T., & Feldmann, J. Optical injection of gold nanoparticles into living cells. *Nano Lett.* **15**, 770-775 (2015).

61. Reul, R. *et al*. Near infrared labeling of PLGA for in vivo imaging of nanoparticles. *Polym. Chem.* **3**, 694-702 (2012).

62. Qiao, M., Chen, D., Ma, X., & Liu, Y. Injectable biodegradable temperature-responsive PLGA-PEG-PLGA copolymers: synthesis and effect of copolymer composition on the drug release from the copolymer-based hydrogels. *Int J Pharm.* **294(1-2)**, 103-112; doi:10.1016/j.ijpharm.2005.01.017 (2005).

63. Zhang, K. *et al*. PEG–PLGA copolymers: Their structure and structure-influenced drug delivery applications. *J Control Release* **183**, 77–86 (2014).

64. Danhier, F. *et al*. PLGA-based nanoparticles: An overview of biomedical applications. *J Control Release* **161**, 505–522 (2012).

65. Liang, G. F. et al. PLGA-based gene delivering nanoparticle enhance suppression effect of miRNA in HePG2 cells. *Nanoscale Res. Lett.* **6**, 447 (2011).

66. Mendoza-Muñoz, N., Alcalá-Alcalá, S., & Quintanar-Guerrero, D. Preparation of polymer nanoparticles by the emulsification-solvent evaporation method: From Vanderhoff's pioneer approach to recent adaptations in *Polymer Nanoparticles for Nanomedicines - A guide for their design, preparation and development*, (eds. Vauthier, C. & Ponchel, G.) 87-121 (Springer, Cham, 2016).

Achievements

Journal publications

1. Enzyme-assisted photoinjection of megadalton molecules into intact plant cells using femtosecond laser amplifier; Taufiq Indra Rukmana, Gabriela Moran, Rachel Méallet-Renault, Misato Ohtani, Taku Demura, Ryohei Yasukuni and Yoichiroh Hosokawa; 2019, *Scientific Reports*, 9, 17530. (Chapter 3 and 5)
2. Photoinjection of fluorescent nanoparticles into intact plant cells using femtosecond laser amplifier; Taufiq Indra Rukmana, Gabriela Moran, Rachel Méallet-Renault, Gilles Clavier, Tadashi Kunieda, Misato Ohtani, Taku Demura, Ryohei Yasukuni and Yoichiroh Hosokawa; 2020, *APL Photonics*, 5, 066104. (Chapter 4 and 5)
3. Investigation of diffusion processes in plant cell cytoplasm by photoinjection using femtosecond laser; Taufiq Indra Rukmana, Gabriela Moran, Rachel Méallet-Renault, Gilles Clavier, Tadashi Kunieda, Misato Ohtani, Taku Demura, Ryohei Yasukuni and Yoichiroh Hosokawa; To be submitted to *Applied Physics Express*. [Tentative] (Chapter 6)

Other journal publications

1. Development of a high-performance liquid chromatography method for analyzing disodium 5'-inosinate levels in flavor enhancers; Dwi Karina Natalia, Harmita, Taufiq Indra Rukmana; 2018, *International Journal of Applied Pharmaceutics*, 10, Special Issue 1, 133-137.
2. Isolation and characteristics of bovine skin gelatin and analysis of glycine, proline, and hydroxyproline by high-performance liquid chromatography-fluorescence; Dini Khoirunnisa, Harmita, Taufiq Indra Rukmana; 2018, *International Journal of Applied Pharmaceutics*, 10, Special Issue 1, 269-275.

3. Isolation, purification, and characterization of bovine tendon collagen and analysis of glycine, proline, and hydroxyproline by high-performance liquid chromatography-fluorescence; Dwi Yulianti, Harmita, Taufiq Indra Rukmana; 2018, *International Journal of Applied Pharmaceutics*, 10, Special Issue 1, 311-315.

Conference publications

1. Introduction of megadalton molecules into tobacco BY-2 cells by femtosecond laser photoporation; Taufiq Indra Rukmana, Sohei Yamada, Kazunori Okano, Misato Ohtani, Taku Demura, Ryohei Yasukuni and Yoichiroh Hosokawa; 2018, *PHC Sakura Project Mini Symposium*, Paris, France, (Jun. 2018). [Oral]
2. Introduction of megadalton molecules into tobacco BY-2 cells by femtosecond laser photoporation; Taufiq Indra Rukmana, Sohei Yamada, Kazunori Okano, Misato Ohtani, Gabriela Moran, Taku Demura, Ryohei Yasukuni and Yoichiroh Hosokawa; 2018, *31st International Microprocesses and Nanotechnology Conference (MNC 2018)*, 15P-7-81, Sapporo, Japan, (Nov. 2018). [Poster]
3. Introduction of megadalton molecules into single plant cells by enzyme-assisted femtosecond laser photoporation; Taufiq Indra Rukmana, Gabriela Moran, Rachel Méallet-Renault, Misato Ohtani, Taku Demura, Ryohei Yasukuni and Yoichiroh Hosokawa; 2019, *ISMO-NAIST Symposium*, Paris, France, (Mar. 2019). [Oral]
4. Photoinjection of fluorescent nanoparticles into plant cells using femtosecond laser amplifier with enzyme treatment; Taufiq Indra Rukmana, Gabriela Moran, Rachel Méallet-Renault, Misato Ohtani, Taku Demura, Ryohei Yasukuni and Yoichiroh Hosokawa; 2019, *The 80th JSAP Autumn Meeting, JSAP-OSA Joint Symposia*, 20a-E214-4, Sapporo, Hokkaido, Japan, (Sep. 2019). [Oral]

5. Introduction of large substances into plant cells using femtosecond laser amplifier, Taufiq Indra Rukmana, Taufiq Indra Rukmana, Gabriela Moran, Rachel Méallet-Renault, Misato Ohtani, Taku Demura, Ryohei Yasukuni and Yoichiroh Hosokawa, 2019, *4th Meeting of PHC-JSPS Sakura Program*, Nara, Japan, (Oct. 2019). [Oral]

Other conference publications

1. フェムト秒レーザーを用いた Tobacco BY 植物細胞への巨大高分子導入; 安國　良平, Rukmana Taufiq Indra, 大谷 美沙都, 出村　拓 and 細川　陽一郎; 2019, 光・量子デバイス研究会, 東北大学東京分室, 日本, (Mar. 2019). [Oral]
2. フェムト秒レーザーを用いた単一植物細胞への巨大分子導入; 上田勇真, Taufiq Indra Rukmana, 岡野和宣, 安國良平, 細川陽一郎, 出村　拓 and 大谷美沙都; 2019, 植物構造オプト若手の会, 岡崎市, 愛知県, 日本, (Nov. 2019). [Poster]
3. Target introduction of DNA like large polysaccharide into plant cells by femtosecond laser photoporation; Yuma Ueda, Taufiq Indra Rukmana, Kunieda Tadashi, Misato Ohtani, Taku Demura, Ryohei Yasukuni and Yoichiroh Hosokawa; 2020, *The 2020 Annual Meeting of the Physical Society of Taiwan*, Pingtung, Taiwan, (Feb. 2020). [Poster]

Acknowledgements

Three years have been passed since I started my research in the Bio-Process Engineering Laboratory, Division of Materials Science, Nara Institute of Science and Technology. I am very grateful as I remember how I joined this wonderful group smoothly. I first came to NAIST as an internship student in Prof. *Yoichiroh Hosokawa* sensei laboratory for about two weeks, including pre-screening interview in 2016. After that, there was a party for me, and all group members were very friendly that made me eager to become an international student in NAIST. Then, I was informed that I was selected as a potential awardee of *NAIST International Scholarship* program. With the helps from Prof. *Yoichiroh Hosokawa* sensei and team, and also from International Student Affairs Section of NAIST and a recommendation from the Faculty of Pharmacy, Universitas Indonesia, in which I was a lecturer, I could complete all the requirements for the scholarship. I was very happy and honored that eventually I got the scholarship. I started my doctoral study in NAIST from October 2017 and my amazing experiences in this laboratory began.

First, I would like to thank my main supervisor, Prof. *Yoichiroh Hosokawa* sensei, for the precious opportunity to work in his laboratory. He gave me full supports, advises, and guidance for my research. Especially in his busy schedule, he always made a time for me when needed.

I would also like to thank Dr. *Ryohei Yasukuni* sensei who supervised me during day-to-day work in the laboratory. He always helped me out when encountering problem in my research, and gave me many advises and suggestions to improve my work.

I would also like to thank Prof. *Shun Hirota* sensei and Prof. *Hironari Kamikubo* sensei as my advisors for all the great suggestions and questions during my research evaluation so I could improve and modify my research accordingly.

I would also like to thank Prof. *Taku Demura* sensei, Assoc. Prof. *Misato Ohtani* sensei, Dr. *Tadashi Kunieda* sensei, and team for providing the tobacco BY-2 cells and giving me valuable discussion and knowledge in conducting plant research.

I would also like to thank Prof. *Rachel Méallet-Renault*, Prof. *Gilles Clavier*, Dr. *Gabriela Moran*, and all French colleagues for all their supports during this project, particularly for providing the fluorescent nanoparticles and their warm welcome when I was in France.

I would also like to thank Dr. *Nicolas Tsapis* and group in Institut Galien Paris Sud, Faculty of Pharmacy, Paris Sud University (UMR CNRS 8612), Paris, France for giving me a precious chance of two-month lab stay to study the preparation of biodegradable nanoparticles.

I would also like to thank Assoc. Prof. *Yalikun Yaxiaer* sensei for the suggestions and discussion so I could improve my knowledge, especially during lab meeting.

I would also like to thank Dr. *Sohei Yamada* sensei for the supports he gave to me, particularly in the early step of preparing biological materials.

I would also like to thank Dr. *Kazunori Okano* sensei who was very helpful when I got a problem during my research.

I would also like to thank Dr. *Eri Akita* sensei who was always helpful to me, especially when I needed plant samples other than TBY-2 cells.

I would also like to thank *Keiko Tada* san, secretary of the laboratory, for all her supports to me, especially in dealing with many paper works.

I would also like to thank all my fellow students and graduates of the laboratory for always giving me all kinds of supports in my research and daily life. Also special thanks to *Hong Zhen-yi* san as my senior who gave me useful advises, *Yoichi Uekuri* san as my tutor during my first months in Japan, *Akari Koyanagi* san who helped me conducting my first experiments with the instruments, *Yuma Ueda* san who was very eager to learn and continue this research topic, *Zhang Tianlong* san for his suggestions, particularly in English proofing, and *Dian Anggraini*

san as the other Indonesian lab mate here who I could discuss many things.

I would also like to thank the International Student Affairs Section and the Student Administration of the Materials Science division for giving me all the supports that I needed for studying here.

I would also like to thank the *NAIST International Scholarship* program for awarding me the scholarship to study here, and also the Ministry of Education, Culture, Sports, Science and Technology (MEXT) of Japan, for all the supports. Studying in NAIST offered me many great experiences, including an English training in UC Davis, USA; an internship/laboratory stay in Paris Sud University, France; attending conferences; and many others.

I would also like to thank the following grants which, in part, funded this research: the Grant-in-Aid for Scientific Research (C) (No. JP18042069), Scientific Research on Innovative Areas (No. JP18H05493) from the Japan Society for the Promotion of Science (JSPS), and the NAIST Special Fund [2018 Competitive Research Fund (Grant in Aid)]. The collaboration between Japan and France was supported by JSPS and MEAE-MESRI under the Japan - France Integrated Action Program (PHC Sakura 40951TG).

I would also like to thank the Faculty of Pharmacy, Universitas Indonesia, for all the supports, including the letter of recommendation from the faculty dean, Dr. *Mahdi Jufri*, to NAIST; and particularly to Prof. *Arry Yanuar* for giving me the first information and recommendation about NAIST; and to Prof. *Harmita* (my supervisor in master and bachelor degree), Dr. *Herman Suryadi* (my supervisor in bachelor degree), Dr. *Hayun* (the head of Laboratory of Pharmaceutical-Medicinal Chemistry and Bioanalysis, to which I belonged), Dr. *Fadlina Chany Saputri* (my superior in the Division of Cooperation, Ventura, and Alumni Relations, back then), and Dr. *Rani Sauriasari* (my superior in the Pharmaceutical Sciences and Research journal), for their continuous supports; and also to all Professors, lecturers, and members of the faculty for their supports, suggestions, and encouragements in my study.

I would also like to thank fellow young lecturers in the Faculty of Pharmacy, Universitas Indonesia, for their continuous supports, suggestions, and encouragements which keep me being motivated in work and life in general.

I would also like to thank all my friends in NAIST, especially fellow Indonesian students in NAIST, and also in Osaka and Nara, for their supports and helps so I could feel at home when studying abroad.

Last, but not the least, I would also like to thank my family: my parents, my brother, and all the big family members, and also my friends, for their continuous supports and encouragements, especially in their pray for me throughout this work and life in general.